

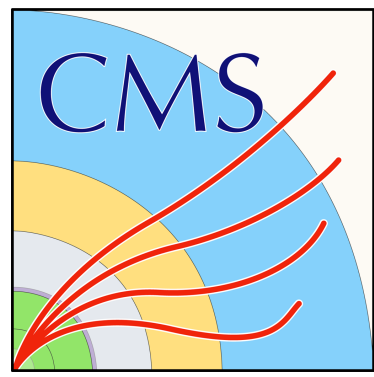
VBF/VBS measurements in ATLAS and CMS

Costanza Carrivale

(Università degli Studi di Perugia, INFN Perugia)

on behalf of the CMS and ATLAS Collaborations

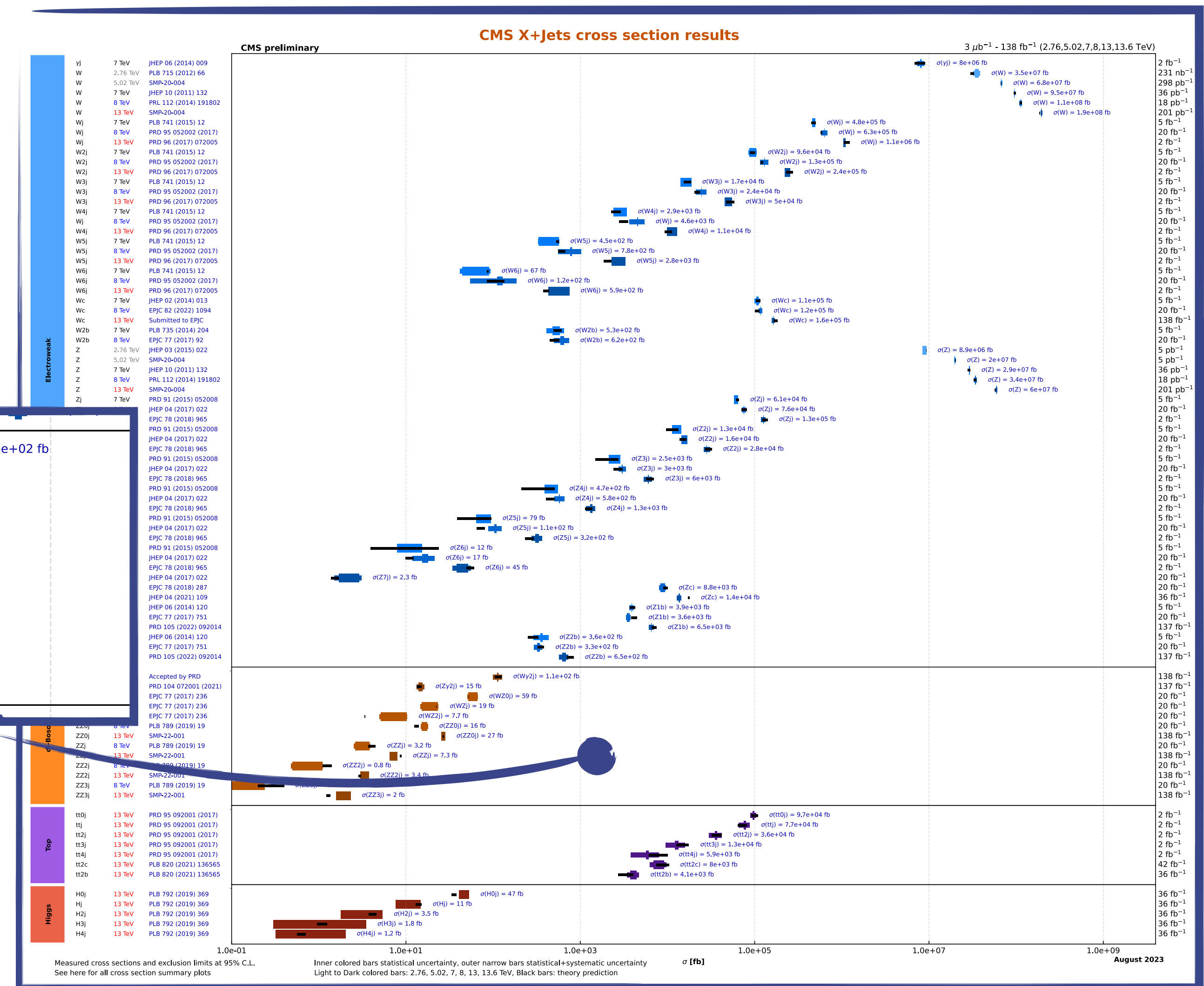
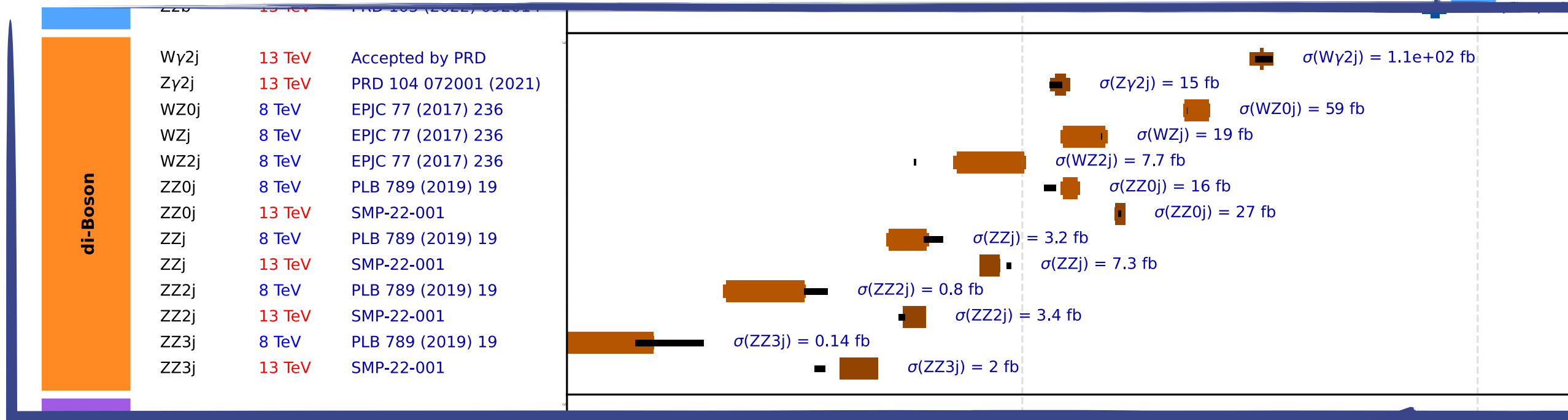
QCD@LHC - Freiburg, 8th October 2024



Vector Boson Fusion/Scattering at LHC

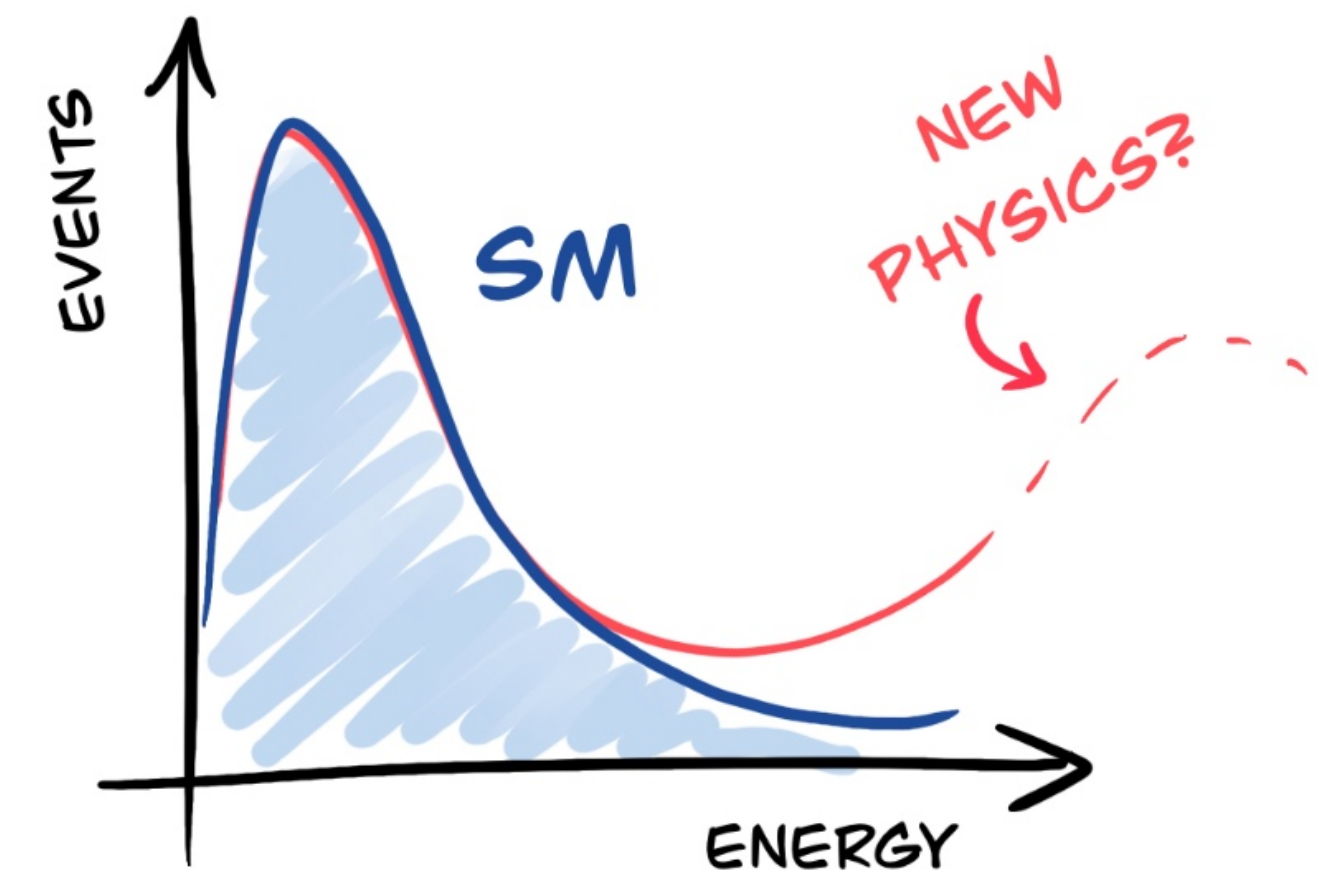
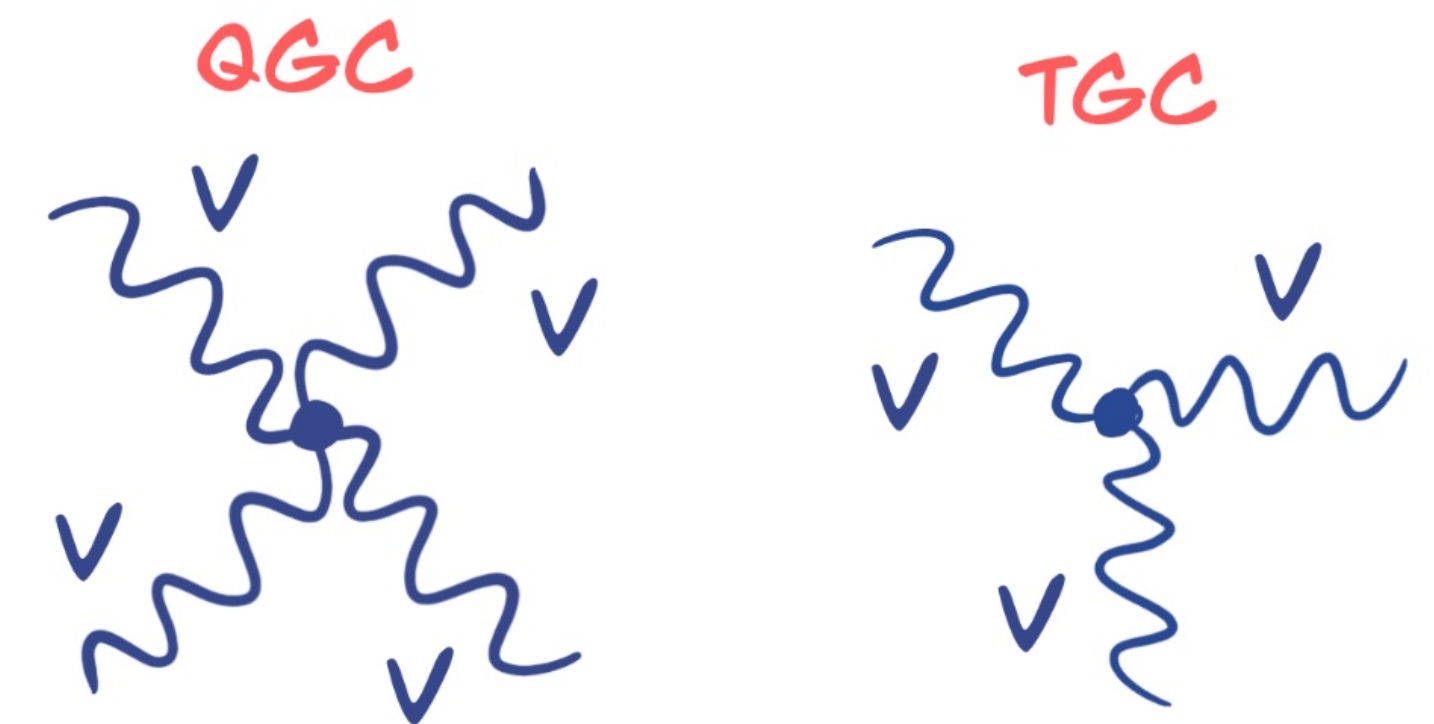


Diagrams in which two Vector Bosons interact, giving either one or two Vector Bosons in the final state, are among the rarest processes measured.



Why are VBF and VBS so charming?

- EW sector of the Standard Model is based on $SU(2)_L \otimes SU(1)_Y$ symmetry group. The non-abelian nature of the group results in self-interaction of the gauge bosons (triple and quartic gauge couplings, **TGCs and QGCs**). VBF/VBS processes exhibit both types of interaction.
- VBF/VBS processes are strictly related to **unitarity violation** in SM and precise measurements can probe the nature of the Higgs sector
- Powerful instrument to search for **effects beyond the SM** using model-independent approaches



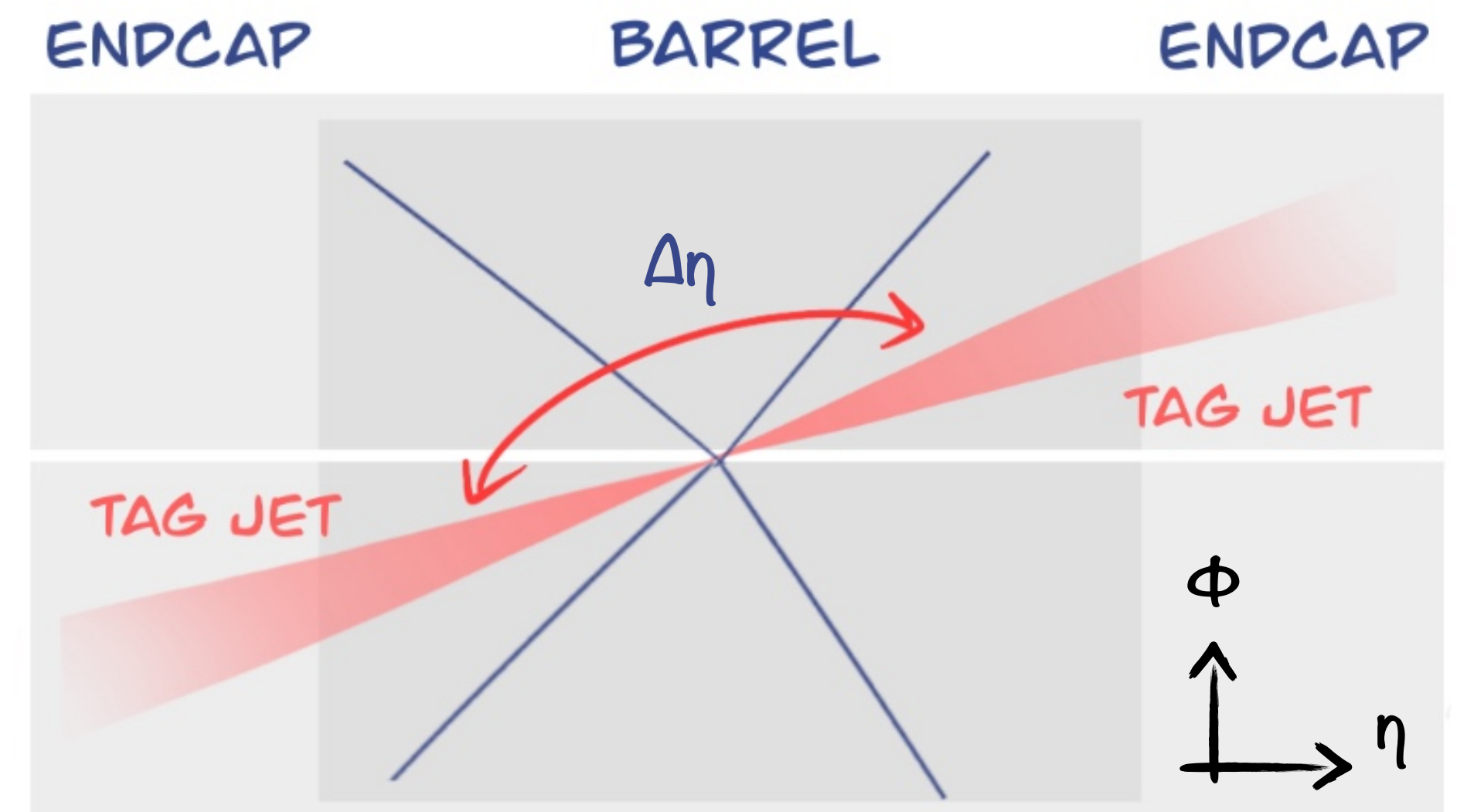
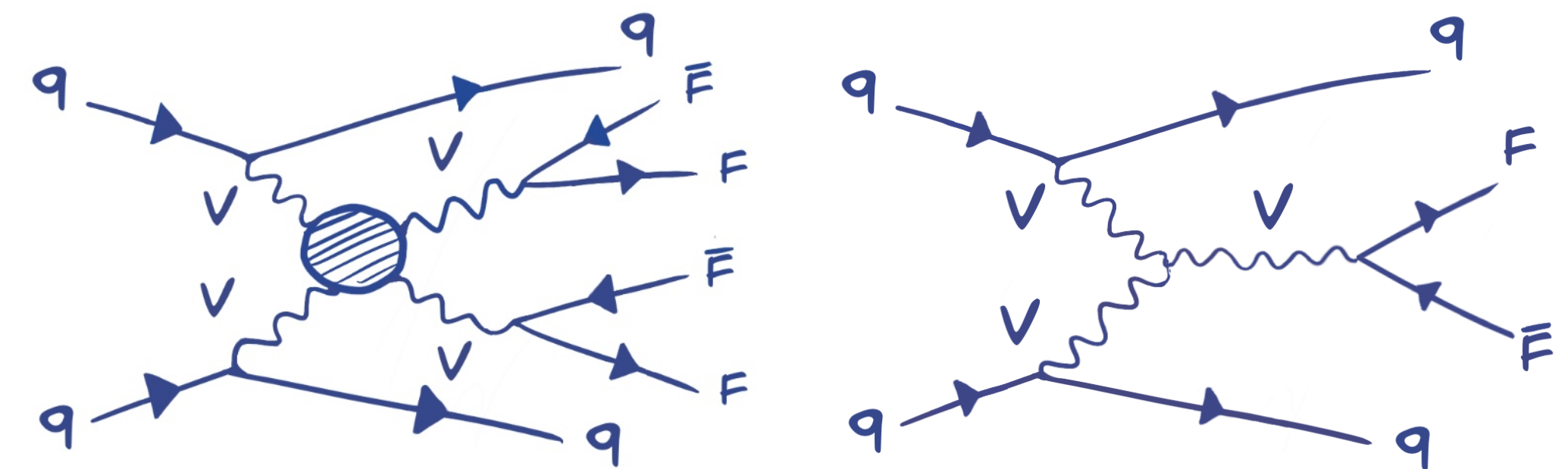
Topology in proton-proton collisions

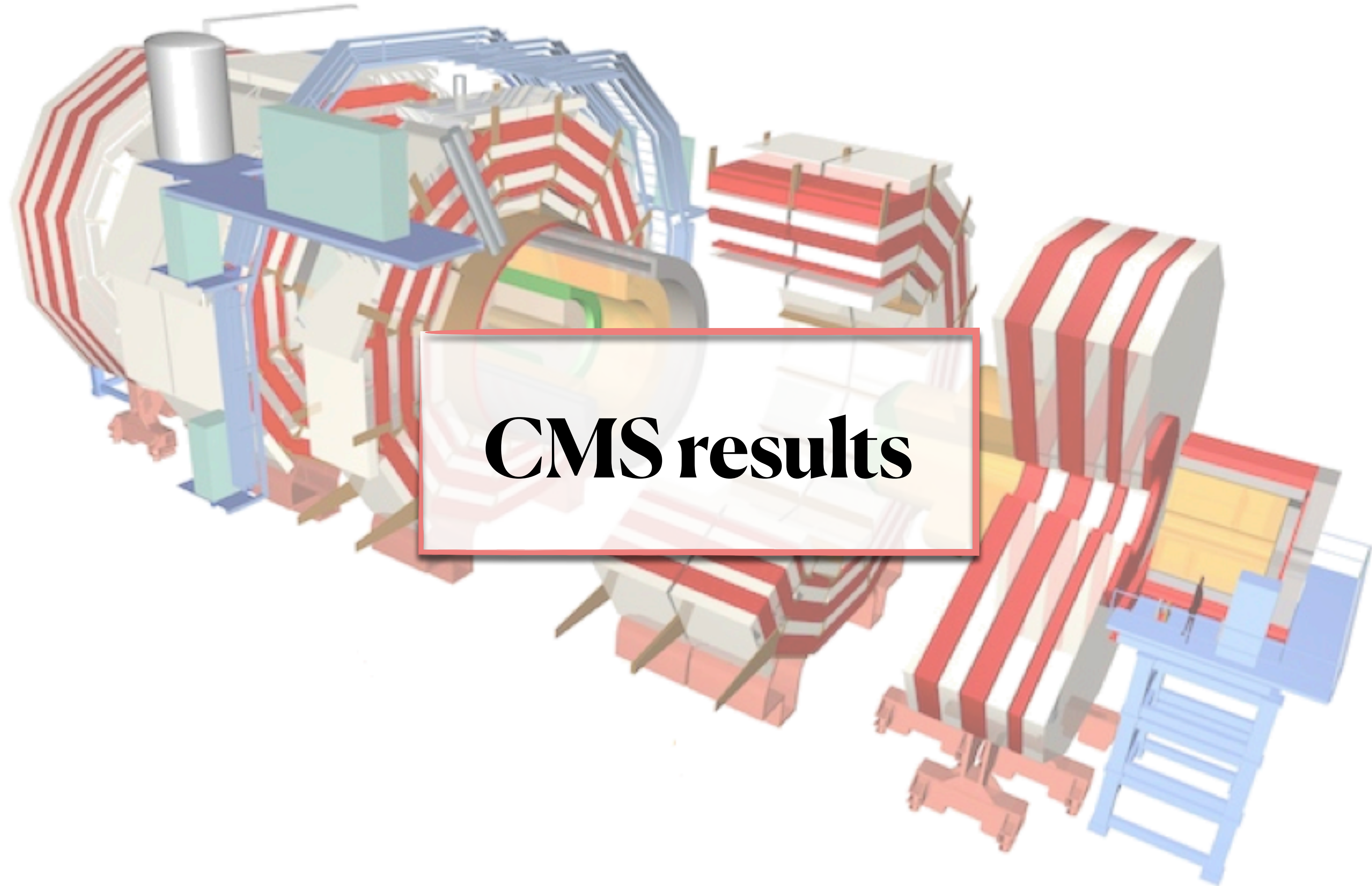
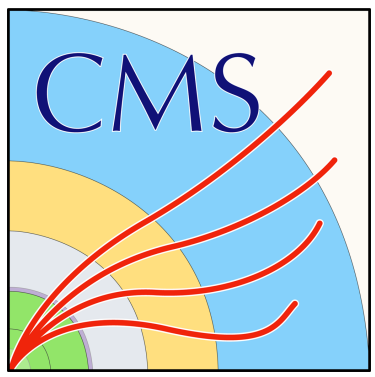
VBS and VBF contribute to EW-induced diboson production at tree level $\mathcal{O}(\alpha^4)$.

At LHC interactions from VBS are characterized by:

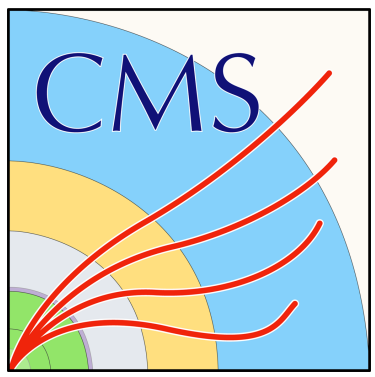
- Presence of **vector bosons** decay products in the central part of the detector;
- Two forward-backward **jets** with high dijet invariant mass and large pseudorapidity separation.

Typical observables in VBF/VBS measurements at LHC are cross sections in detector fiducial regions.



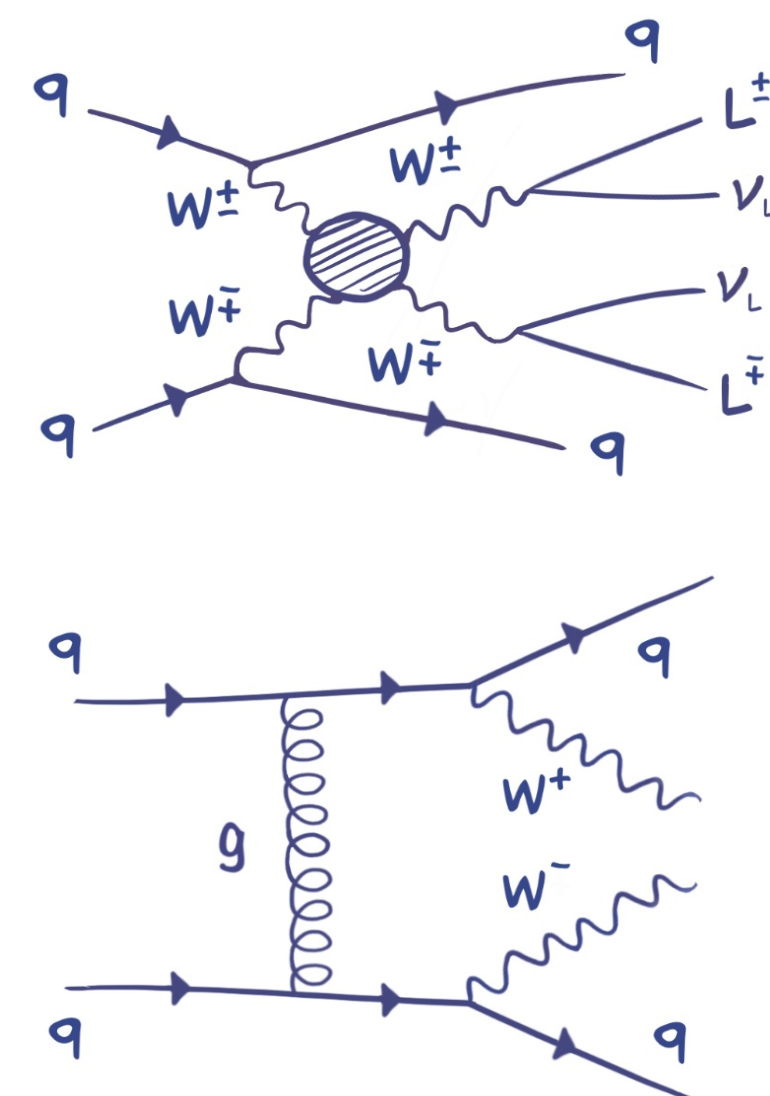


CMS results



Opposite-sign WW VBS

EWK production of a pair of opposite-sign Ws and two jets, with both W decaying leptonically.



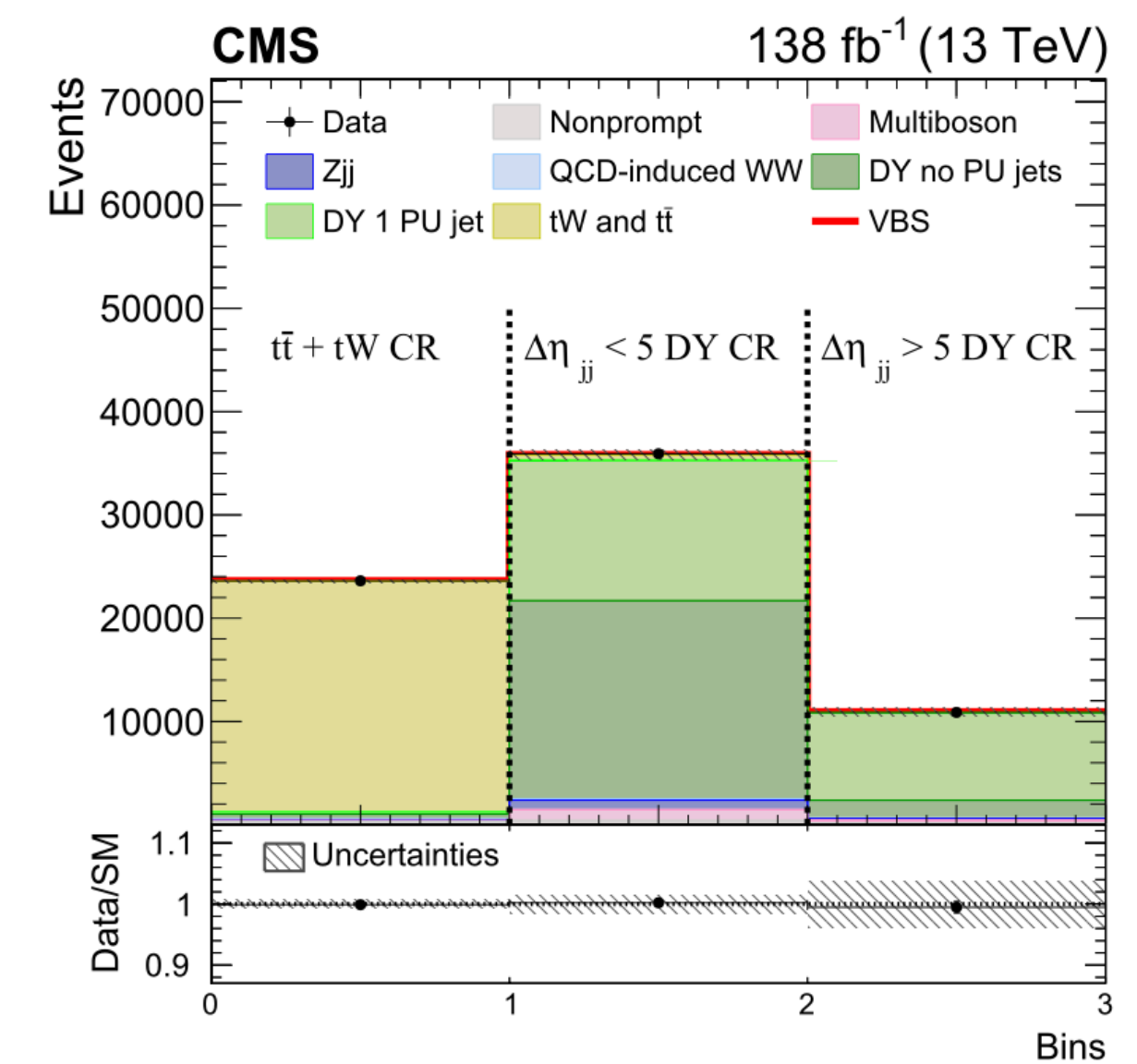
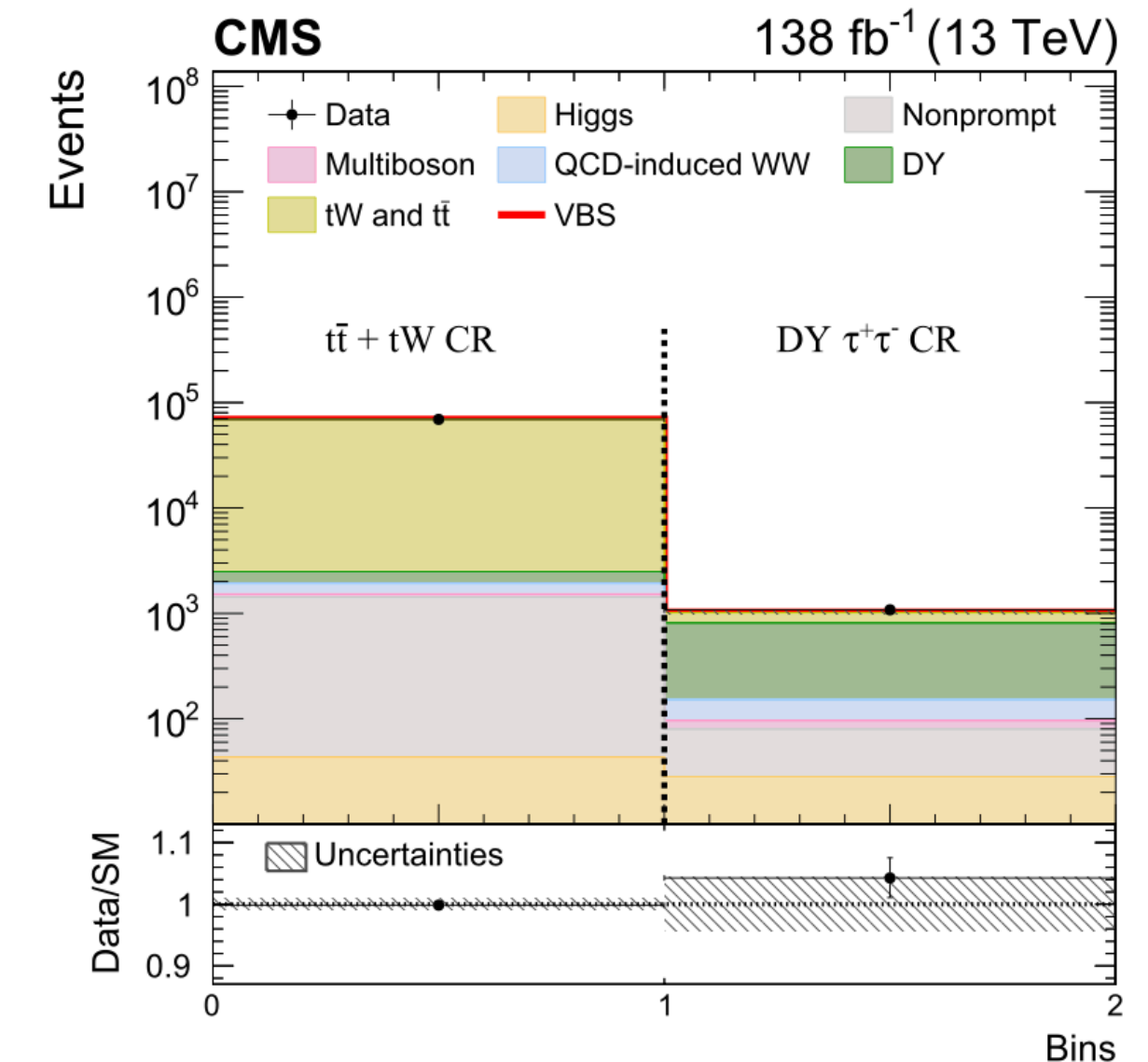
The analysis selects final states with two OS leptons: e^+e^- , $\mu^+\mu^-$, $e^\pm\mu^\mp$.
Sources of background:

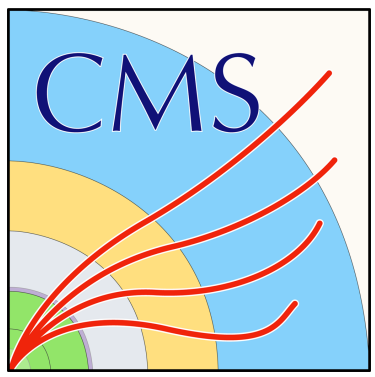
- **Top pair production** makes the measurement quite challenging. Studied in a dedicated CR (~95% pure sample $t\bar{t}$)
- **Drell Yan** is one of the leading backgrounds in ee and $\mu\mu$ categories (~91% wrt 64% in $e\mu$), comes from different sources
- Non-prompt (data driven)
- QCD-induced WW, Higgs, multiboson

Events where at least one jet comes from a pileup vertex
 $|\Delta\eta_{jj}| > 5$

Events where both jets are generated in hard interaction
 $|\Delta\eta_{jj}| < 5$

$\tau\tau$





Opposite-sign WW VBS

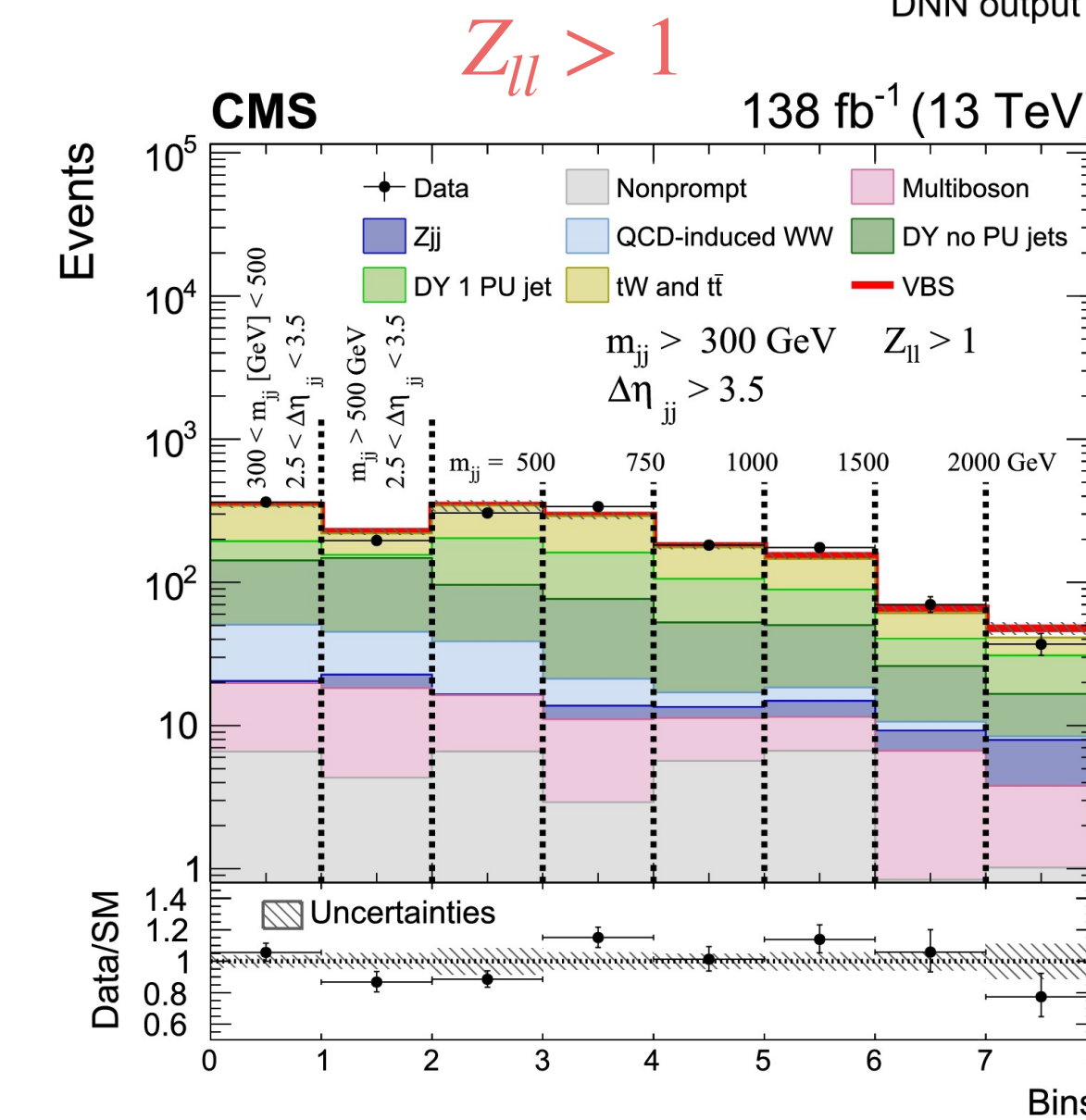
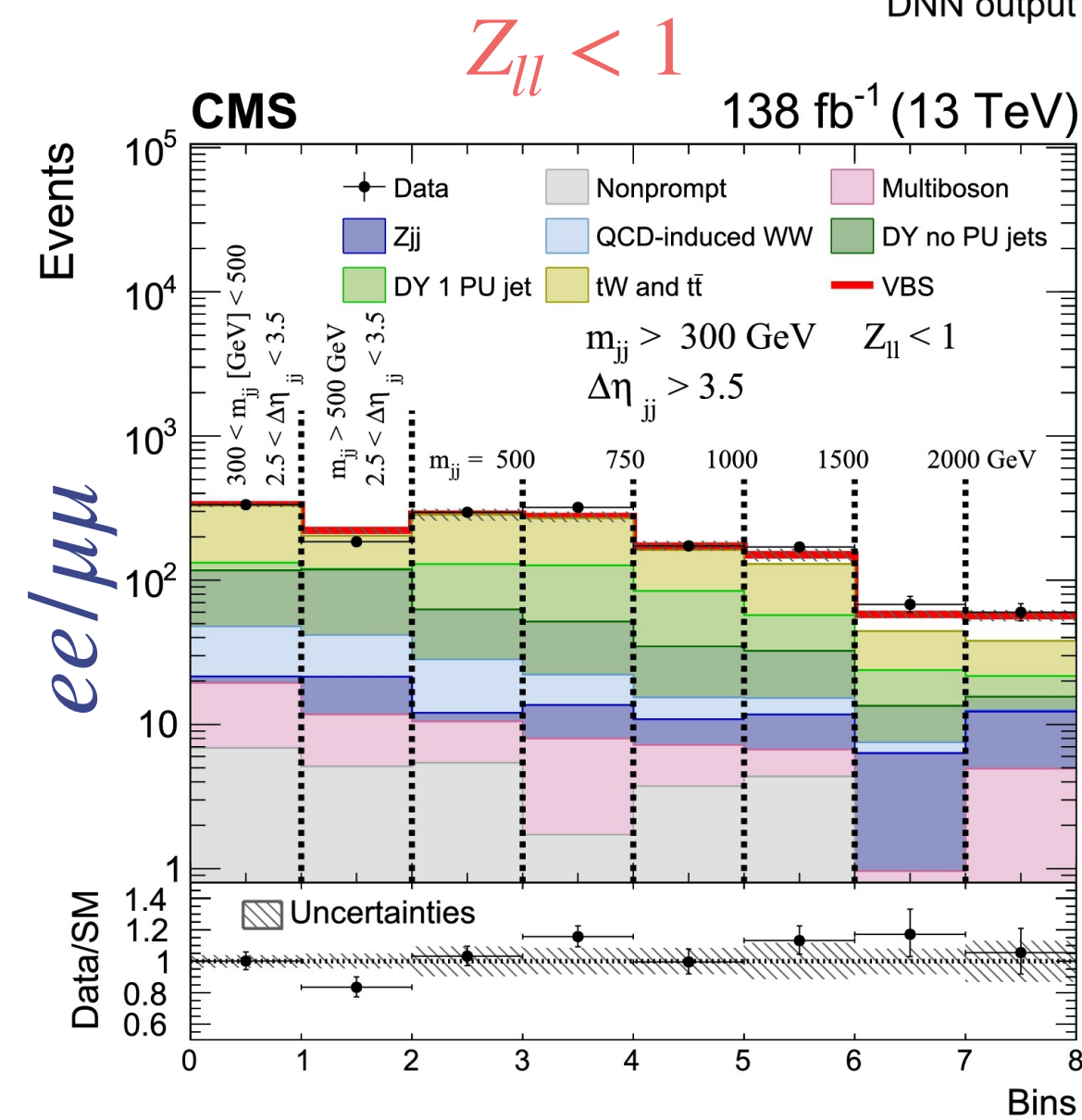
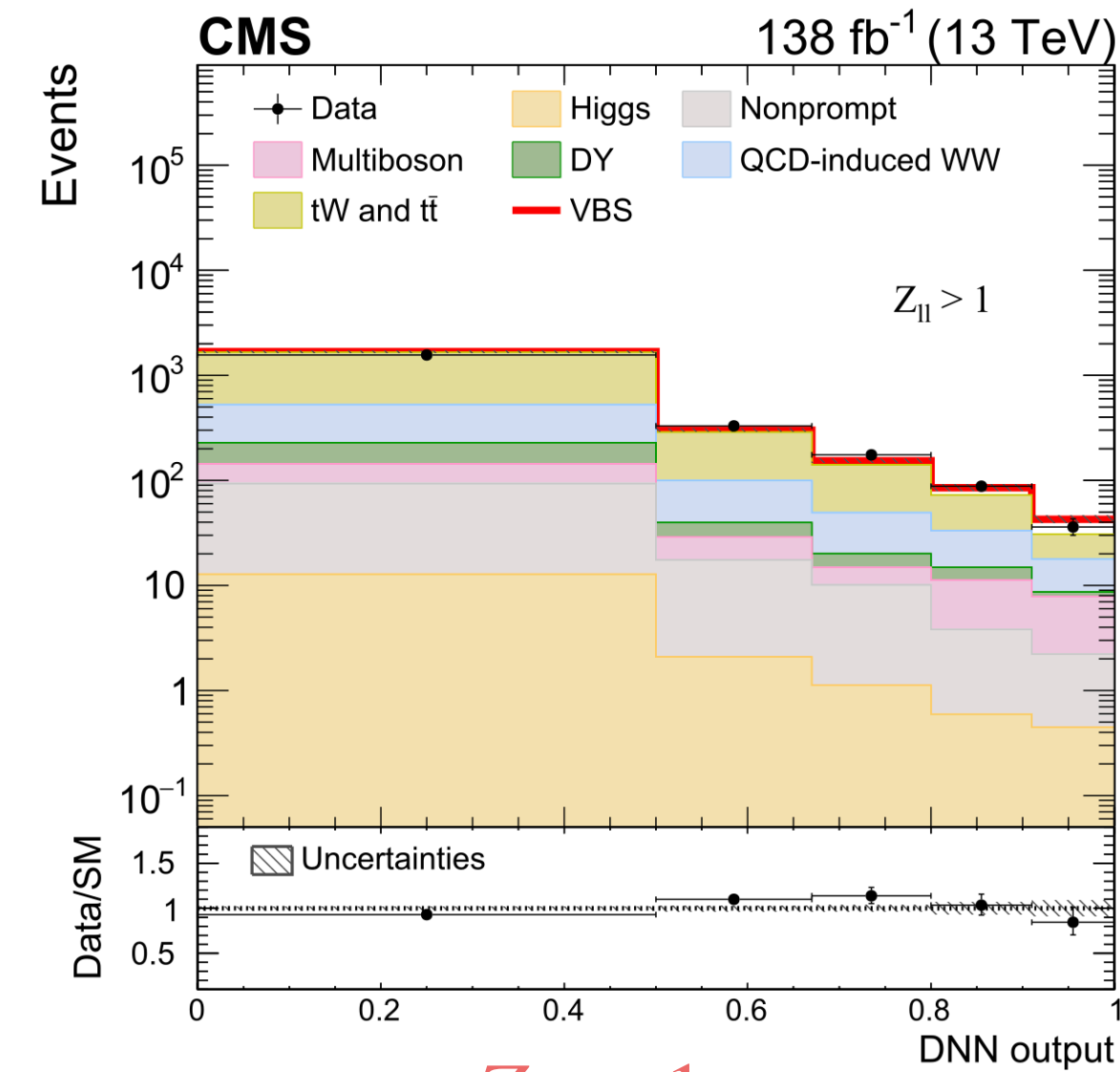
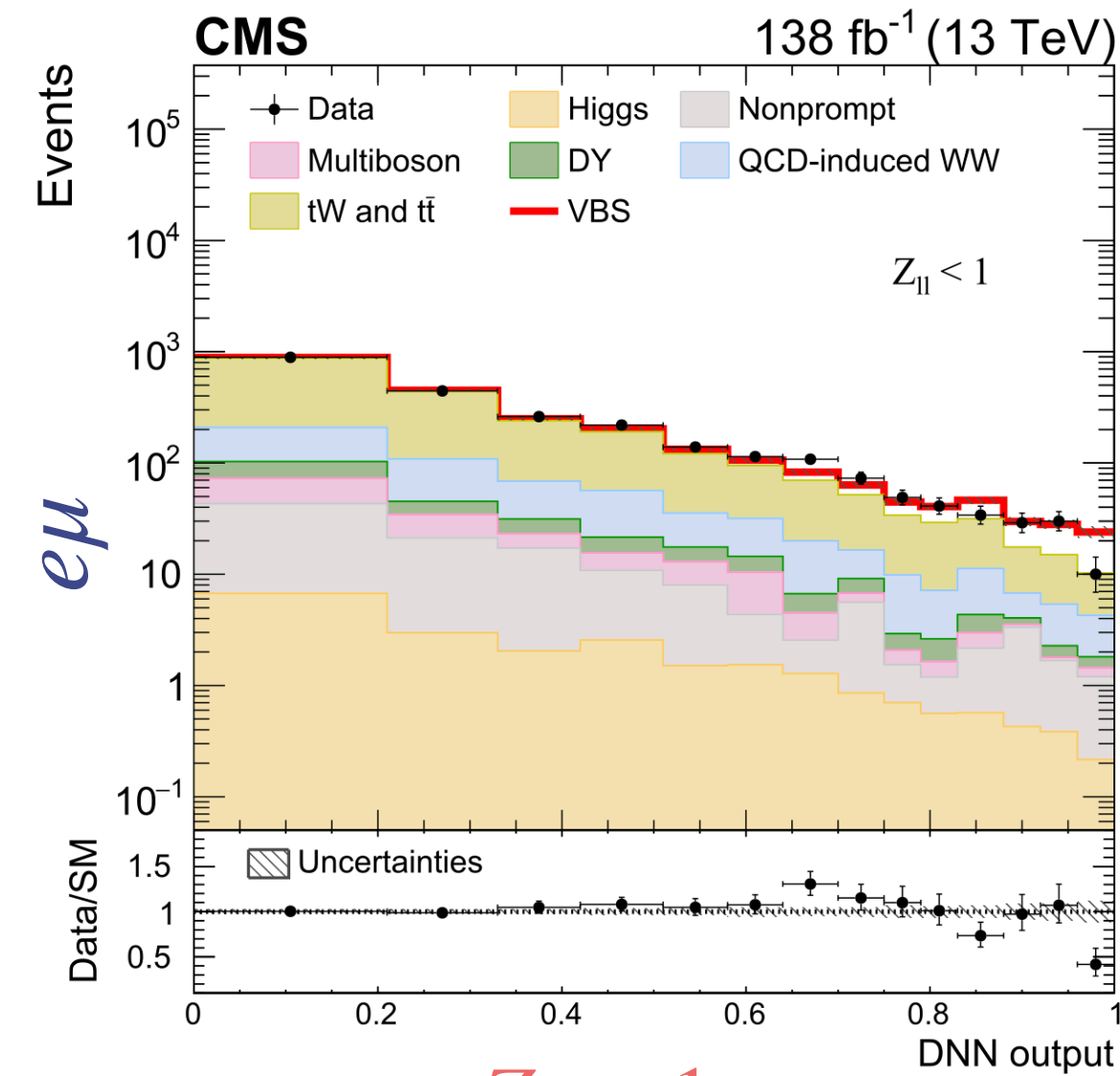
SR is split in two regions to optimize the signal significance, based on centrality of dilepton system with respect to the tagging jets, quantified by Zeppenfeld variable $Z_{ll} = \frac{1}{2} |\eta_{l1} + \eta_{l2} - (\eta_{j1} + \eta_{j2})|$.

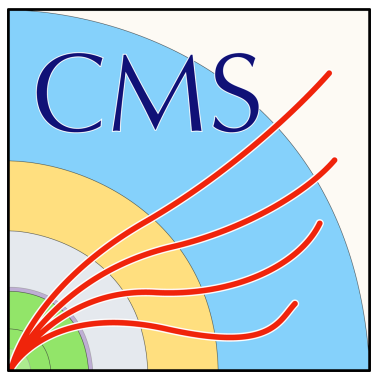
All categories are fit to data using a maximum likelihood fit and different discriminating variables:

- A feed-forward deep neural network (DNN) for $e\mu$
- Different variables in different regions for ee and $\mu\mu$:

n. events	{	$m_{jj} \in [300; 500] \text{ and } \Delta\eta_{jj} \in [2.5; 3.5]$	bin 1
		$m_{jj} > 500 \text{ and } \Delta\eta_{jj} \in [2.5; 3.5]$	bin 2
		$m_{jj} \in [300; 500] \text{ and } \Delta\eta_{jj} > 3.5$	bin 3
		$m_{jj} > 500 \text{ and } \Delta\eta_{jj} > 3.5$	bins 4-8

The observed (expected) significance is 5.6 (5.2) σ .



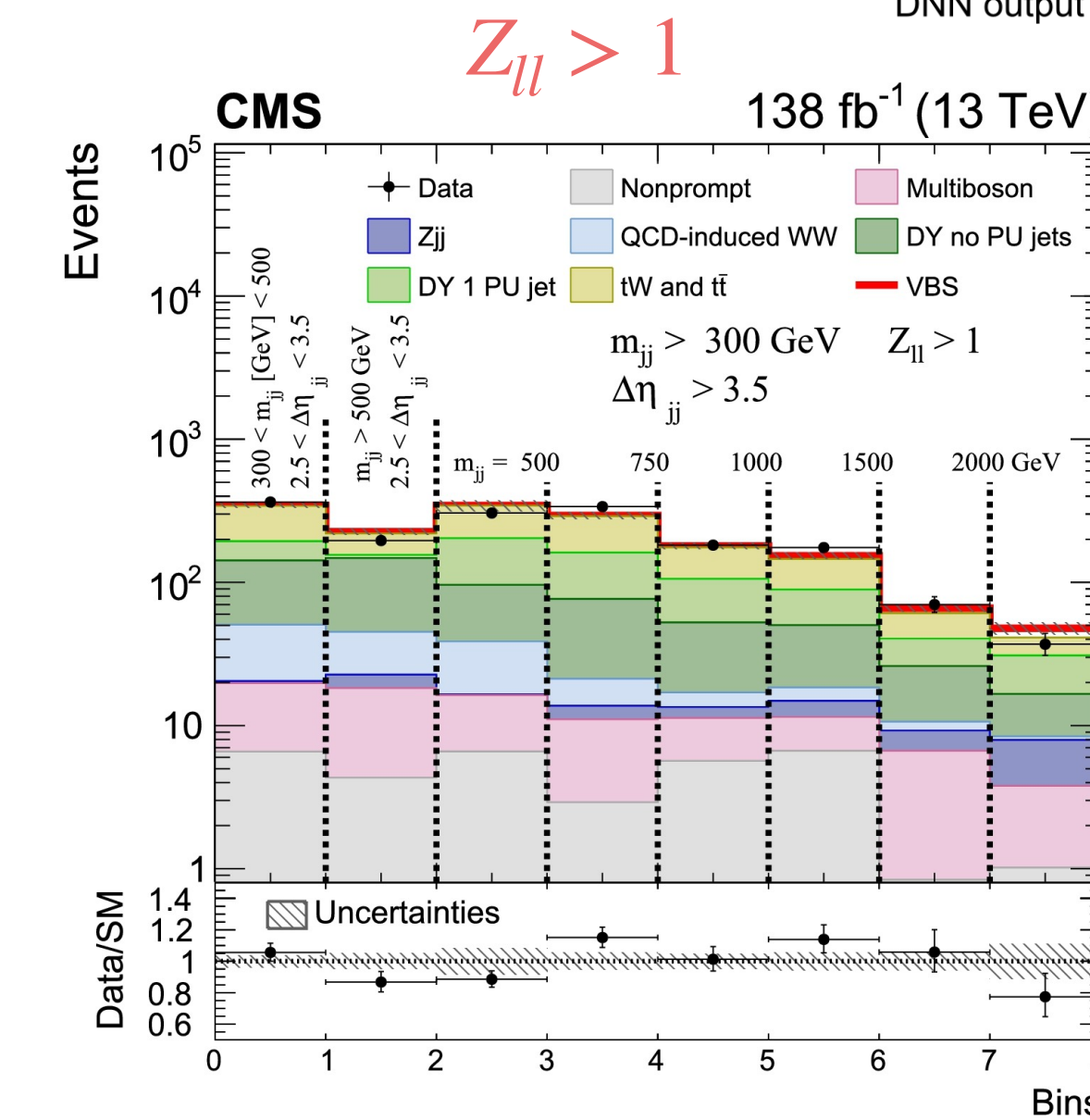
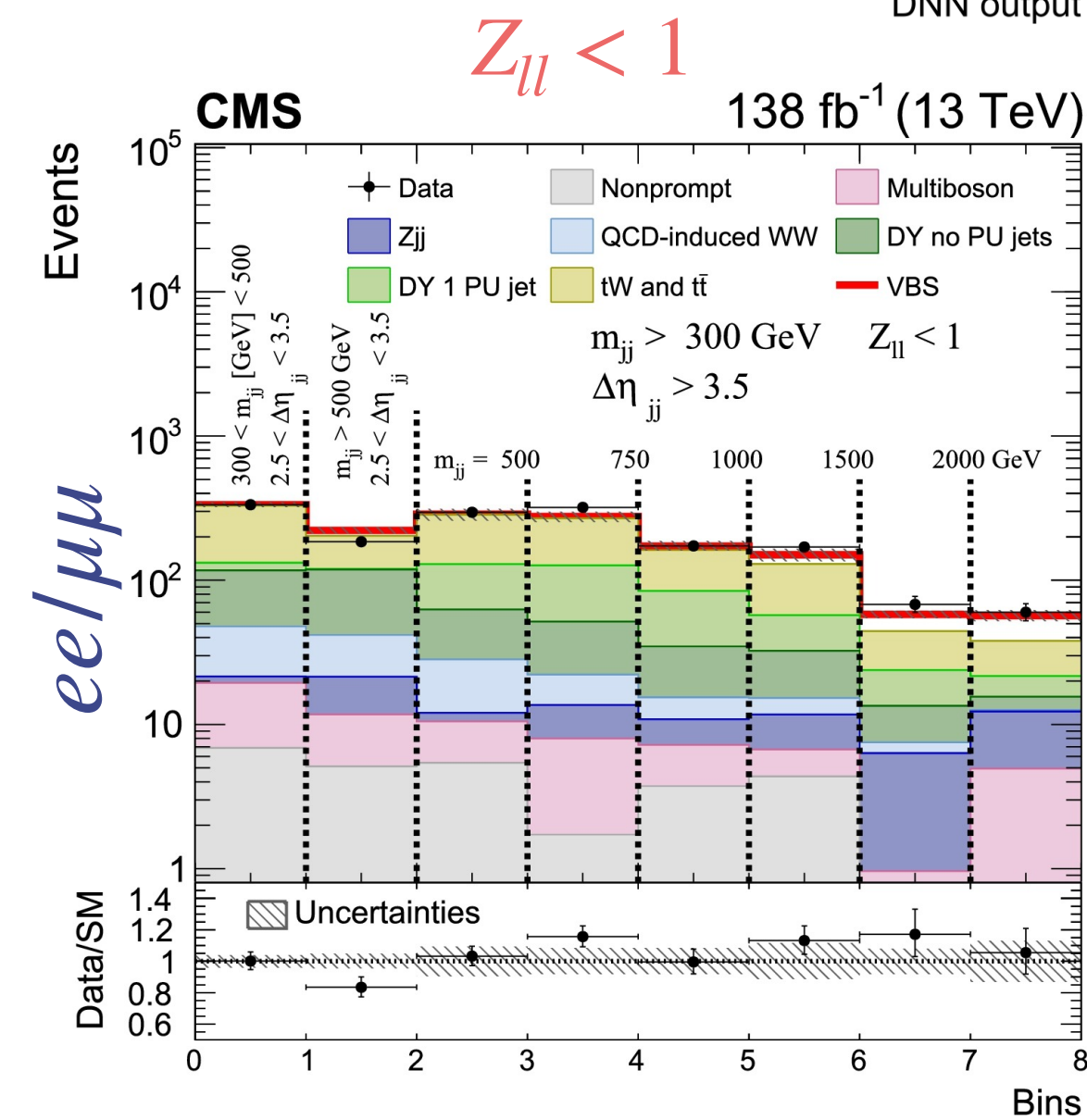
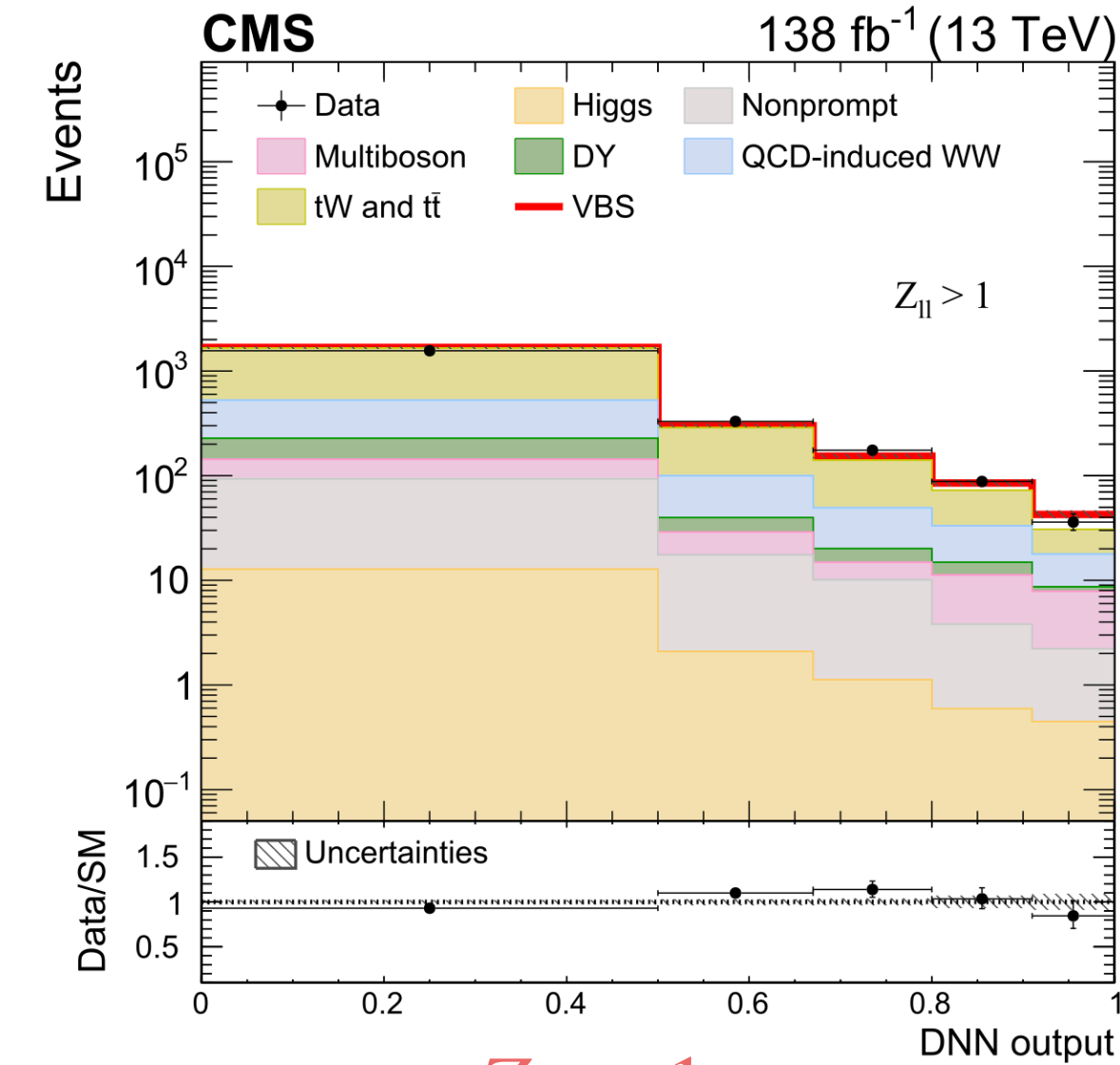
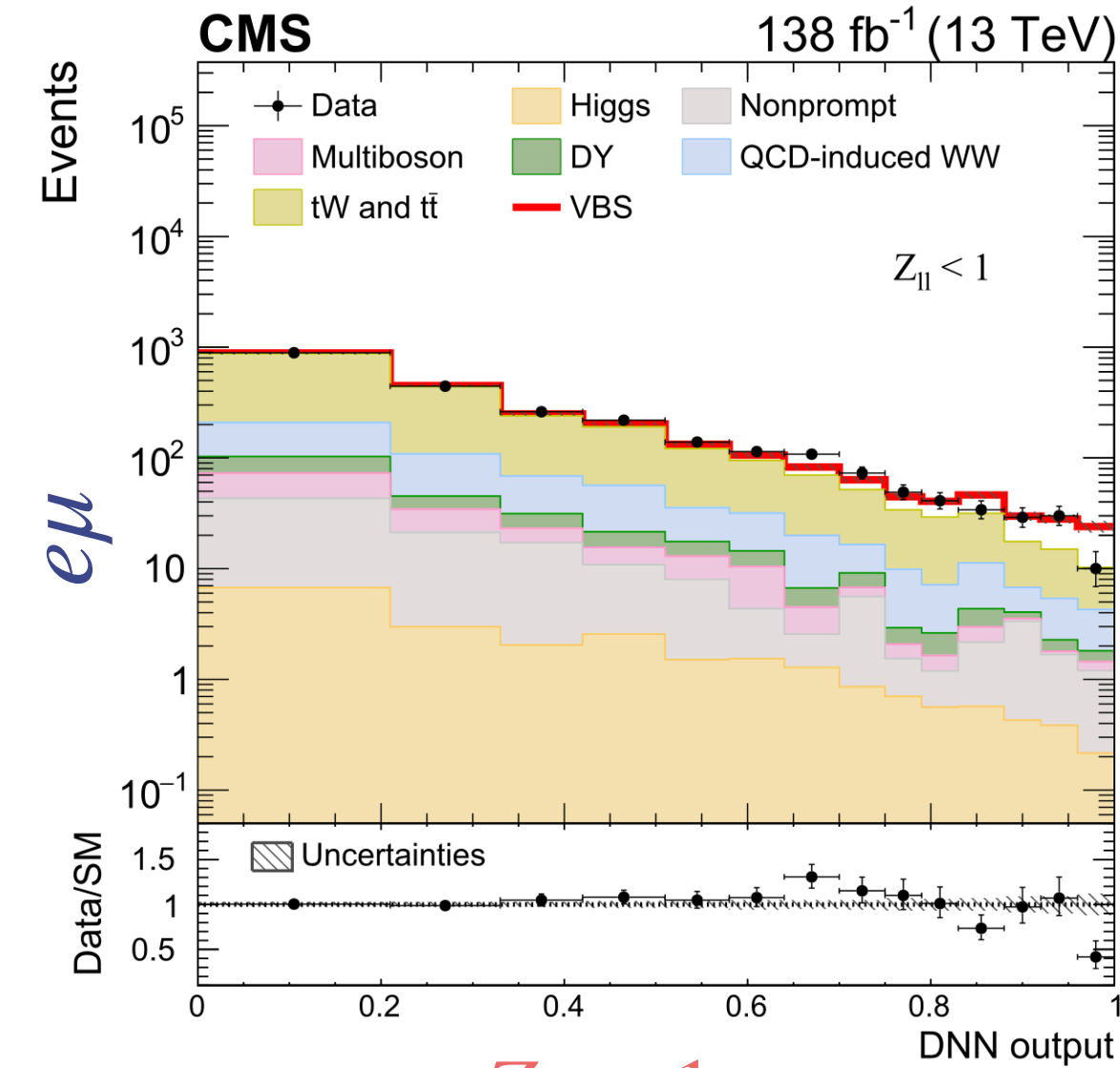


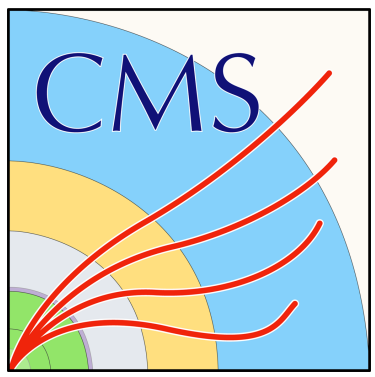
Opposite-sign WW VBS

EW osWW production cross section is measured in two different fiducial volumes:

- Inclusive volume (no tau veto, outgoing partons with $p_T > 10$ GeV and $m_{qq'} > 100$ GeV): $\sigma_{obs} = 99 \pm 20$ fb, $\sigma_{exp} = 89 \pm 5$ (scale) fb
- Fiducial volume similar to reconstructed SR: $\sigma_{obs} = 10.2 \pm 2.0$ fb, $\sigma_{exp} = 9.1 \pm 0.6$ (scale) fb

Objects	Requirements
	$e\mu, ee, \mu\mu$ (not from τ decay), opposite charge
	$p_T^{\text{dressed } \ell} = p_T^\ell + \sum_i p_T^{\gamma_i}$ if $\Delta R(\ell, \gamma_i) < 0.1$
Leptons	$p_T^{\ell_1} > 25$ GeV, $p_T^{\ell_2} > 13$ GeV, $p_T^{\ell_3} < 10$ GeV
	$ \eta < 2.5$
	$p_T^{\ell\ell} > 30$ GeV, $m_{\ell\ell} > 50$ GeV
	$p_T^j > 30$ GeV
	$\Delta R(j, \ell) > 0.4$
Jets	At least 2 jets, no b jets
	$ \eta < 4.7$
	$m_{jj} > 300$ GeV, $ \Delta\eta_{jj} > 2.5$
p_T^{miss}	$p_T^{\text{miss}} > 20$ GeV





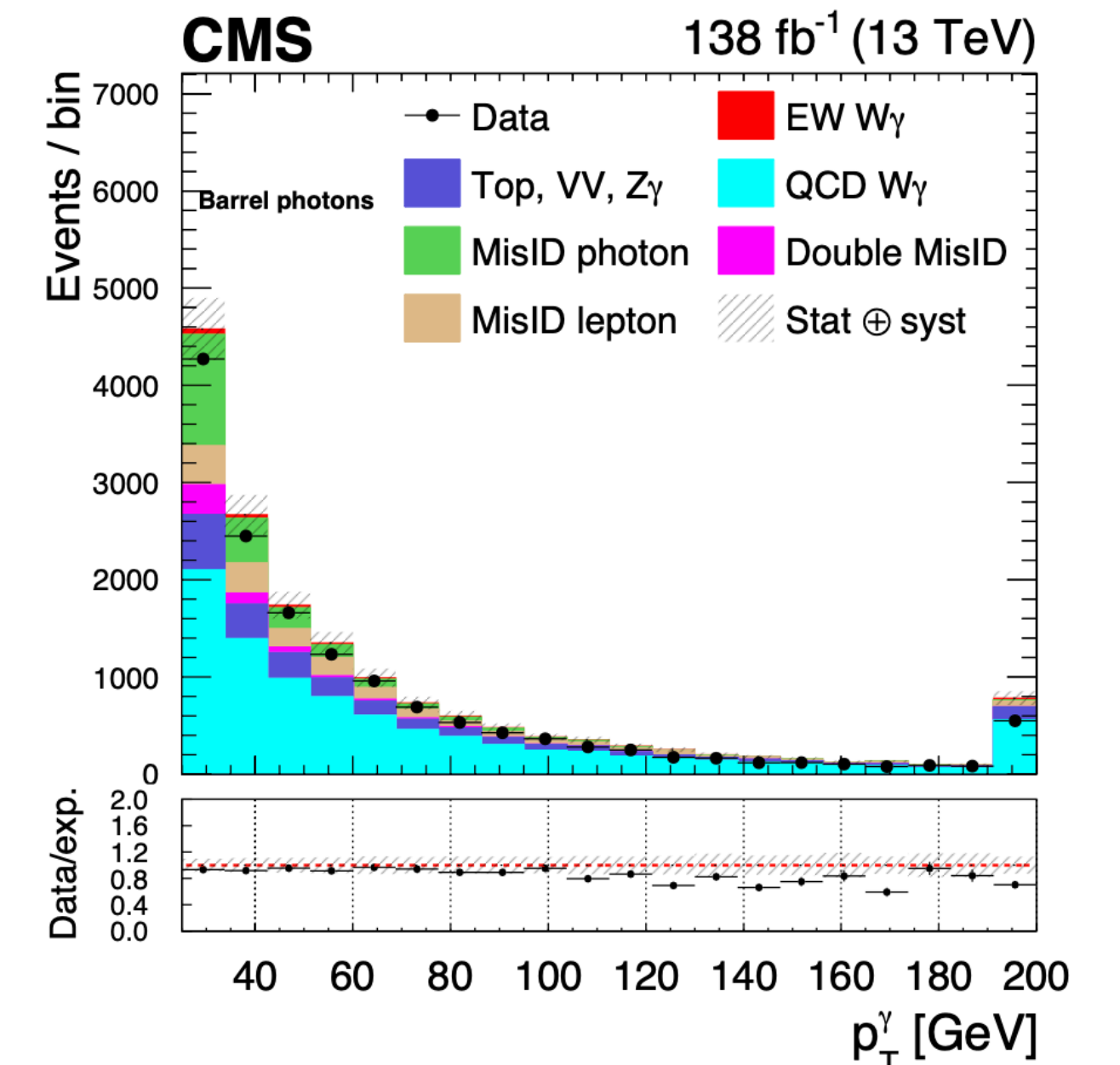
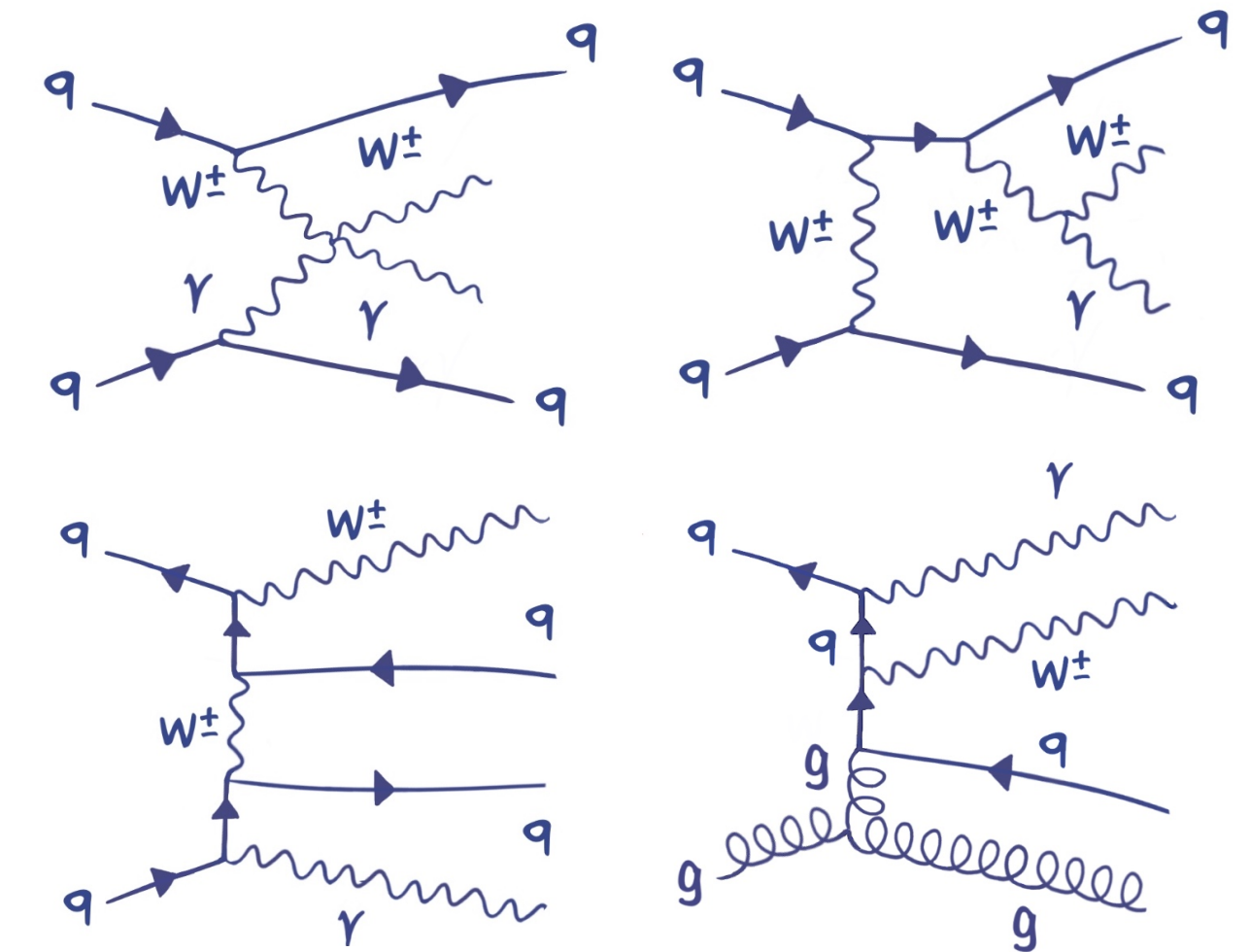
EWK production of $W\gamma + 2\text{jets}$

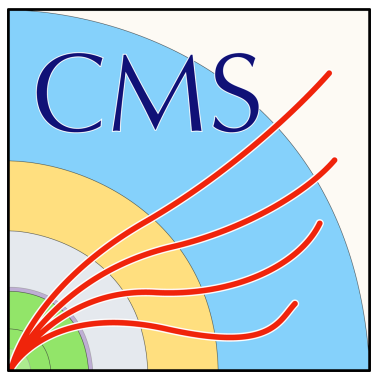
EWK production of W, γ and two jets, with W boson decaying in the leptonic channel.

Main background sources are:

- $W + \text{jets}$
- Top quark processes with jet misidentified as photon
- Top, $VV, Z\gamma$

Scale factors for non-prompt photons are extrapolated in a loose- γ Control Region and are applied in the Signal Region. Discrimination relies on the **photon $\sigma_{\eta\eta}$** , an observable that quantifies the lateral extension of the shower.



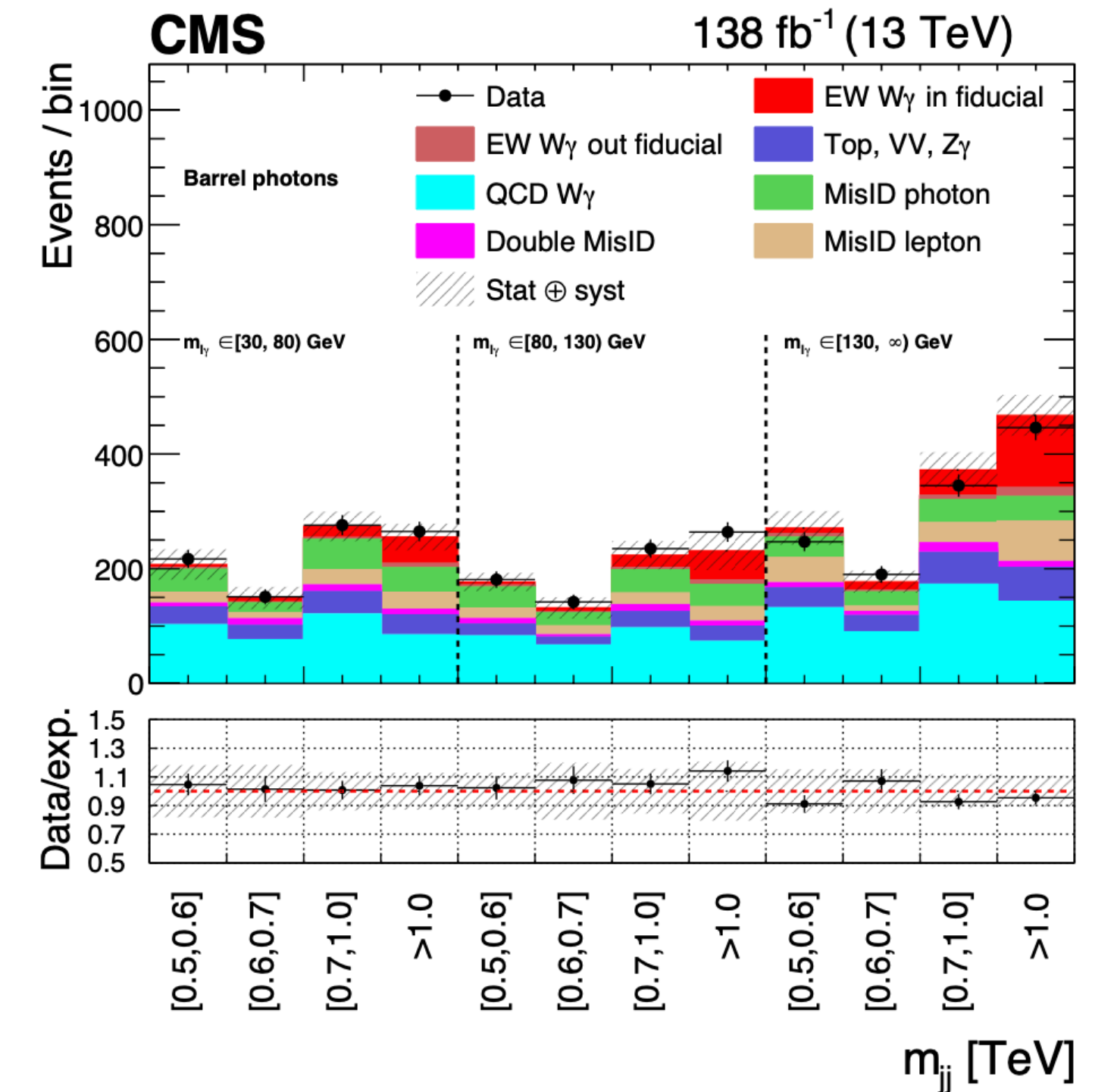


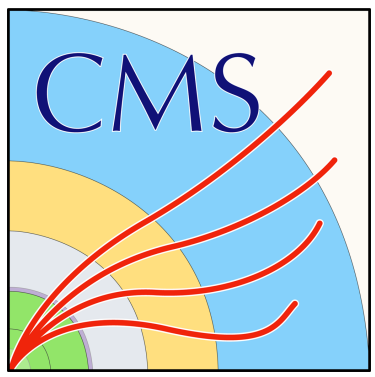
EWK production of $W\gamma + 2\text{jets}$

- Measurement of EW $W\gamma$ production rate is extracted using a binned likelihood fit to a 2D distribution in $m_{l\gamma}$ and m_{jj} . The observed (expected) significance is **6.0 (6.8) σ** .
- The purely EW ($\mu_{\text{QCD}} = 1$) and EW+QCD W fiducial cross section is measured in a fiducial region as $\sigma^{\text{fid}} = \sigma_g \hat{\mu} \alpha$, where σ_g is the cross section calculated with MadGraph5 at LO in QCD.

Signal	$\mu = \sigma_{\text{OBS}}/\sigma_{\text{SM}}$	Cross Section [fb]
EWK $W\gamma$	$0.88^{+0.19}_{-0.18}$	$23.5 \pm 2.8(\text{stat})^{+1.9}_{-1.7}(\text{th})^{+3.5}_{-3.4}(\text{stat})$
EWK+QCD $W\gamma$	$0.98^{+0.12}_{-0.11}$	$113 \pm 2.0(\text{stat})^{+2.5}_{-2.3}(\text{th})^{+13}_{-13}(\text{stat})$

All the results are in agreement with SM predictions.



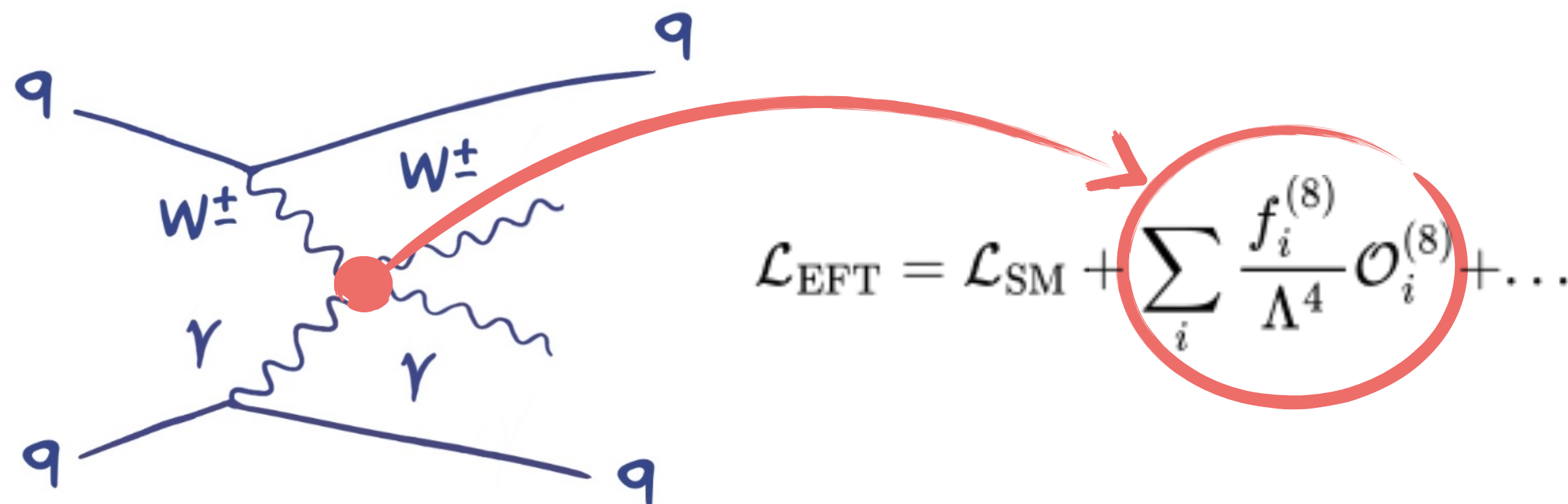


EWK production of $W\gamma + 2\text{jets}$

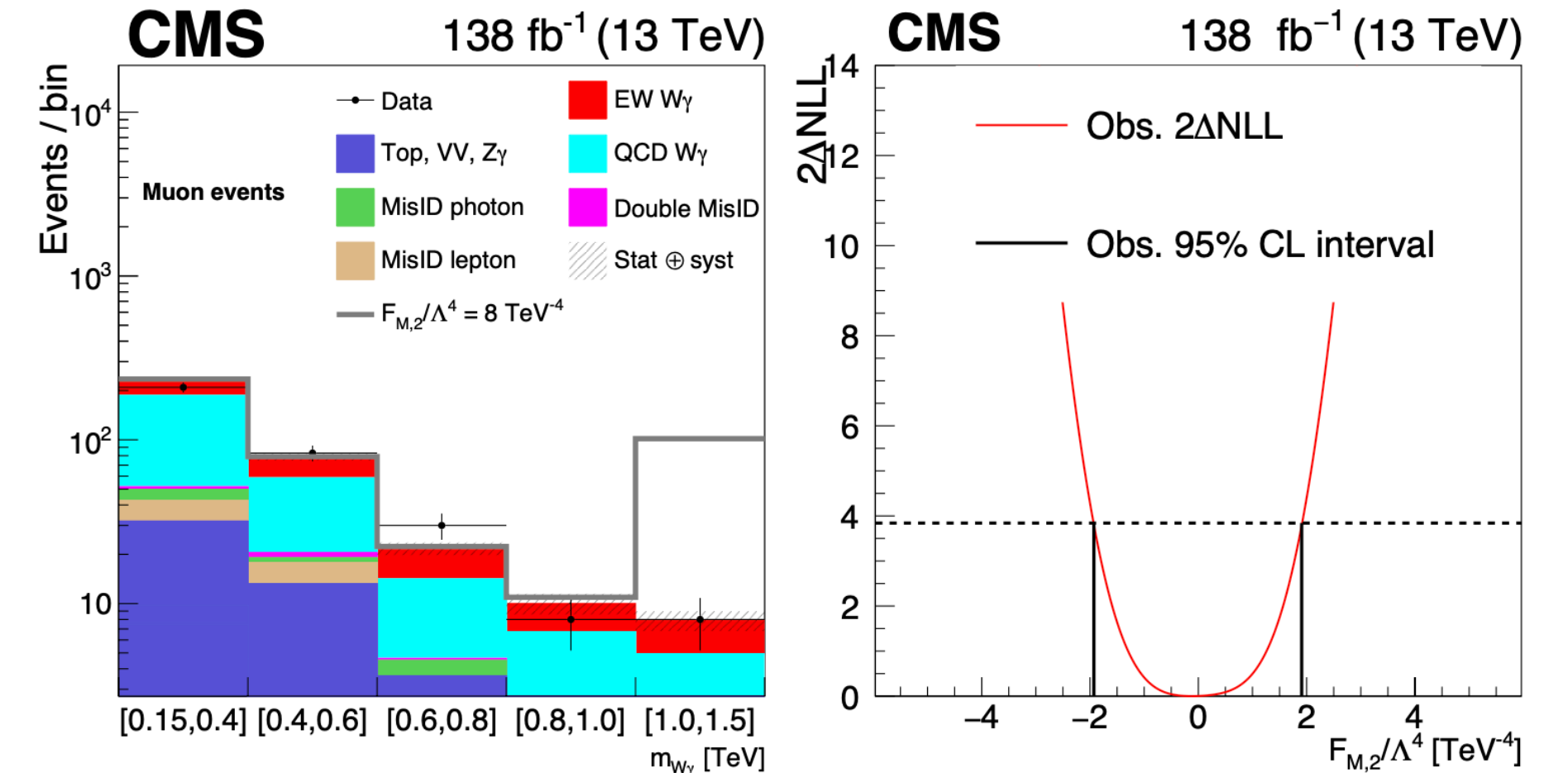
EFT interpretation

Constraints on anomalous quartic gauge couplings for EFT@dim8 operators are extracted @95%CL via likelihood scan approach.

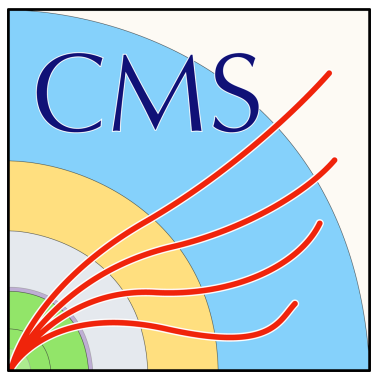
- One operator at the time (other EFT couplings set to zero)
- $m_{W\gamma}$ distribution built in the VBS phase-space region to enhance sensitivity to aQGC



Most stringent limits to date on several aQGC parameters.

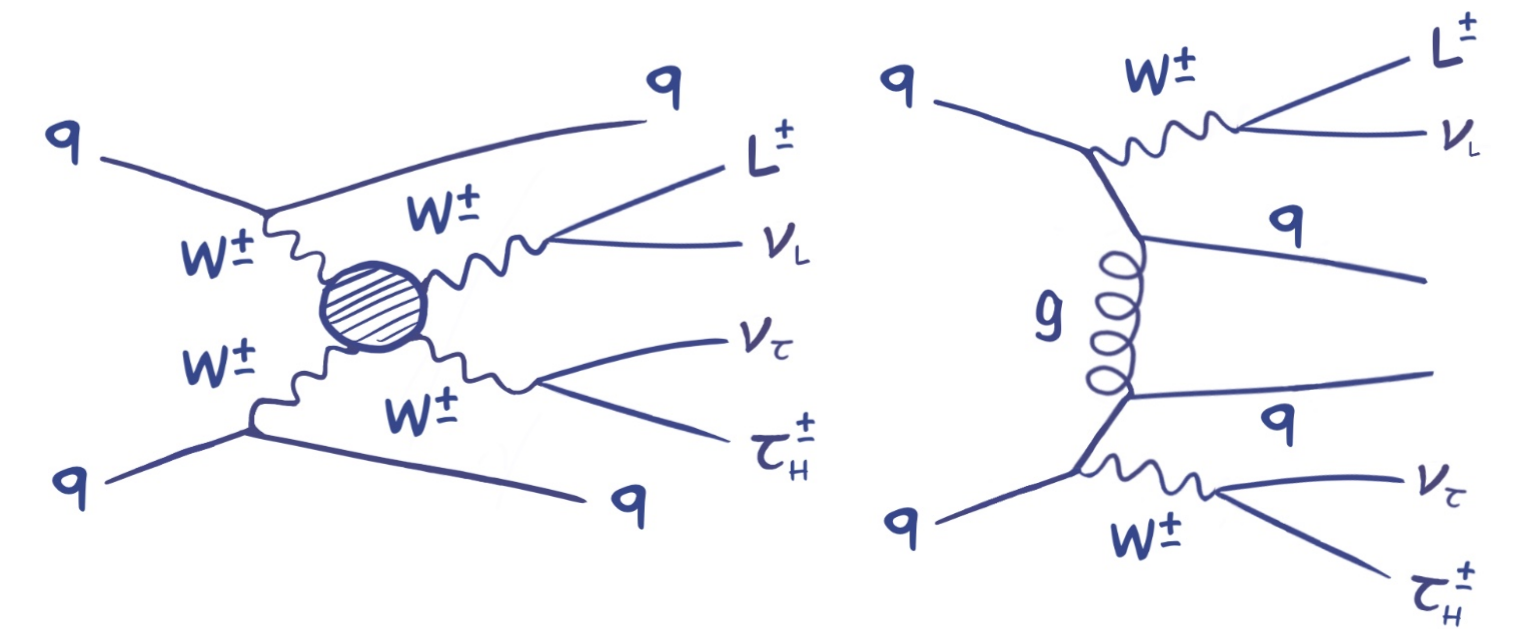


Expected limit	Observed limit	U_{bound}
$-5.1 < f_{M,0}/\Lambda^4 < 5.1$	$-5.6 < f_{M,0}/\Lambda^4 < 5.5$	1.7
$-7.1 < f_{M,1}/\Lambda^4 < 7.4$	$-7.8 < f_{M,1}/\Lambda^4 < 8.1$	2.1
$-1.8 < f_{M,2}/\Lambda^4 < 1.8$	$-1.9 < f_{M,2}/\Lambda^4 < 1.9$	2.0
$-2.5 < f_{M,3}/\Lambda^4 < 2.5$	$-2.7 < f_{M,3}/\Lambda^4 < 2.7$	2.7
$-3.3 < f_{M,4}/\Lambda^4 < 3.3$	$-3.7 < f_{M,4}/\Lambda^4 < 3.6$	2.3
$-3.4 < f_{M,5}/\Lambda^4 < 3.6$	$-3.9 < f_{M,5}/\Lambda^4 < 3.9$	2.7
$-13 < f_{M,7}/\Lambda^4 < 13$	$-14 < f_{M,7}/\Lambda^4 < 14$	2.2
$-0.43 < f_{T,0}/\Lambda^4 < 0.51$	$-0.47 < f_{T,0}/\Lambda^4 < 0.51$	1.9
$-0.27 < f_{T,1}/\Lambda^4 < 0.31$	$-0.31 < f_{T,1}/\Lambda^4 < 0.34$	2.5
$-0.72 < f_{T,2}/\Lambda^4 < 0.92$	$-0.85 < f_{T,2}/\Lambda^4 < 1.0$	2.3
$-0.29 < f_{T,5}/\Lambda^4 < 0.31$	$-0.31 < f_{T,5}/\Lambda^4 < 0.33$	2.6
$-0.23 < f_{T,6}/\Lambda^4 < 0.25$	$-0.25 < f_{T,6}/\Lambda^4 < 0.27$	2.9
$-0.60 < f_{T,7}/\Lambda^4 < 0.68$	$-0.67 < f_{T,7}/\Lambda^4 < 0.73$	3.1



Same-sign WW with hadronic tau

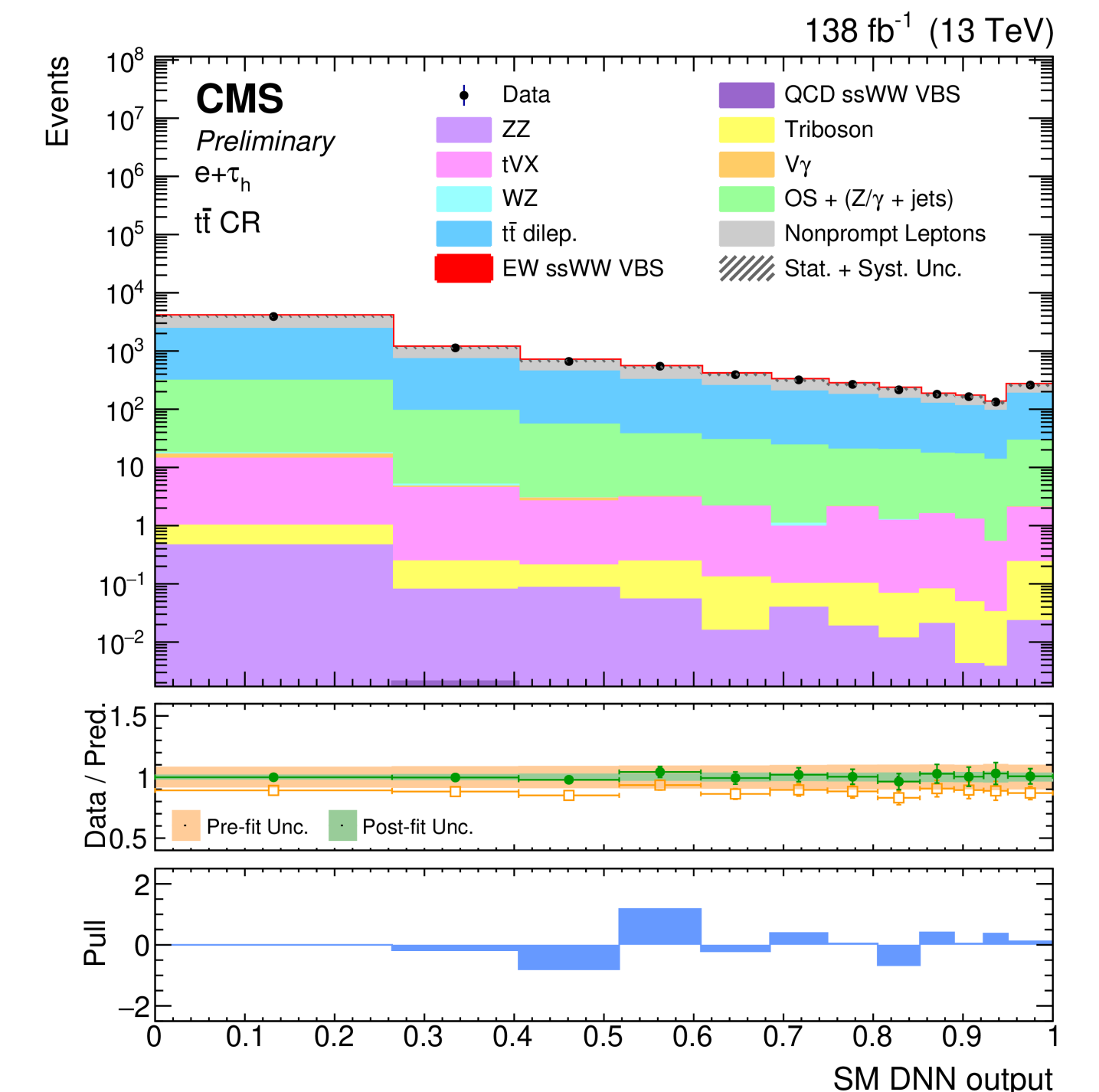
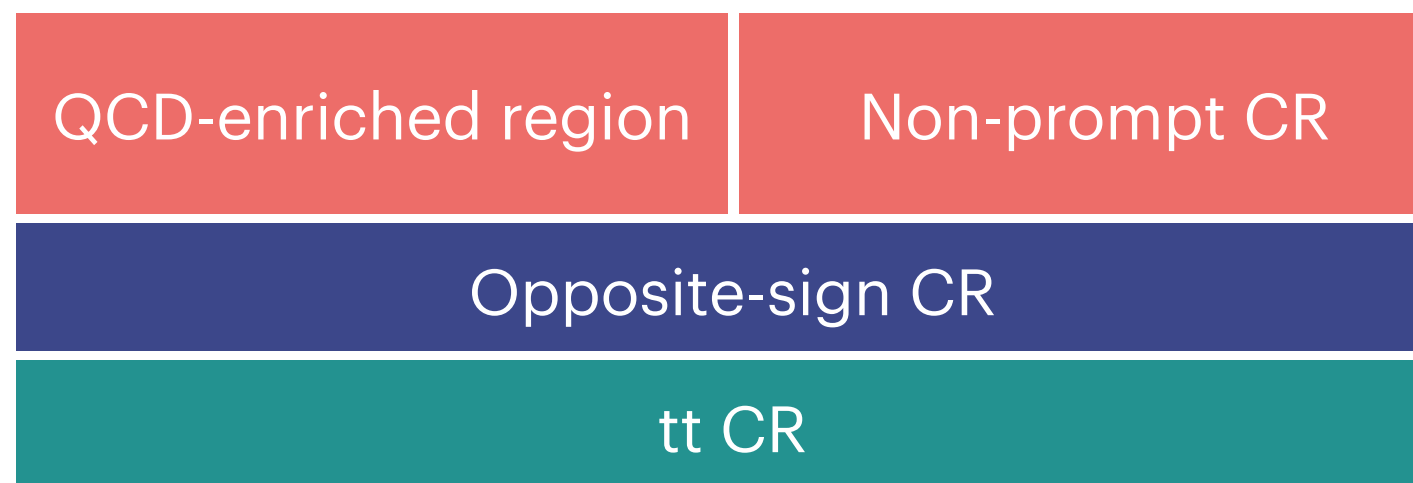
EWK production of same-sign W boson pairs with a hadronically decaying τ in the final state.

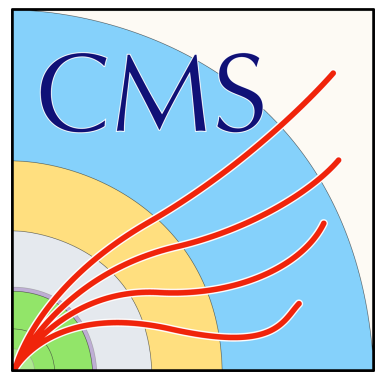


Same-sign WW is the golden channel for VBS studies due to good separation between EWK and QCD components and full availability of NLO corrections.

Main backgrounds sources in SR are:

- events containing **nonprompt** leptons from QCD-mediated multijet, W+jets, hadr. and semi-leptonic tt (**95%**)
- $Z/\gamma^* + \text{jets}$ (2%)
- Dileptonic tt production (1%)





Same-sign WW with hadronic tau

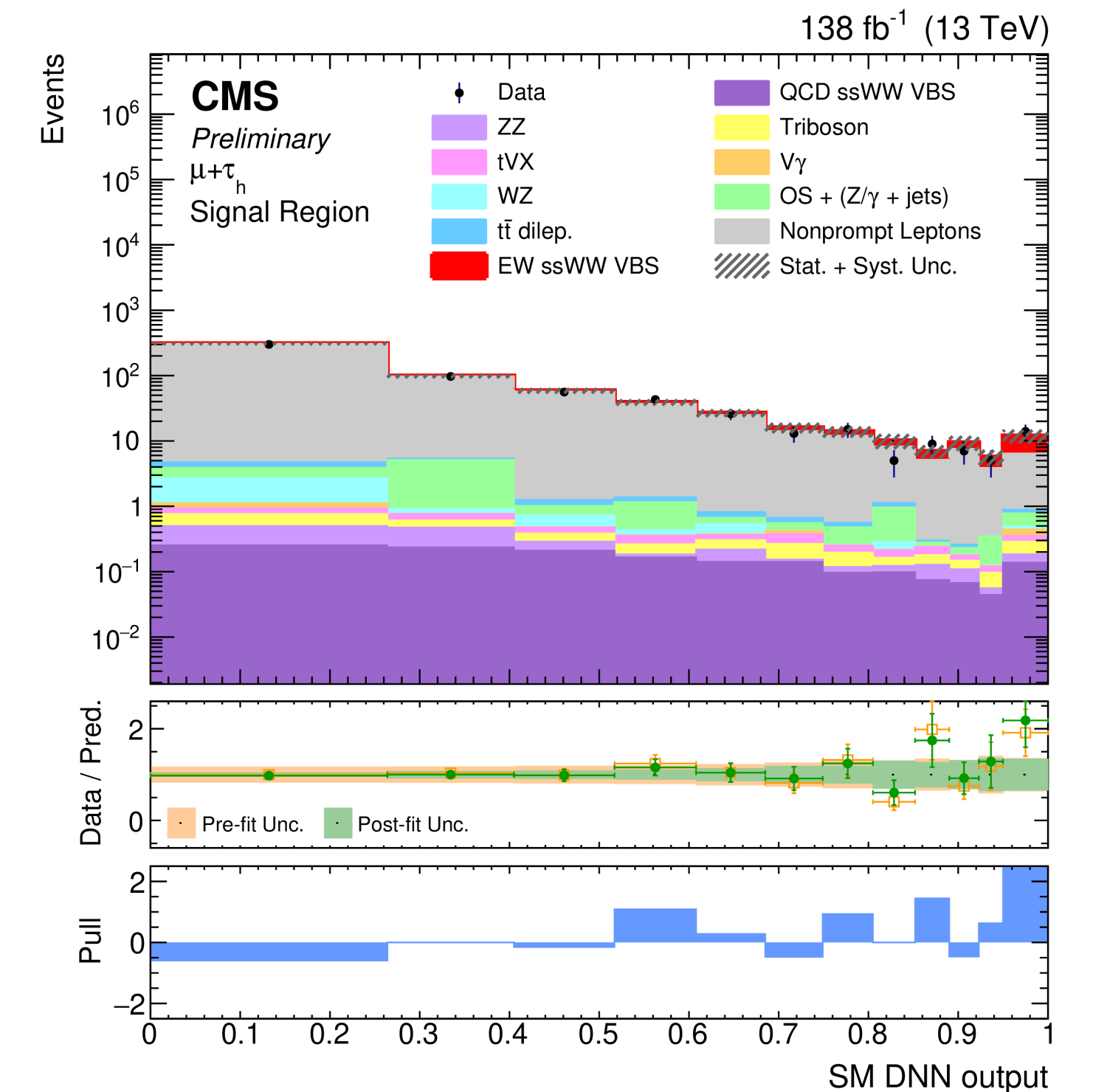
- 9 significant observables are combined in a single ML discriminator (DNN) to separate signal and background. Two dedicated transverse masses are defined:

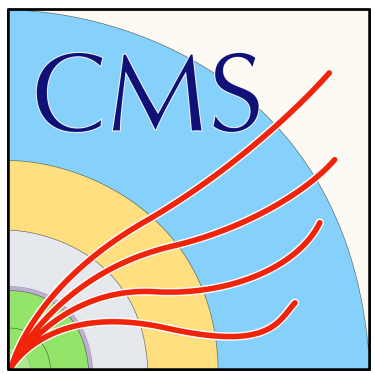
$$M_{1T}^2 = \left(\sqrt{M_{\tau l}^2 + p_T^{\tau l 2} + p_T^{\text{miss}} \right)^2 - |\vec{p}_T^{\tau l} + \vec{p}_T|^2$$

$$M_{o1}^2 = \left(p_T^\tau + p_T^l + p_T \right)^2 - |\vec{p}_T^{\tau l} + \vec{p}_T^l + \vec{p}_T|^2$$

- Measurement of purely EW ssWW signal strength ($\mu_{\text{QCD}} = 1$) and EWK+QCD ssWW signal strength:

Signal	$\mu = \sigma_{\text{OBS}}/\sigma_{\text{SM}}$	Significance [σ]
EWK ssWW	$1.44_{-0.56}^{+0.63}$	2.7 (1.9 exp)
EWK+QCD ssWW	$1.43_{-0.54}^{+0.60}$	2.9 (2.0 exp)



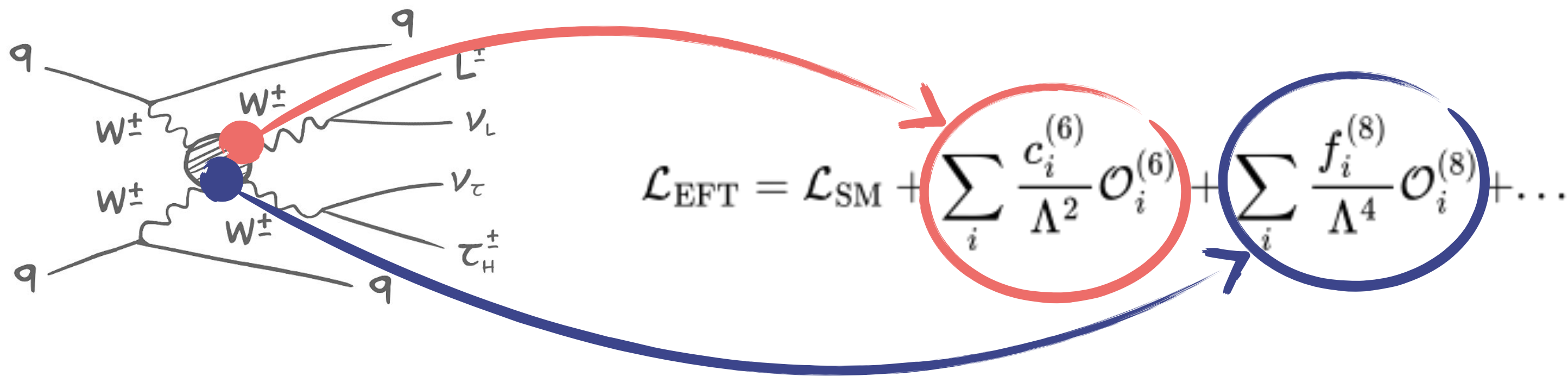


Same-sign WW with hadronic tau

EFT interpretation

Constraints on bosonic dim6 and dim8 EFT Wilson coefficients are derived via likelihood scan approach. Both 1D and 2D limits are extrapolated.

First analysis considering pairs of different dimension operators in 2D scan.



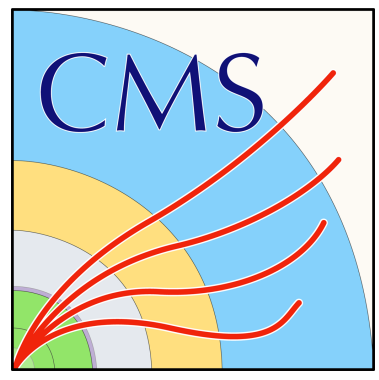
- 1D limits consider one operator at the time
- 2D limits couple operators that give similar contributions to the $WW \rightarrow WW$ scattering amplitude and that have a similar ratio between quadratic and linear terms.

dimension 6

$$\begin{aligned} \mathcal{O}_W &= \epsilon^{ijk} W_\mu^{\nu i} W_\nu^{\rho j} W_\rho^{\mu k} \\ \mathcal{O}_{\varphi\Box} &= (\varphi^\dagger \varphi) \Box (\varphi^\dagger \varphi) \\ \mathcal{O}_{\varphi D} &= (\varphi^\dagger D^\mu \varphi) * (\varphi^\dagger D_\mu \varphi) \\ \mathcal{O}_{\varphi W} &= \varphi^\dagger \varphi W_{\mu\nu}^i W^{\mu\nu i} \\ \mathcal{O}_{\varphi WB} &= \varphi^\dagger \tau^i \varphi W_{\mu\nu}^i B^{\mu\nu} \end{aligned}$$

dimension 8

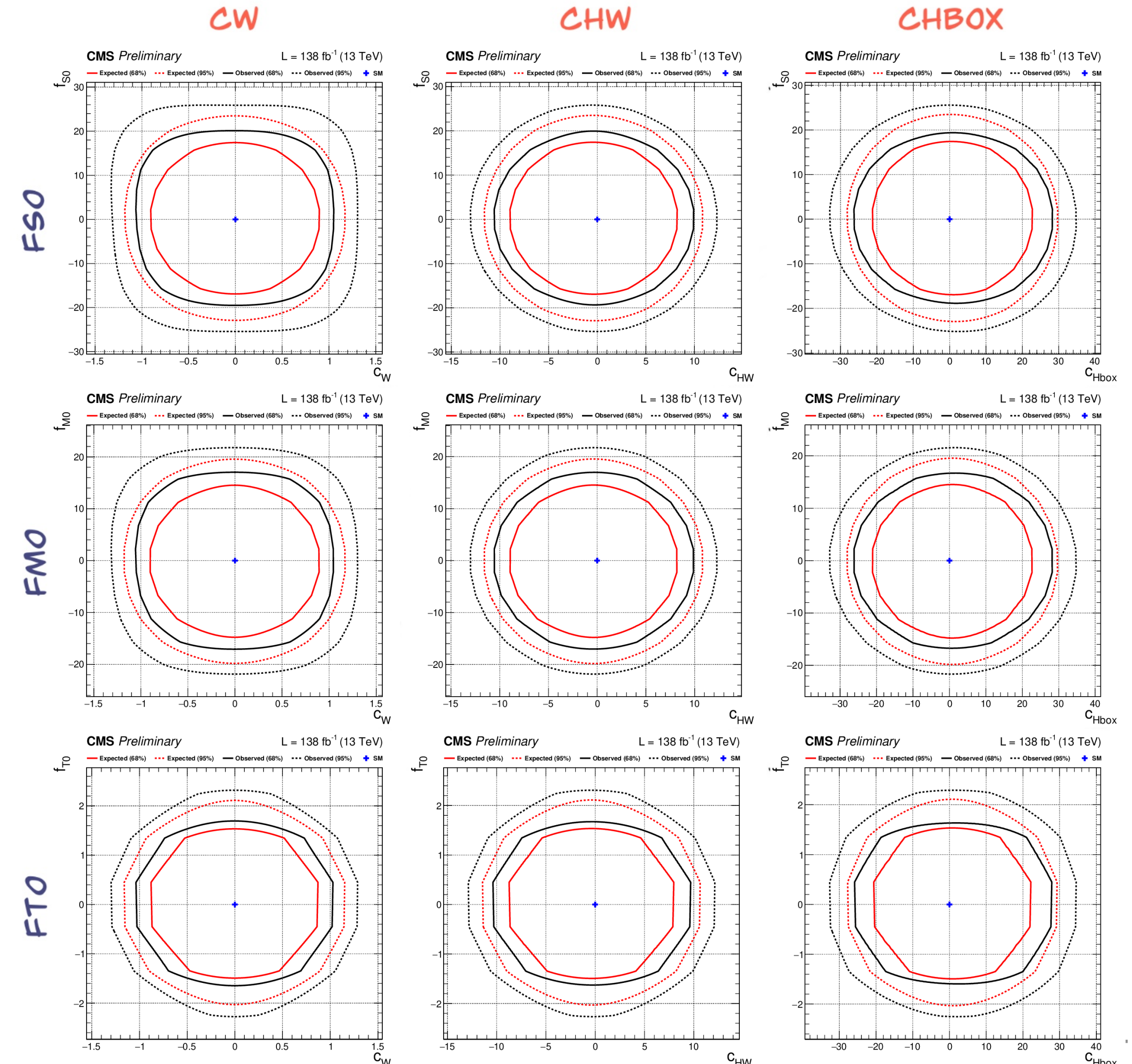
$$\begin{aligned} \mathcal{O}_{S,0} &= [(D_\mu \Phi)^\dagger D_\nu \Phi] \times [(D^\mu \Phi)^\dagger D^\nu \Phi] \\ \mathcal{O}_{S,1} &= [(D_\mu \Phi)^\dagger D^\mu \Phi] \times [(D_\nu \Phi)^\dagger D^\nu \Phi] \\ \mathcal{O}_{S,2} &= [(D_\mu \Phi)^\dagger D_\nu \Phi] \times [(D^\nu \Phi)^\dagger D^\mu \Phi] \\ \mathcal{O}_{M,0} &= \text{Tr}[\hat{W}_{\mu\nu} \hat{W}^{\mu\nu}] \times [(D_\beta \Phi)^\dagger D^\beta \Phi] \\ \mathcal{O}_{M,1} &= \text{Tr}[\hat{W}_{\mu\nu} \hat{W}^{\nu\beta}] \times [(D_\beta \Phi)^\dagger D^\mu \Phi] \\ \mathcal{O}_{M,7} &= [(D_\mu \Phi)^\dagger \hat{W}_{\beta\nu} D^\nu \Phi] \\ \mathcal{O}_{T,0} &= \text{Tr}[\hat{W}_{\mu\nu} \hat{W}^{\mu\nu}] \times \text{Tr}[\hat{W}_{\alpha\beta} \hat{W}^{\alpha\beta}] \\ \mathcal{O}_{T,1} &= \text{Tr}[\hat{W}_{\alpha\nu} \hat{W}^{\mu\beta}] \times \text{Tr}[\hat{W}_{\mu\beta} \hat{W}^{\alpha\nu}] \\ \mathcal{O}_{T,2} &= \text{Tr}[\hat{W}_{\alpha\mu} \hat{W}^{\mu\beta}] \times \text{Tr}[\hat{W}_{\beta\nu} \hat{W}^{\nu\alpha}] \end{aligned}$$

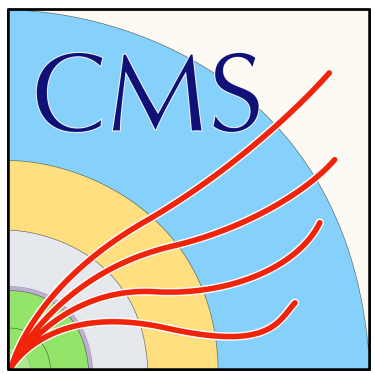


Same-sign WW with hadronic tau

EFT interpretation

Wilson coefficient	68% CL interval(s)		95% CL interval	
	Expected	Observed	Expected	Observed
$c_{ll}^{(1)}$	$[-12.9, -8.03] \cup [-2.95, 1.91]$	$[-11.6, 0.045]$	$[-14.6, 3.53]$	$[-13.5, 2.11]$
$c_{qq}^{(1)}$	$[-0.501, 0.576]$	$[-0.341, 0.416]$	$[-0.742, 0.818]$	$[-0.605, 0.681]$
c_W	$[-0.681, 0.669]$	$[-0.513, 0.481]$	$[-0.987, 0.974]$	$[-0.842, 0.818]$
c_{HW}	$[-7.00, 6.09]$	$[-5.48, 4.31]$	$[-9.99, 9.05]$	$[-8.68, 7.60]$
c_{HWB}	$[-41.7, 69.6]$	$[30.7, 89.2]$	$[-66.6, 96.4]$	$[-49.7, 110]$
$c_{H\Box}$	$[-16.6, 18.1]$	$[-12.0, 14.0]$	$[-24.7, 26.3]$	$[-20.9, 22.7]$
c_{HD}	$[-24.6, 34.7]$	$[-15.3, 31.5]$	$[-38.2, 48.8]$	$[-31.4, 45.5]$
$c_{HI}^{(1)}$	$[-28.8, 29.9]$	$[-38.2, 39.5]$	$[-49.4, 49.7]$	$[-69.3, 68.3]$
$c_{HI}^{(3)}$	$[-1.43, 2.23] \cup [5.88, 9.54]$	$[-0.045, 8.58]$	$[-2.64, 10.8]$	$[-1.59, 9.94]$
$c_{Hq}^{(1)}$	$[-4.53, 4.42]$	$[-3.27, 3.44]$	$[-6.56, 6.44]$	$[-5.55, 5.60]$
$c_{Hq}^{(3)}$	$[-2.39, 1.37]$	$[-1.88, 0.705]$	$[-3.24, 2.16]$	$[-2.82, 1.61]$
f_{T0}	$[-1.02, 1.08]$	$[-0.774, 0.842]$	$[-1.52, 1.58]$	$[-1.32, 1.38]$
f_{T1}	$[-0.426, 0.480]$	$[-0.319, 0.381]$	$[-0.640, 0.695]$	$[-0.552, 0.613]$
f_{T2}	$[-1.15, 1.37]$	$[-0.851, 1.12]$	$[-1.75, 1.98]$	$[-1.51, 1.76]$
f_{M0}	$[-9.89, 9.74]$	$[-8.07, 7.70]$	$[-14.6, 14.5]$	$[-13.1, 12.8]$
f_{M1}	$[-12.5, 13.3]$	$[-9.54, 11.15]$	$[-18.7, 19.6]$	$[-16.4, 17.7]$
f_{M7}	$[-20.3, 19.2]$	$[-17.6, 15.3]$	$[-29.9, 28.8]$	$[-27.6, 25.8]$
f_{S0}	$[-11.6, 12.0]$	$[-9.60, 9.82]$	$[-17.4, 17.9]$	$[-15.9, 16.1]$
f_{S1}	$[-37.4, 38.8]$	$[-40.9, 41.3]$	$[-57.2, 58.6]$	$[-60.9, 61.8]$
f_{S2}	$[-37.4, 38.8]$	$[-40.9, 41.3]$	$[-57.2, 58.6]$	$[-60.9, 61.8]$





VBF measurements at CMS

Zjj production (Z to 2L)

Measurement of EWK production cross section of a Z boson in association with 2 jets at $\sqrt{s} = 13$ TeV (35.9 fb^{-1}) in l^+l^- decay channel.

Results in agreement with MC predictions:

$$\text{Meas.: } \sigma_{LO}(\text{EWK } lljj) = 534 \pm 20(\text{stat}) \pm 57(\text{syst}) \text{ fb}$$

$$\text{Exp.: } \sigma_{LO}^{MG5}(\text{EWK } lljj) = 543 \pm 24(\text{total}) \text{ fb}$$

Limits on bosonic dimension-6 EFT operators with no evidence of BSM physics.

Reference: [Eur. Phys. J. C \(2018\) 78:589](#)

Wjj production (W to LNu)

Measurement of EWK production cross section of a W boson in association with 2 jets at $\sqrt{s} = 13$ TeV (35.9 fb^{-1}) in $l\nu$ decay channel. Results in agreement with MC predictions:

$$\text{Meas.: } \sigma_{LO}(\text{EWK } l\nu jj) = 6.23 \pm 0.12(\text{stat}) \pm 0.61(\text{syst}) \text{ pb}$$

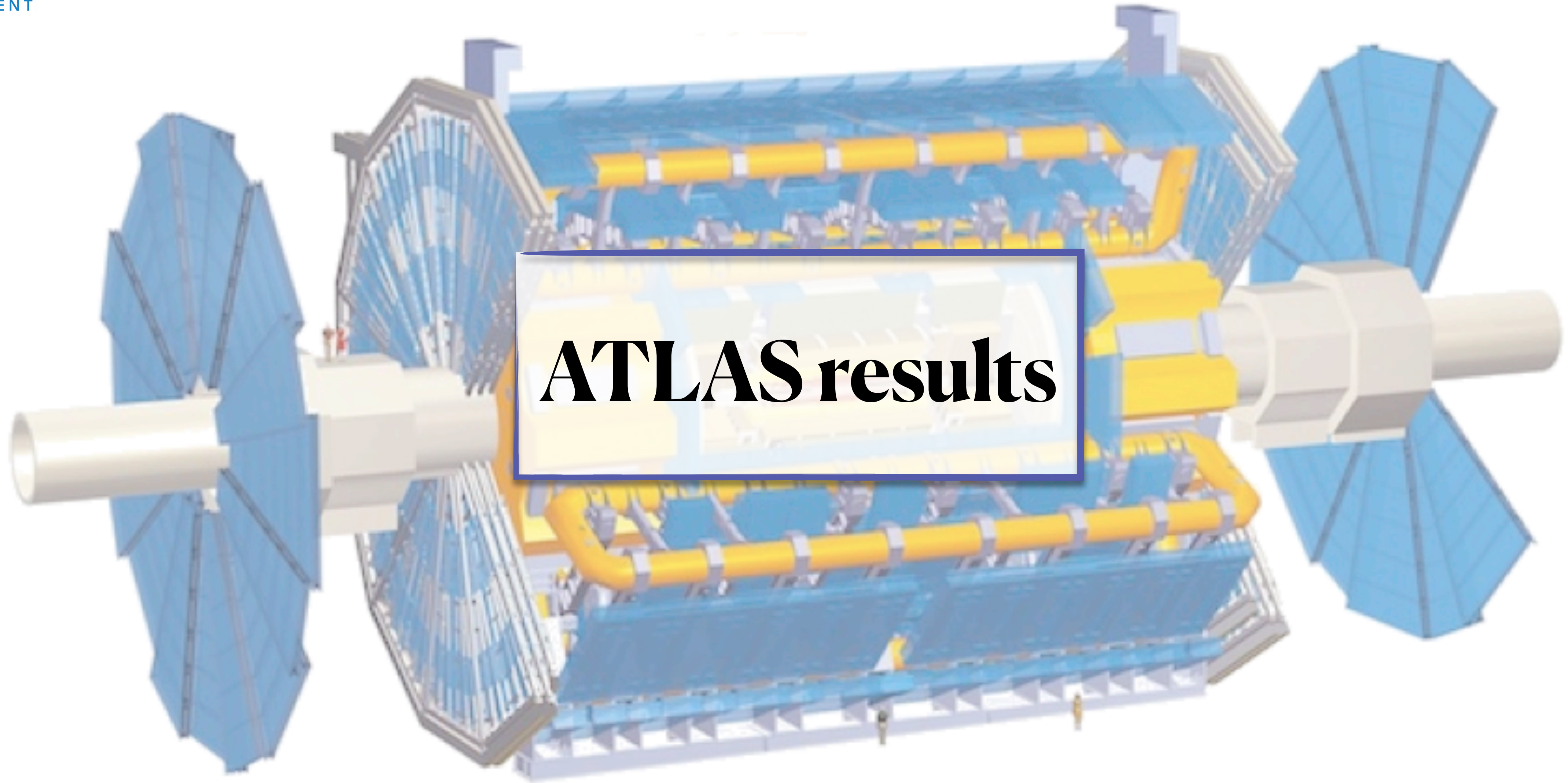
$$\text{Exp.: } \sigma_{LO}^{MG5}(\text{EWK } l\nu jj) = 6.81_{-0.06}^{+0.03}(\text{scale}) \pm 0.26(\text{PDF}) \text{ pb}$$

$$\text{Meas.: } \sigma_{NLO}(\text{EWK } l\nu jj) = 6.07 \pm 0.12(\text{stat}) \pm 0.57(\text{syst}) \text{ pb}$$

$$\text{Exp.: } \sigma_{NLO}^{MG5}(\text{EWK } l\nu jj) = 6.74_{-0.04}^{+0.02}(\text{scale}) \pm 0.26(\text{PDF}) \text{ pb}$$

Limits on bosonic dimension-6 EFT operators with no evidence of BSM physics.

Reference: [Eur. Phys. J. C \(2020\) 80:43](#)



ATLAS results

Opposite-sign WW VBS

EWK production of a pair of opposite-sign Ws and two jets, with both W decaying leptonically.

Tighter cuts wrt CMS to suppress W boson contributions from VBF Higgs production.

In order to reduce contribution from DY background, only $e\mu$ final state is considered. In Signal Region:

- 66% of bkg comes from **Top quark production** (dedicated CR, bkg constrained in simultaneous fit of SR and CR)
- 24% comes from **QCD osWW** (normalised with a scale factor coming from a fake- enriched region, effect of 15%-60% across the NN distribution)

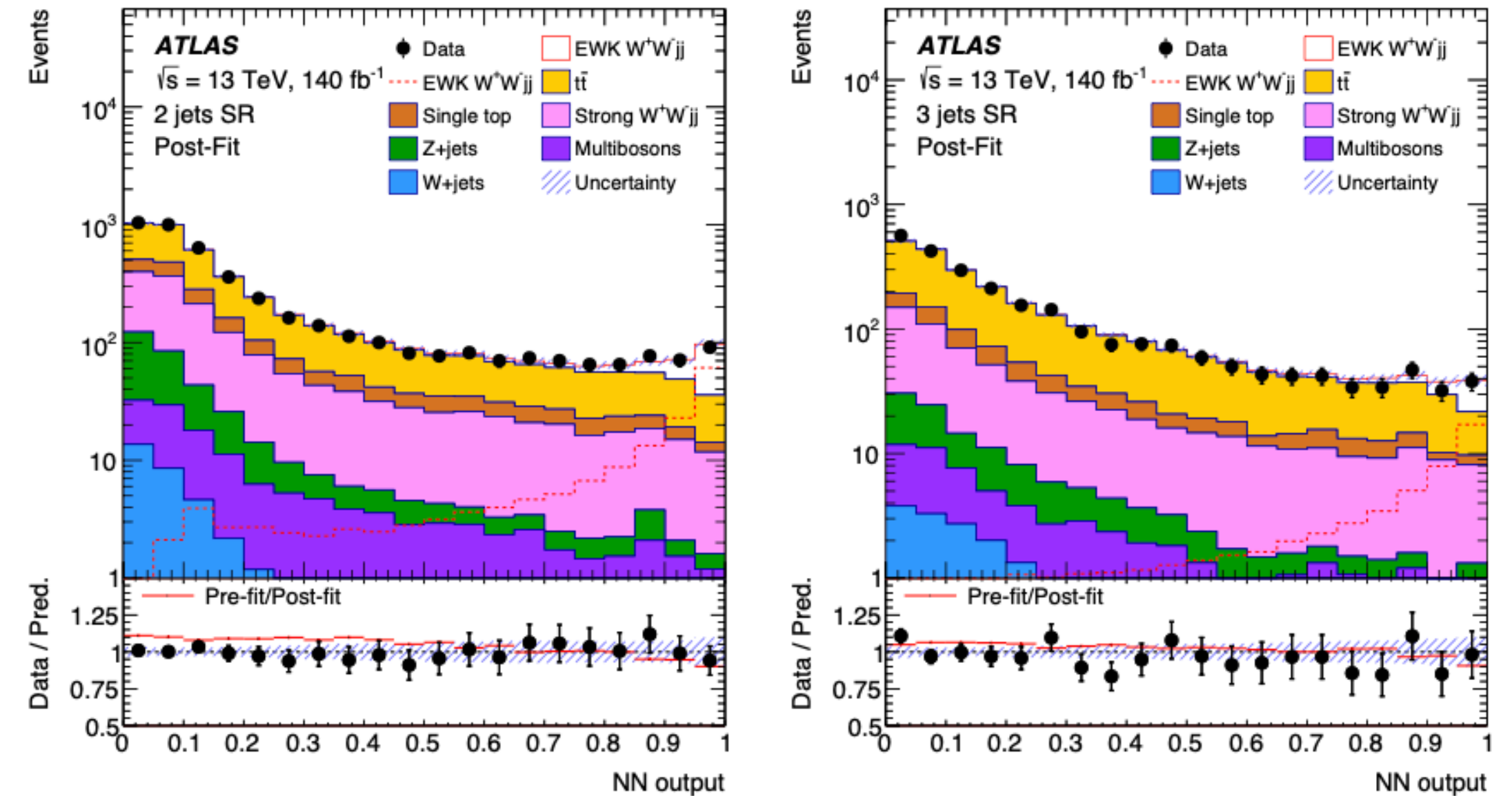
Category	Requirements
Leptons	$p_T > 27$ GeV $ \eta < 2.47$ excluding $1.37 < \eta < 1.52$ (electrons) $ \eta < 2.5$ (muons) Identification: Tight Isolation: Gradient (electrons), Tight_FixedRad (muons) $ d_0/\sigma_{d_0} < 5$ (electrons), $ d_0/\sigma_{d_0} < 3$ (muons) $ z_0 \sin \theta < 0.5$ mm
<i>b</i> -jets	$p_T > 20$ GeV and $ \eta < 2.5$ (DL1r <i>b</i> -tagging with 85% efficiency)
Jets	$p_T > 25$ GeV and $ \eta < 4.5$
Events	One electron and one muon with opposite electric charges No additional lepton with $p_T > 10$ GeV, Loose isolation, Tight/Medium (electrons) and Loose (muons) identification $m_{e\mu} > 80$ GeV $E_T^{\text{miss}} > 15$ GeV No <i>b</i> -jet Two or three jets $\zeta > 0.5$

Opposite-sign WW VBS

Profile likelihood fit is performed on the NN output observable simultaneously in the SR and the CR, with signal strength of osWW, top quark and QCD osWW bkg left as floating parameters.

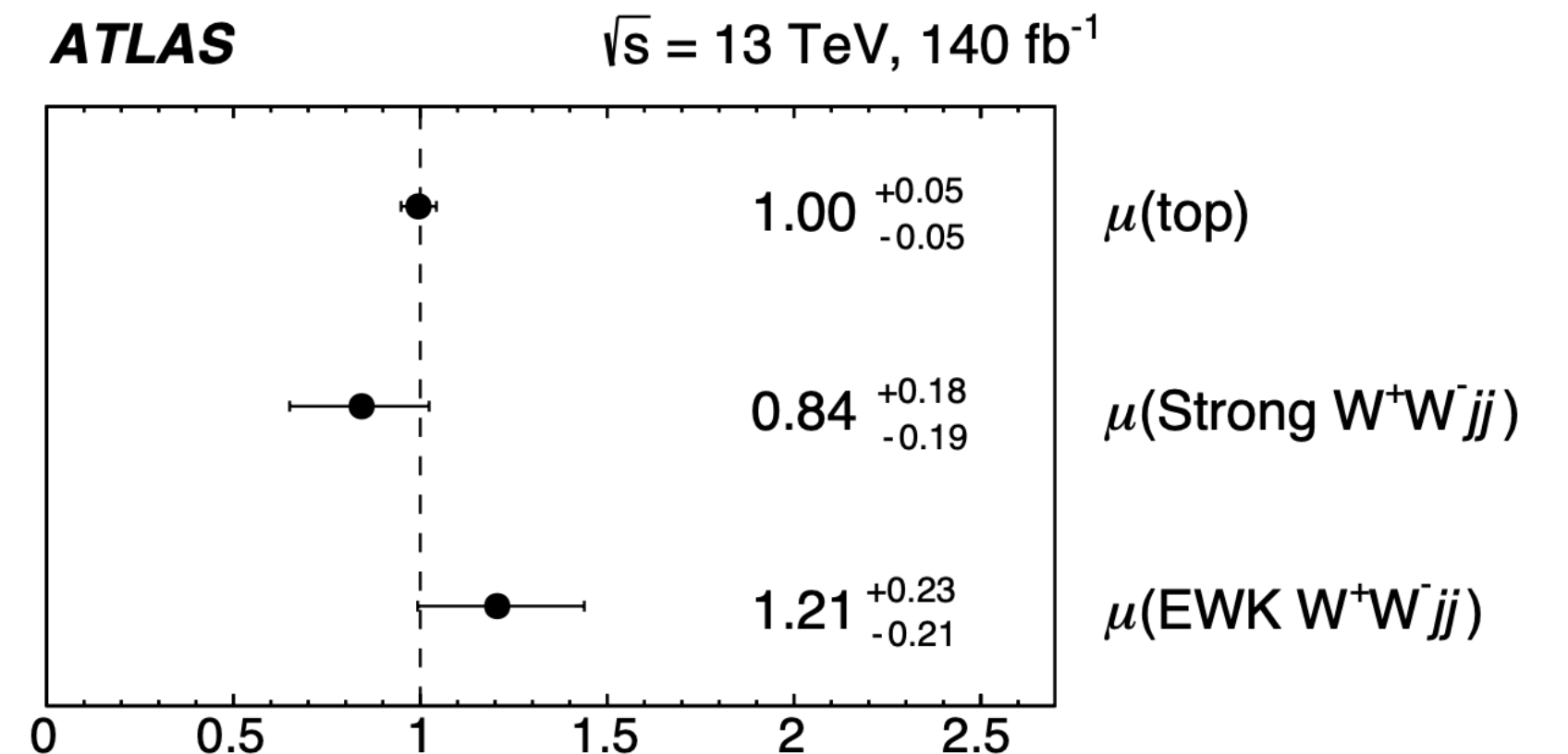
The observed (expected) significance is 7.1 (6.2) σ .

The fiducial cross-section for VBS osWW production is obtained by multiplying μ by the theoretical fiducial cross-section:



Signal	Measured xsec [fb]	Expected* xsec [fb]
EWK osWW	$2.65^{+0.49}_{-0.46}$	$2.20^{+0.14}_{-0.13}$

*POWHEG BOX v2



WZ VBS

EWK production of WZ plus two jets, with both vector bosons decaying leptonically.

Events with three leptons and moderate missing energy in final state are selected.

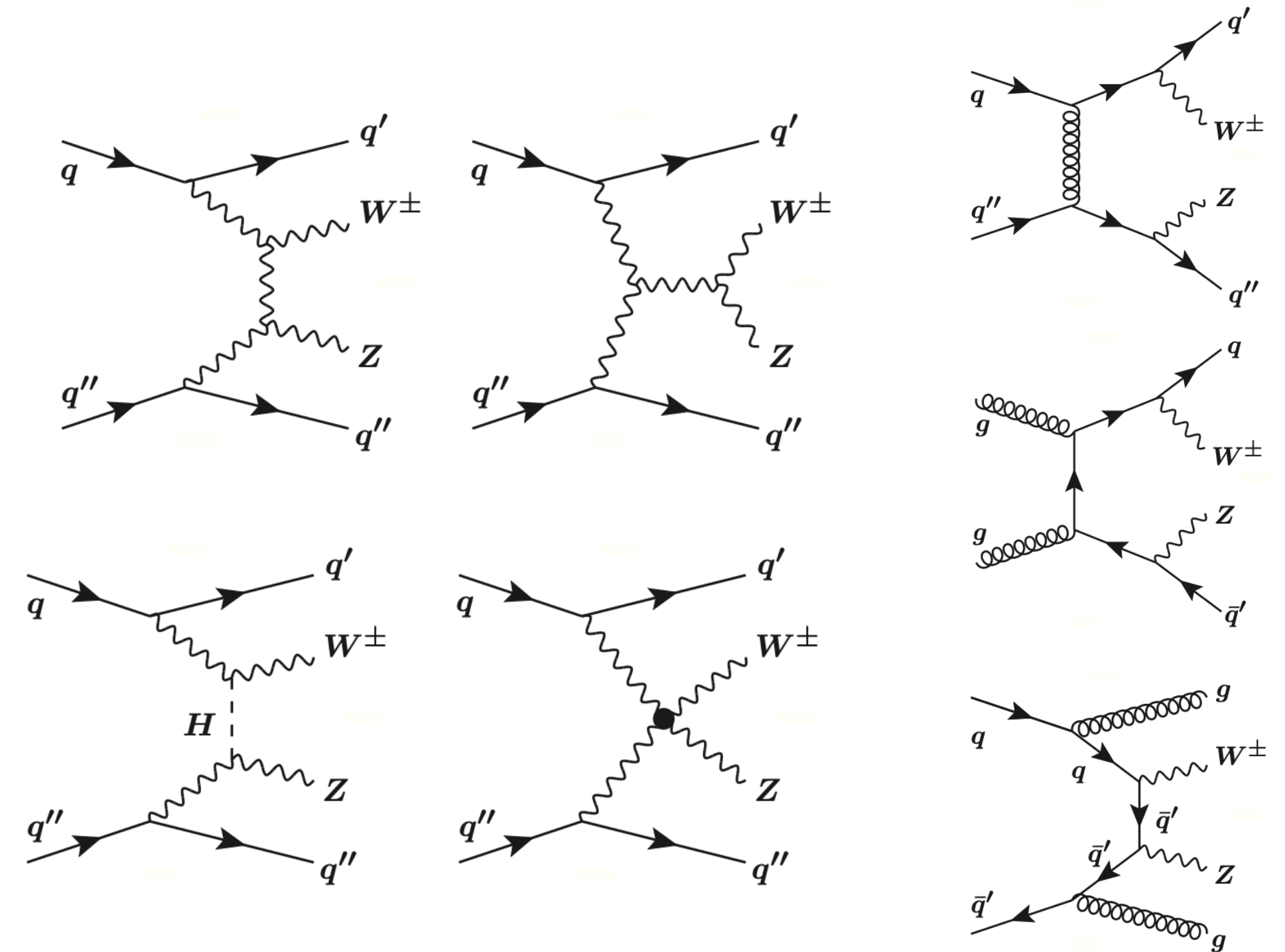
Main sources of irreducible background arise from:

- **ZZ QCD** with a small contribution from ZZ EWK events
- $t\bar{t} + V$ ($V = Z, W$)

Dedicated Control Regions are used to normalize those backgrounds.

Minor sources (VVV) are estimated from MC simulations.

Reducible backgrounds are estimated with data driven methods.

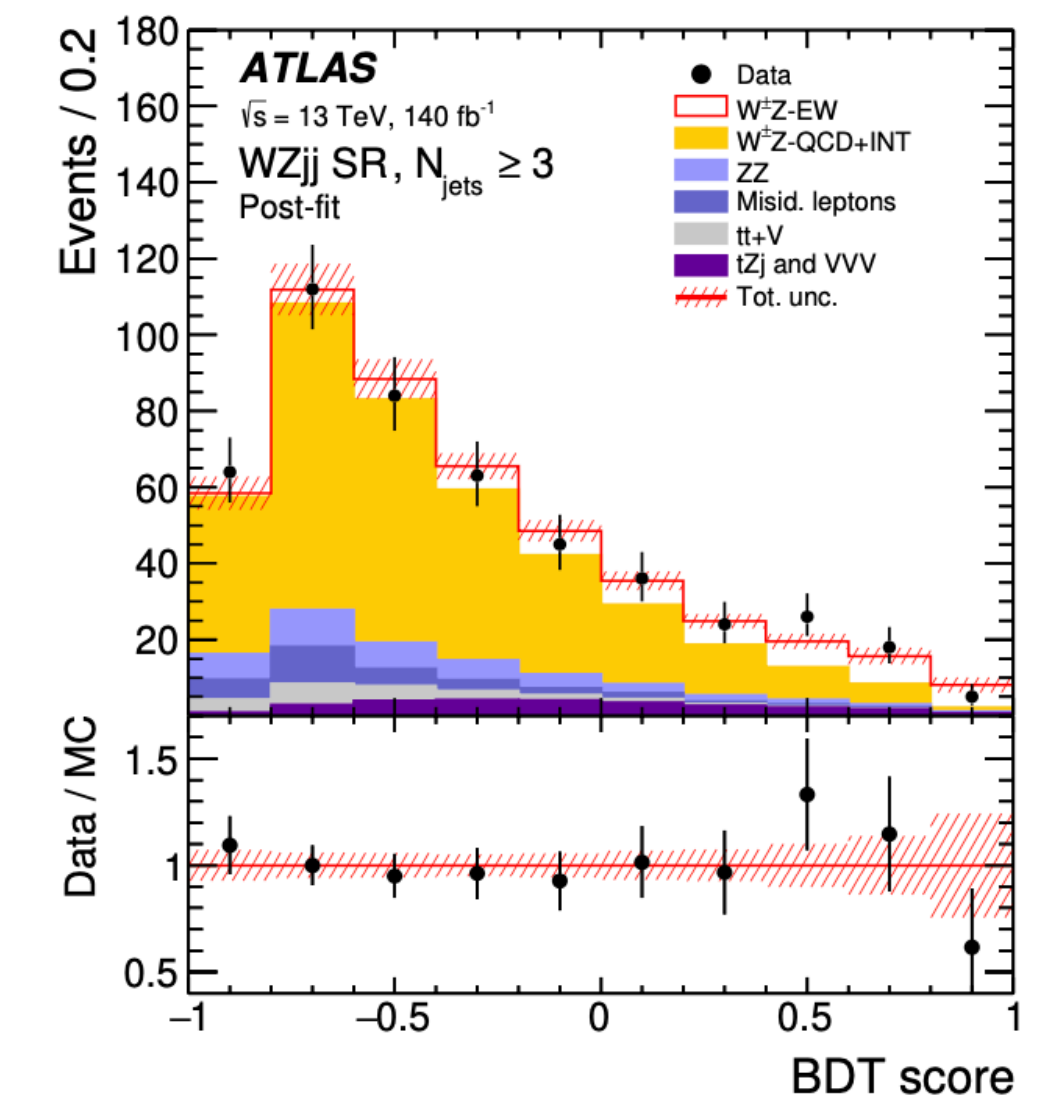
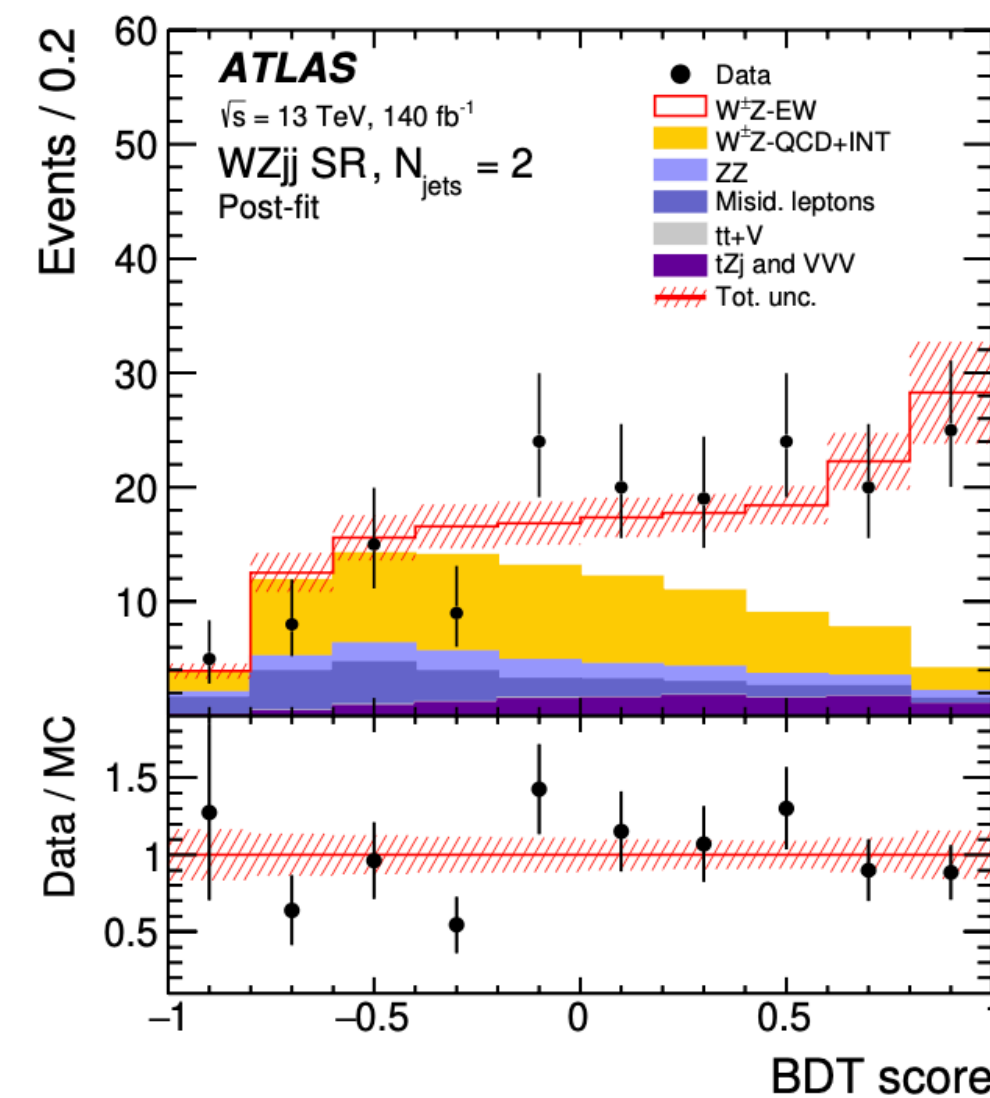
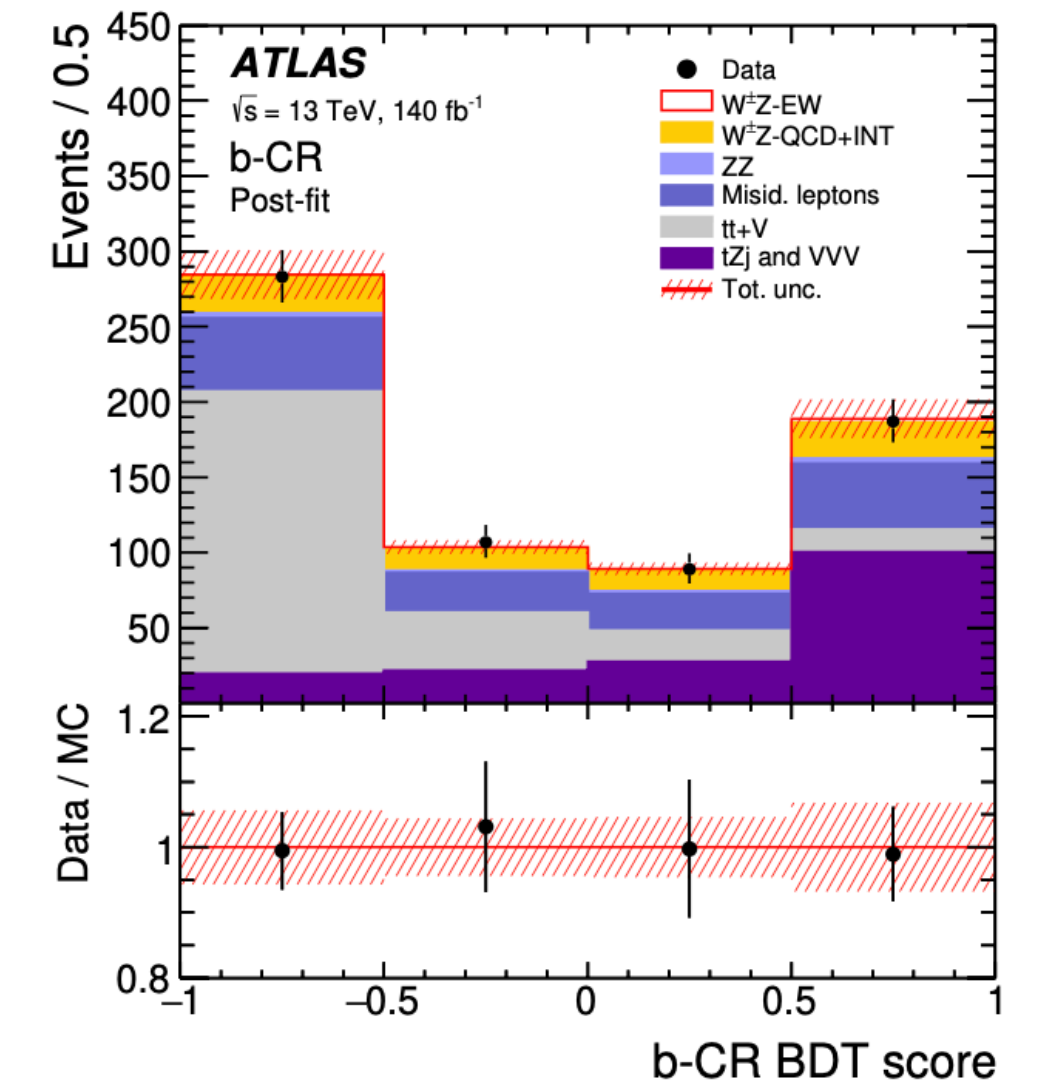
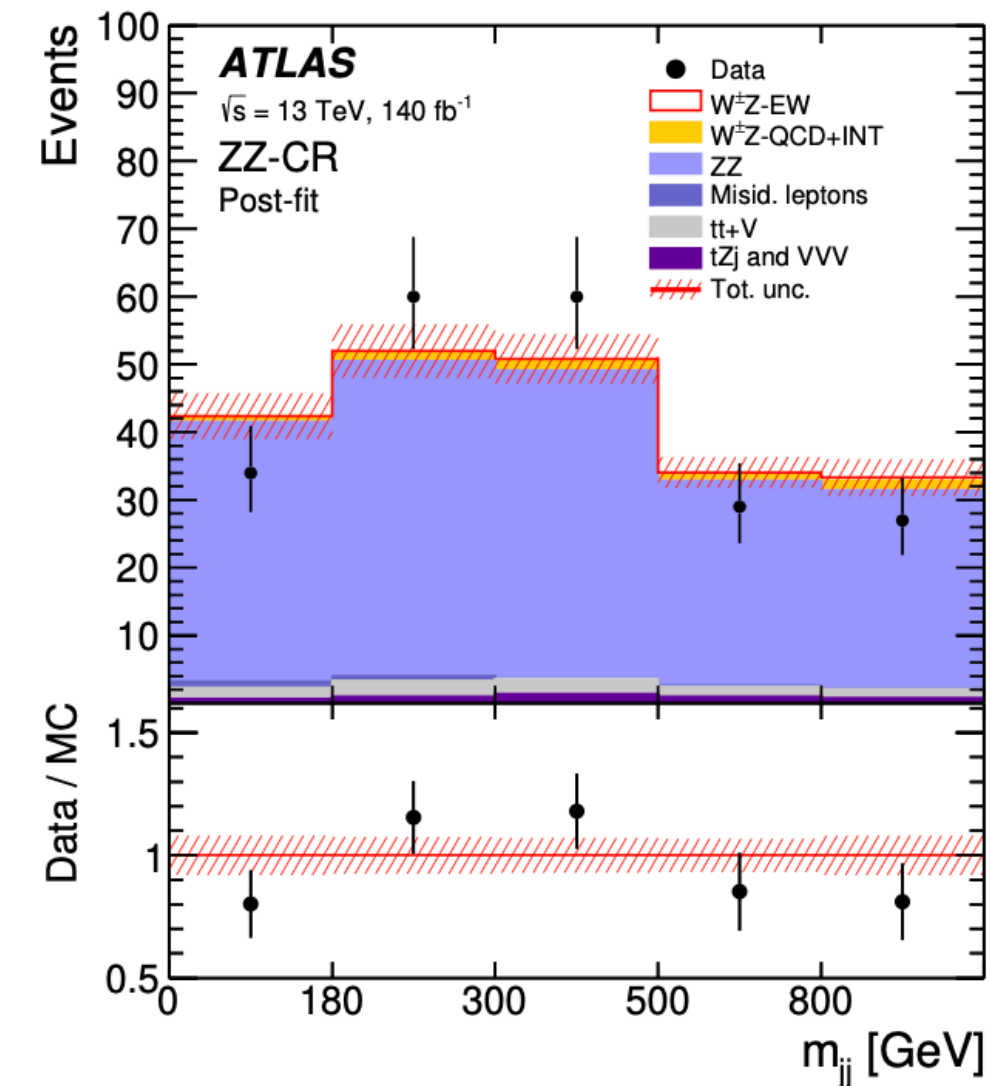


WZ VBS

A Boost Decision Tree (BDT) discriminant is used to separate signal from backgrounds, trained with 15 kinematic distributions.

- To better separate $t\bar{t}V$ and tZj events in b-Control Region, a second BDT discriminant (**b-CR BDT**) is used, trained with an extended set of observables.
- For better modeling SR is divided in two regions, based on **number of jets** in the events (2, 3 or more).
- The good modeling of the background is validated in a region at low m_{jj} .

Background and signal normalisation are adjusted by the profile-likelihood fit.

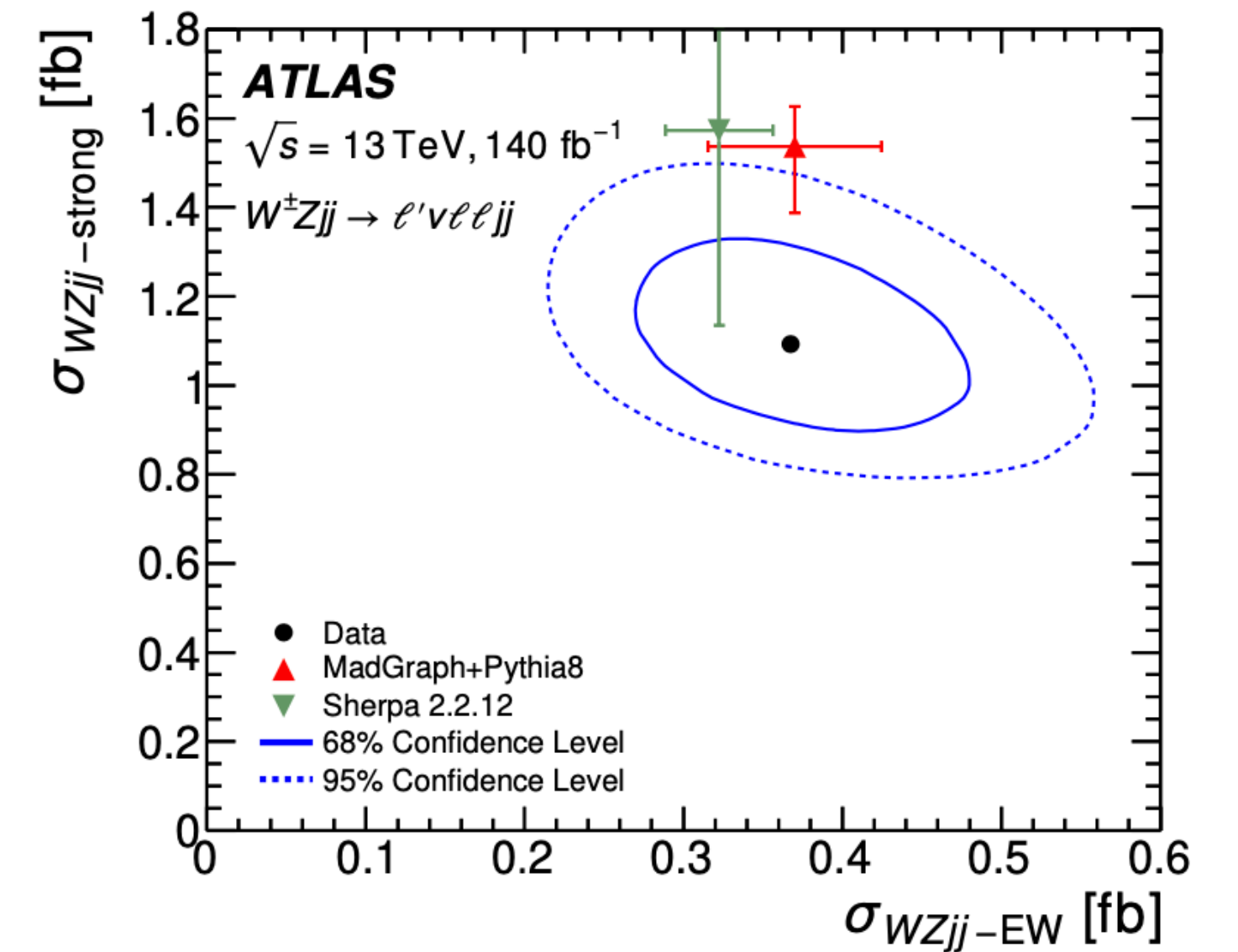


WZ VBS

Cross section measurements of purely EWK, QCD and EWK+QCD WZ show a good agreement with data and theoretical predictions .

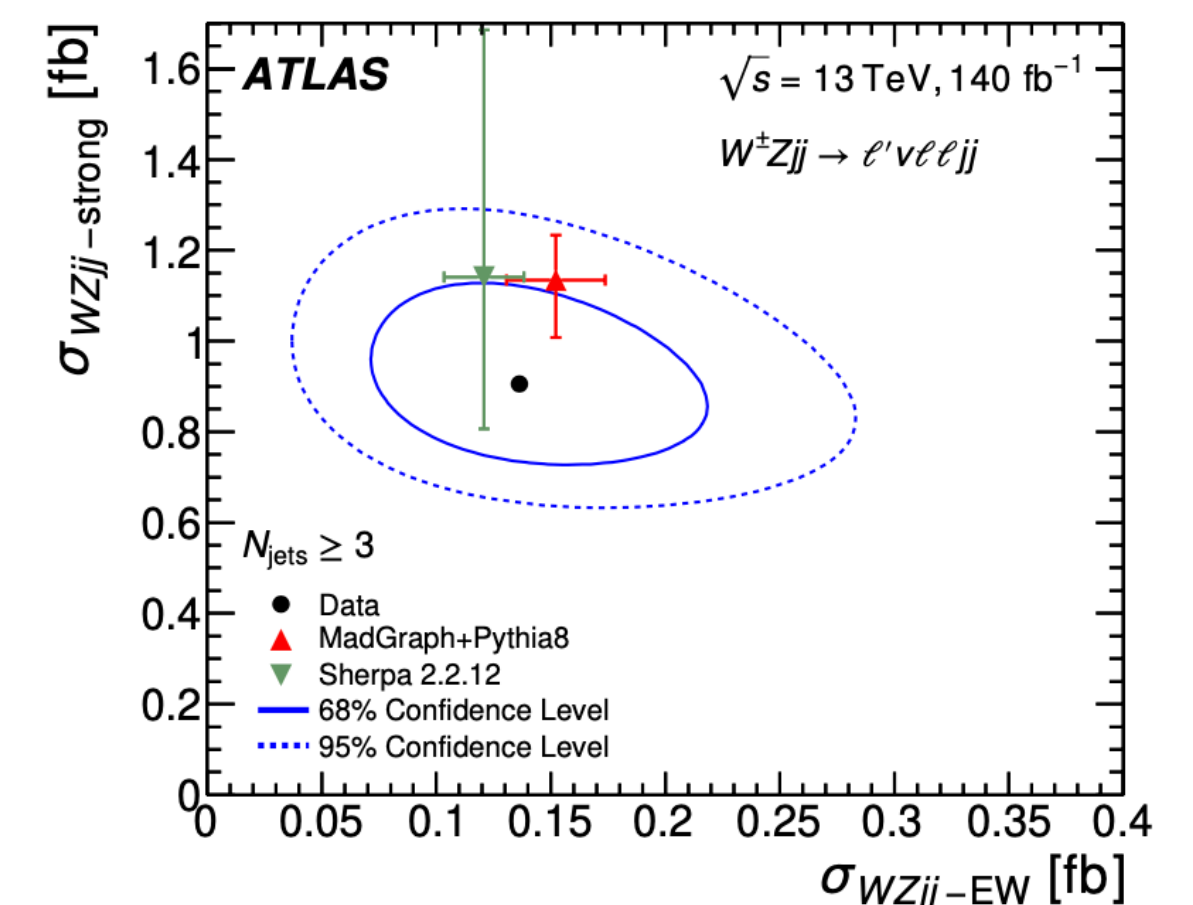
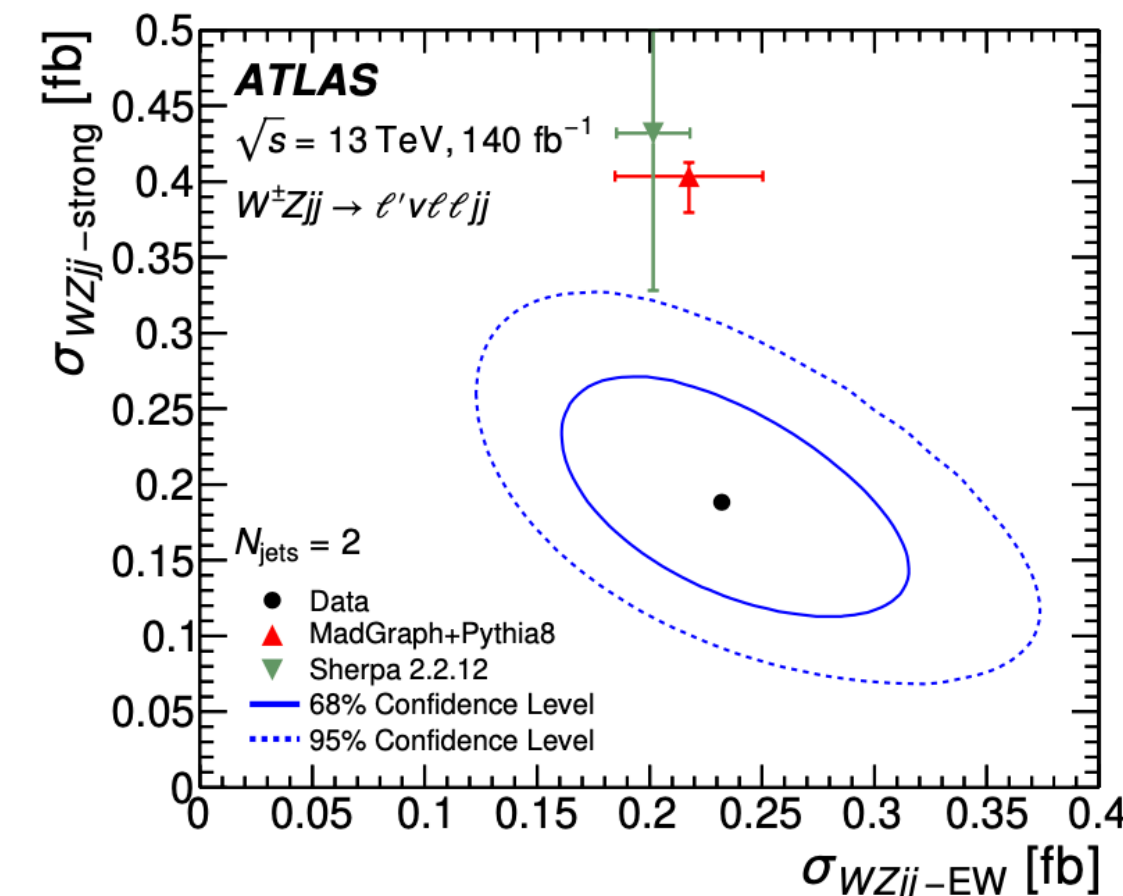
Signal	Measured Cross Section [fb]	Expected* Cross Section [fb]
EWK WZ	$0.368 \pm 0.037(\text{stat}) \pm 0.059(\text{syst}) \pm 0.003(\text{lumi})$	$0.370 \pm 0.001(\text{stat}) \pm 0.006(\text{PDF})^{+0.030}_{-0.026}(\text{scale})$
QCD WZ	$1.093 \pm 0.066(\text{stat}) \pm 0.131(\text{syst}) \pm 0.009(\text{lumi})$	$1.537 \pm 0.009(\text{stat}) \pm 0.016(\text{PDF})^{+0.087}_{-0.149}(\text{scale})$
EWK+QCD WZ	$1.462 \pm 0.063(\text{stat}) \pm 0.118(\text{syst}) \pm 0.012(\text{lumi})$	$1.907 \pm 0.009(\text{stat}) \pm 0.022(\text{PDF})^{+0.117}_{-0.175}(\text{scale})$

*MadGraph+PYTHIA8



Considering separately events with 2 jets and events with three or more jets leads to a disagreement with MC prediction in the first channel.

Differential measurements are also performed, showing similar agreement with data (for more, take a look to Backup slides).

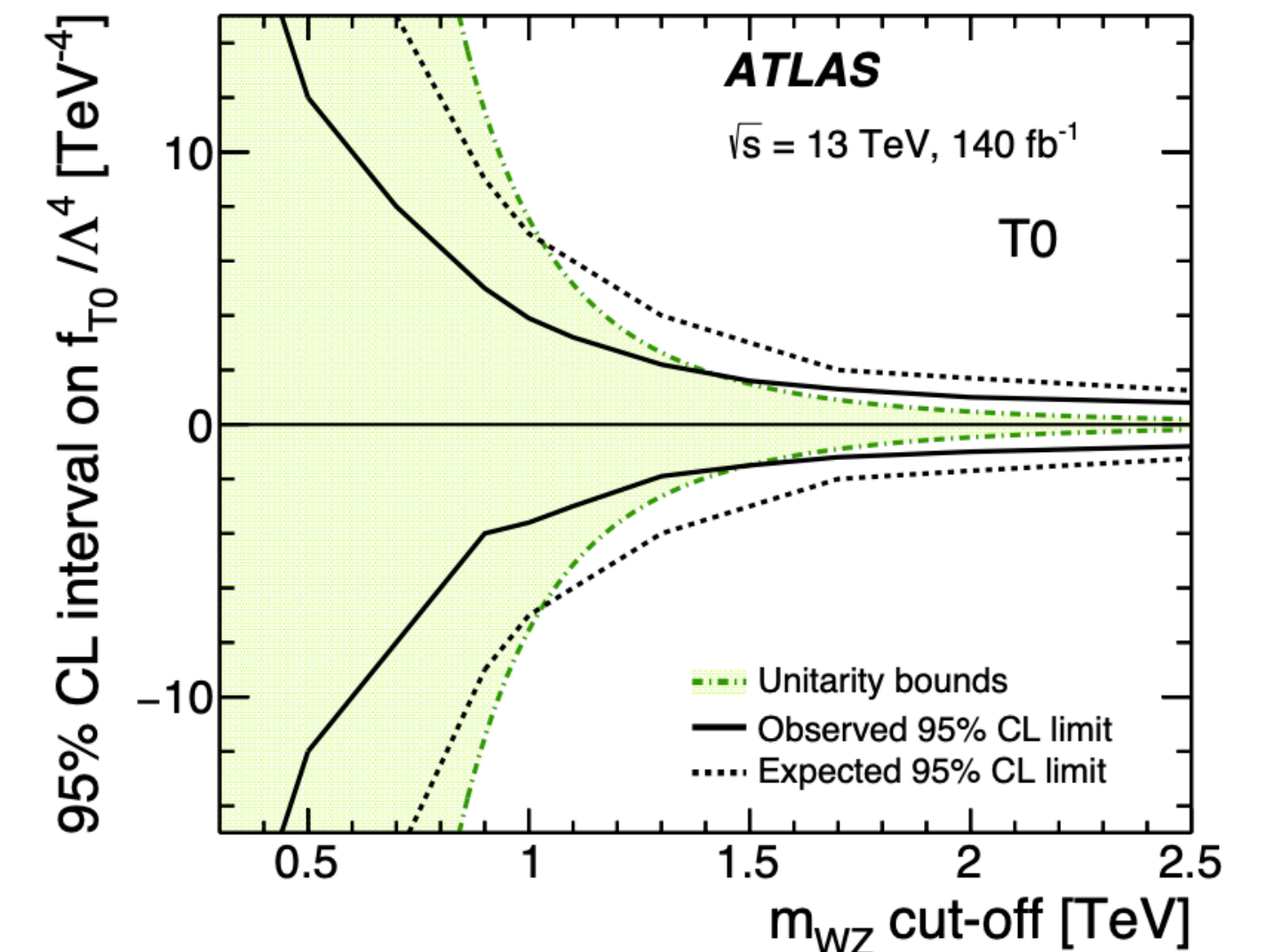
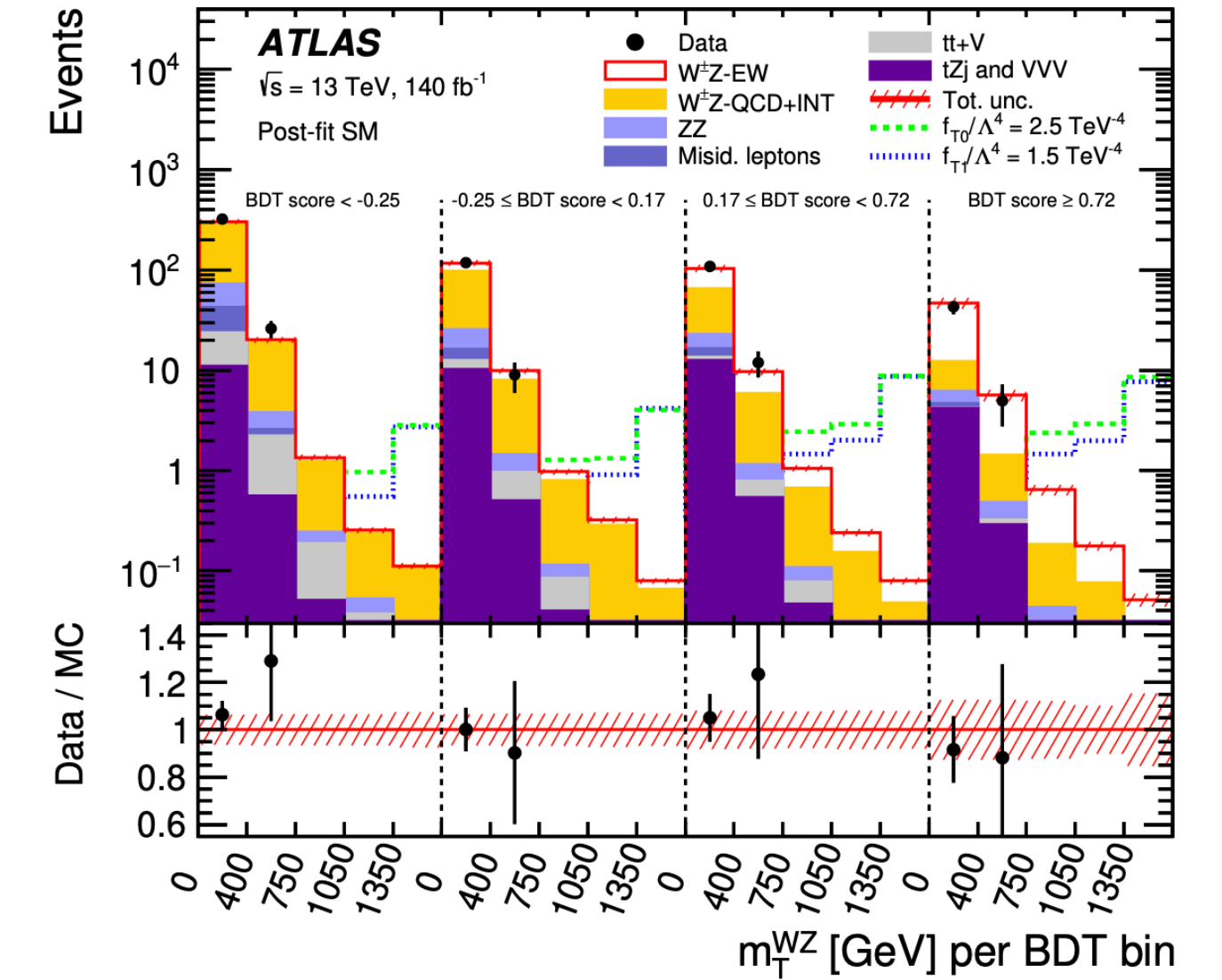


WZ VBS

Limits on aQGCs are set with the implementation of unitarization techniques.

- A profile-likelihood ratio test statistics is used on 2D combination of BDT score and transverse mass of WZ system;
- **Unitarization procedure** consists in a comparison between the curve of the limits obtained varying cutoff on m_{WZ} and unitarity bounds of reference [Phys. Rev. D 101, 113003](#).

Before	Expected [TeV ⁻⁴]	Observed [TeV ⁻⁴]	After	Expected [TeV ⁻⁴]	Observed [TeV ⁻⁴]
f_{T0}/Λ^4	[-0.80, 0.80]	[-0.57, 0.56]	f_{T0}/Λ^4	[-7.0, 7.0]	[-1.5, 1.6]
f_{T1}/Λ^4	[-0.52, 0.49]	[-0.39, 0.35]	f_{T1}/Λ^4	[-1.1, 1.0]	[-0.7, 0.6]
f_{T2}/Λ^4	[-1.6, 1.4]	[-1.2, 1.0]	f_{T2}/Λ^4	[-12, 6]	[-2.4, 1.8]
f_{M0}/Λ^4	[-8.3, 8.3]	[-5.8, 5.6]	f_{M0}/Λ^4	[-60, 60]	[-12, 12]
f_{M1}/Λ^4	[-12.3, 12.2]	[-8.6, 8.5]	f_{M1}/Λ^4	[-32, 32]	[-15, 15]
f_{M7}/Λ^4	[-16.2, 16.2]	[-11.3, 11.3]	f_{M7}/Λ^4	[-30, 30]	[-15, 15]
f_{S02}/Λ^4	[-14.2, 14.2]	[-10.4, 10.4]	f_{S02}/Λ^4	[-41, 41]	[-18, 18]
f_{S1}/Λ^4	[-42, 41]	[-30, 30]	f_{S1}/Λ^4	—	—

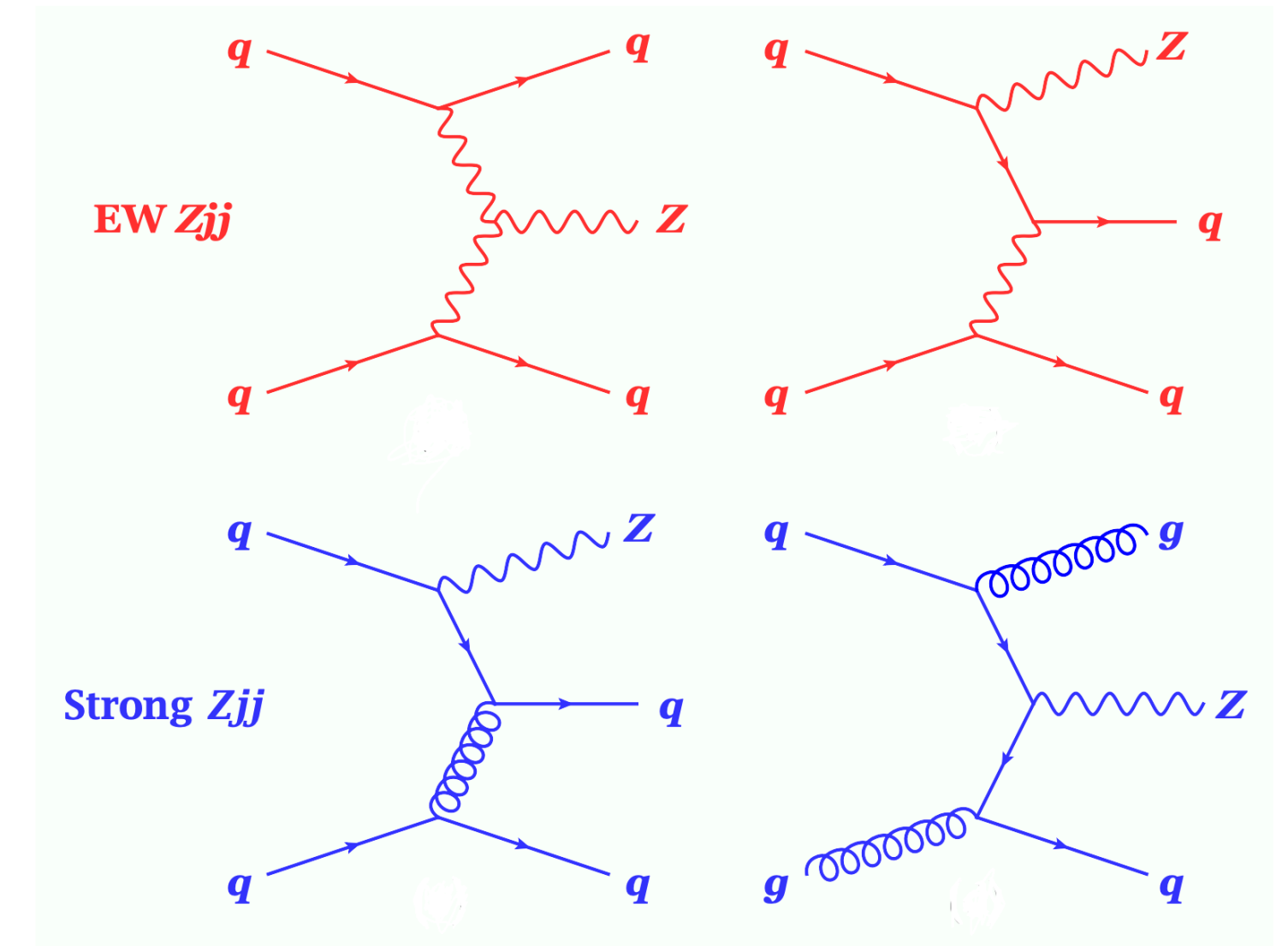


VBF Zjj

EWK production of two jets in association with a Z boson, where Z decays leptonically (e, mu)

This study aims to determine which event generator predictions can be used reliably in VBF and VBS analyses at LHC, using measurements to constraint generator parameters.

Different MC generators are used to simulate signal sample and main background.

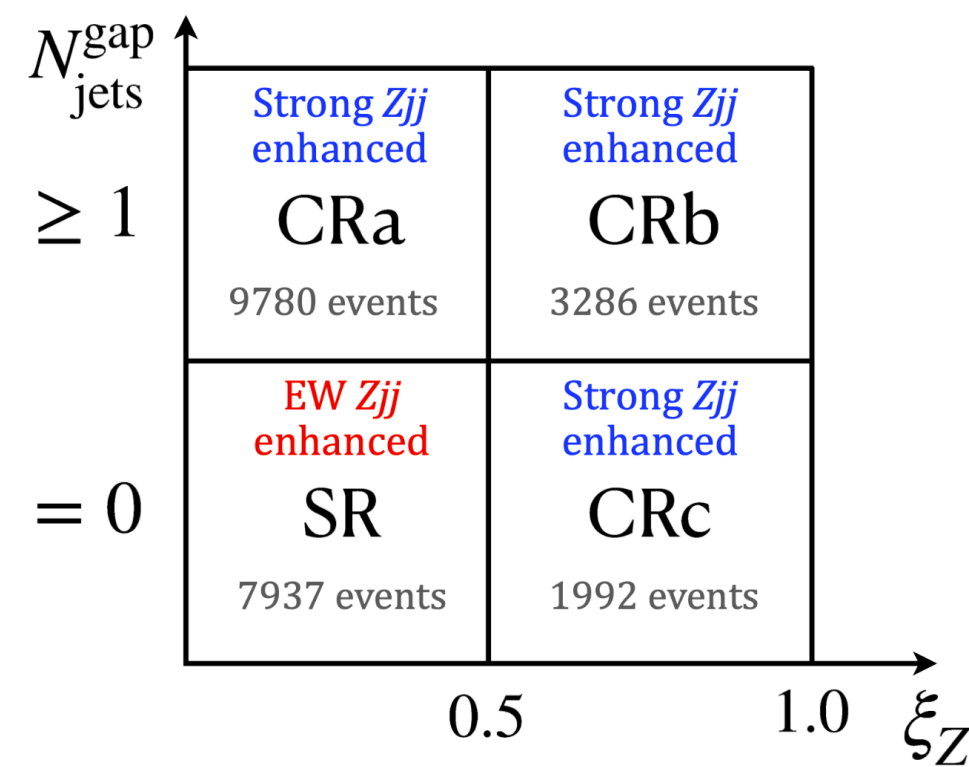


Process	Generator	ME accuracy	PDF	Shower and hadronisation	Parameter set
EW Zjj	POWHEG-BOX v1	NLO	CT10nlo	PYTHIA8 + EVTGEN	AZNLO
	HERWIG7 + VBFNLO	NLO	MMHT2014lo	HERWIG7 + EVTGEN	default
	SHERPA 2.2.1	LO (2–4j)	NNPDF3.0nnlo	SHERPA	default
Strong Zjj	SHERPA 2.2.1	NLO (0–2j), LO (3–4j)	NNPDF3.0nnlo	SHERPA	default
	MADGRAPH5_aMC@NLO	NLO (0–2j), LO (3–4j)	NNPDF2.3nlo	PYTHIA8 + EVTGEN	A14
	MADGRAPH5	LO (0–4j)	NNPDF3.0lo	PYTHIA8 + EVTGEN	A14

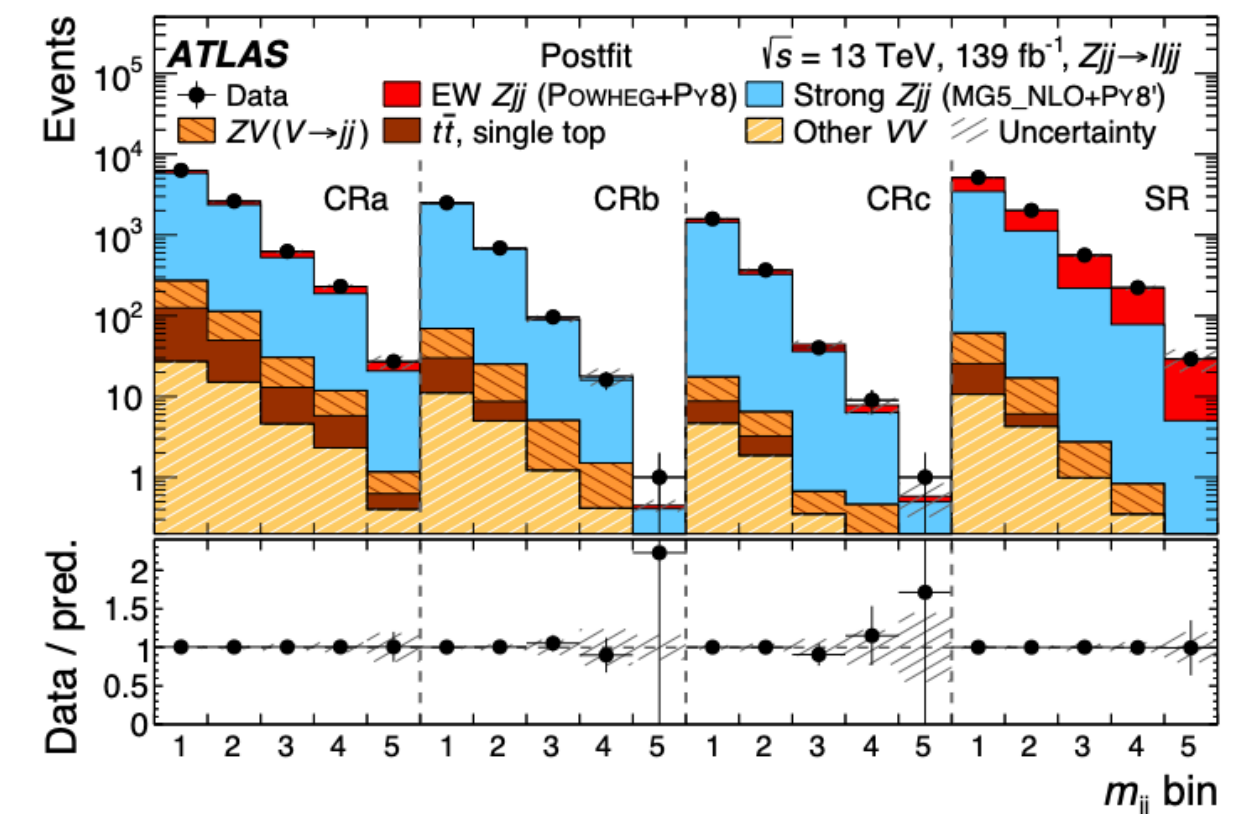
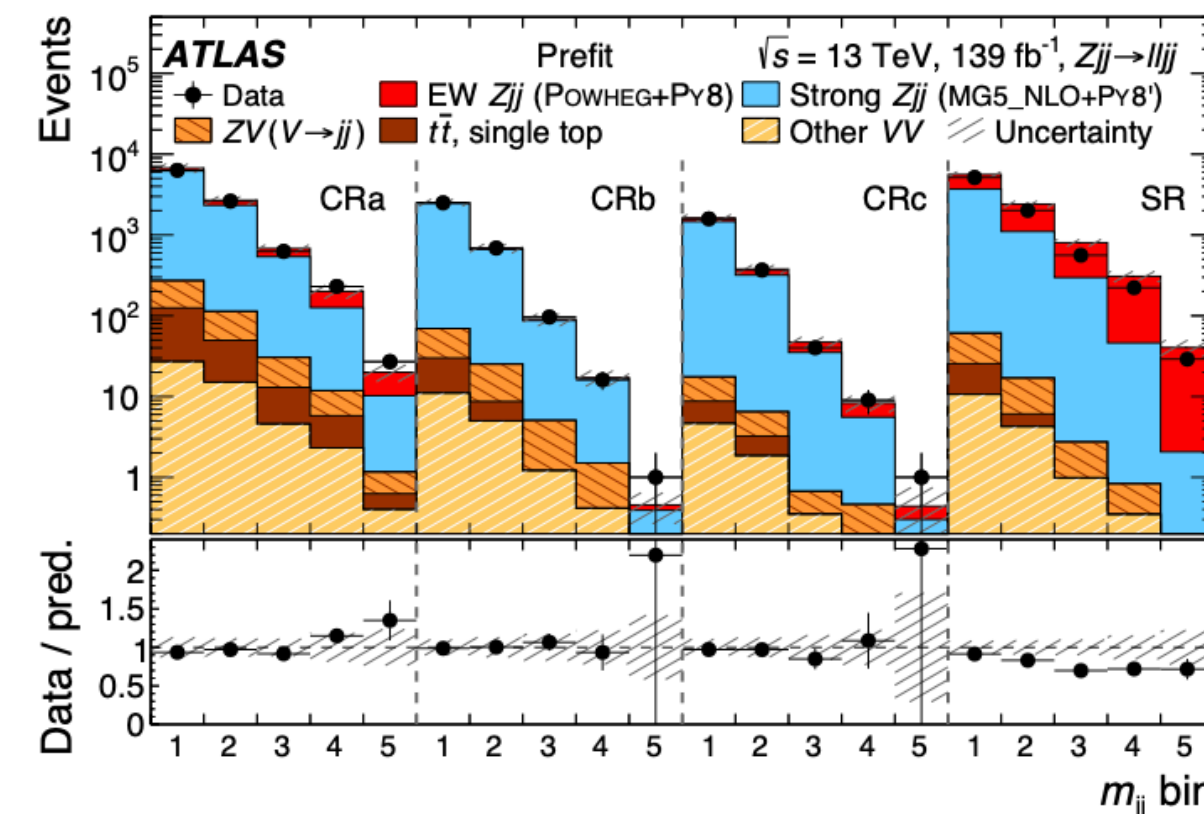
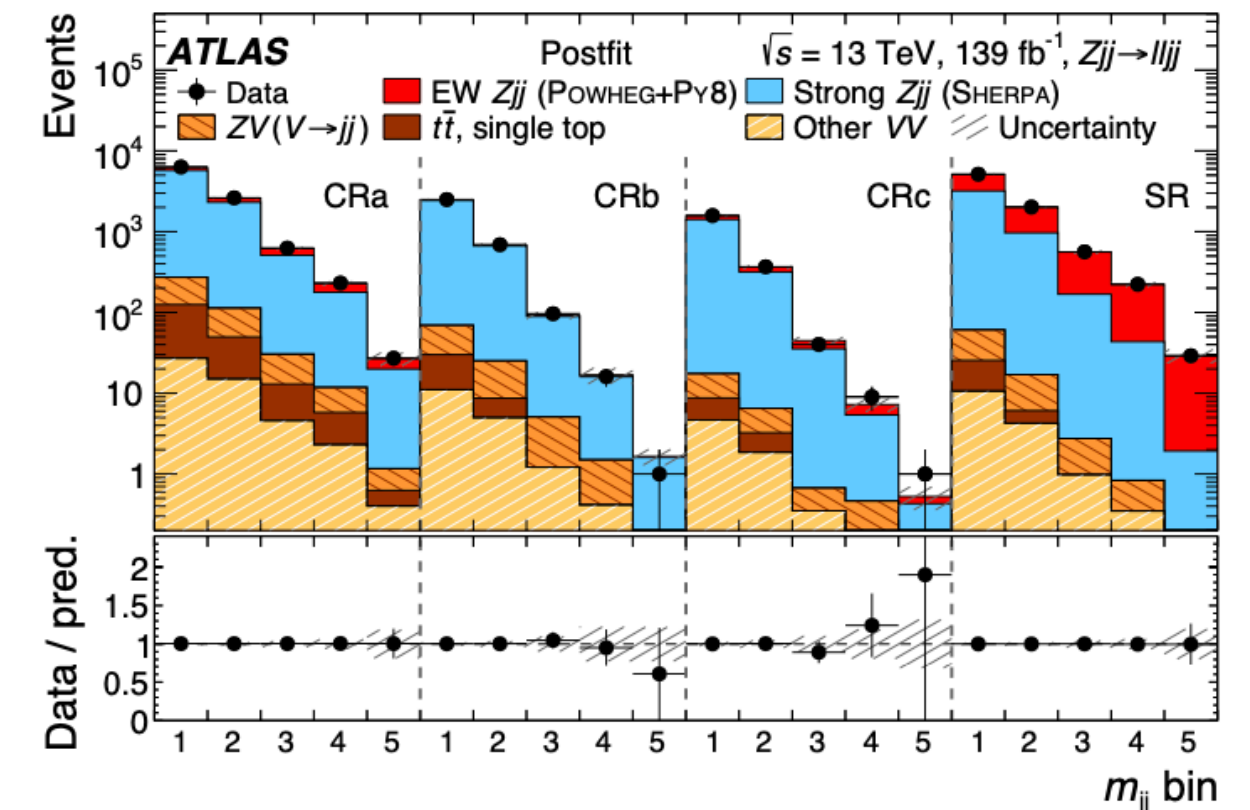
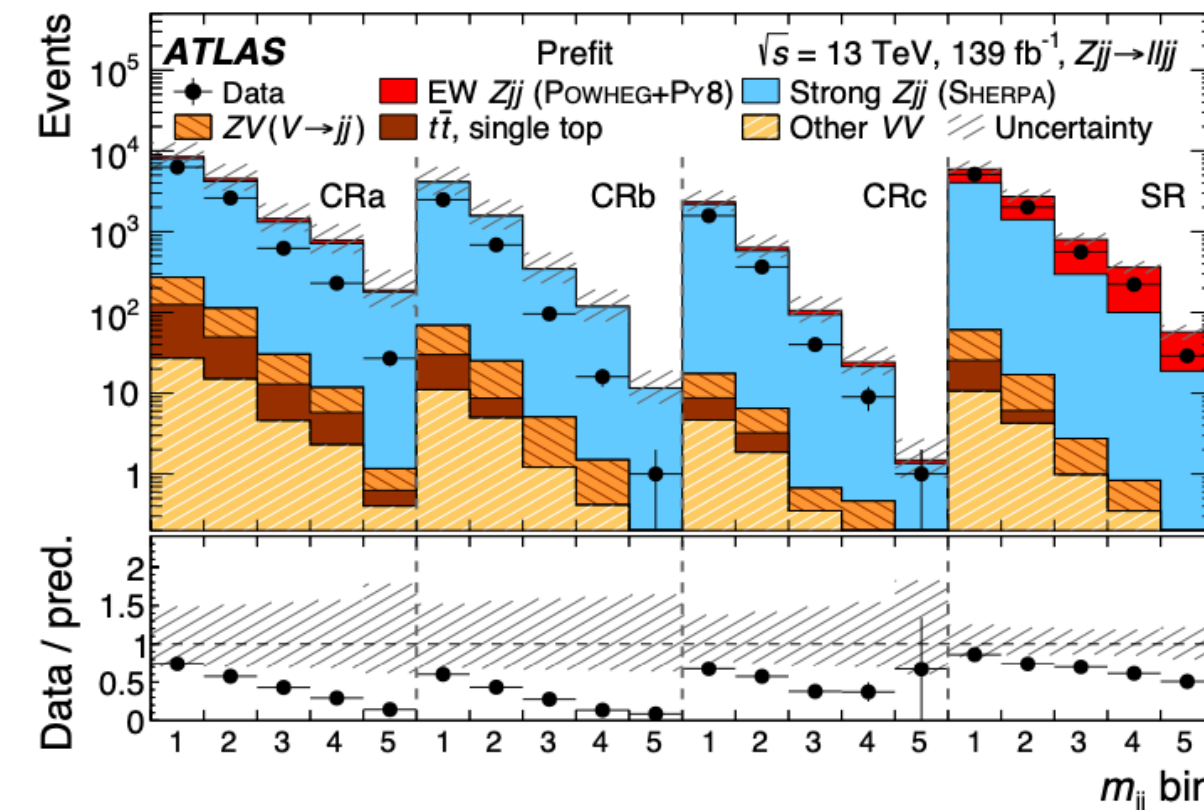
VBF Zjj

Dominant background comes from **strong Zjj** production:

- Dedicated Control Regions, defined by intervals in the centrality of the dijet system and $N_{\text{jets}}^{\text{gap}}$,



- There's no reason to prefer one generator over another for background simulation.



EWK signal yield is obtained as the midpoint of the envelope of three yields with different strong Zjj simulation.

VBF Zjj

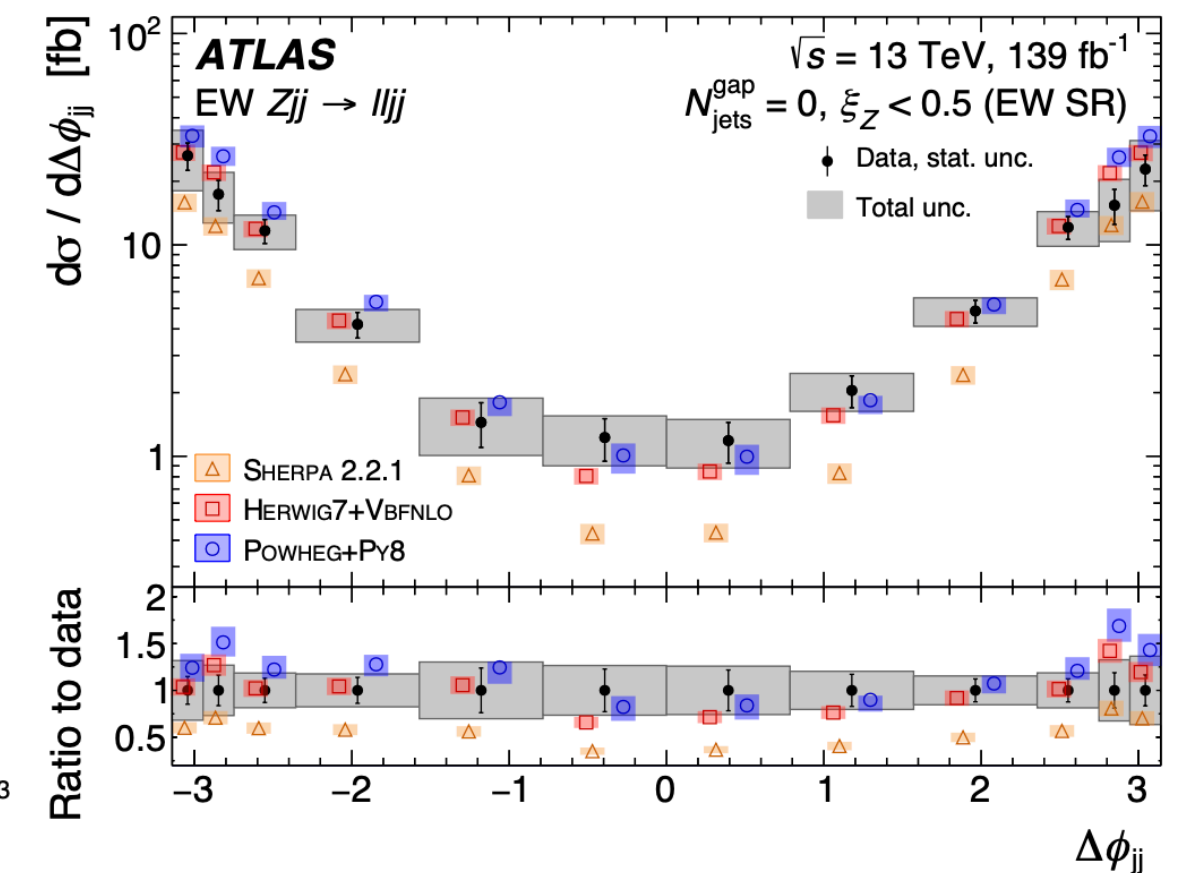
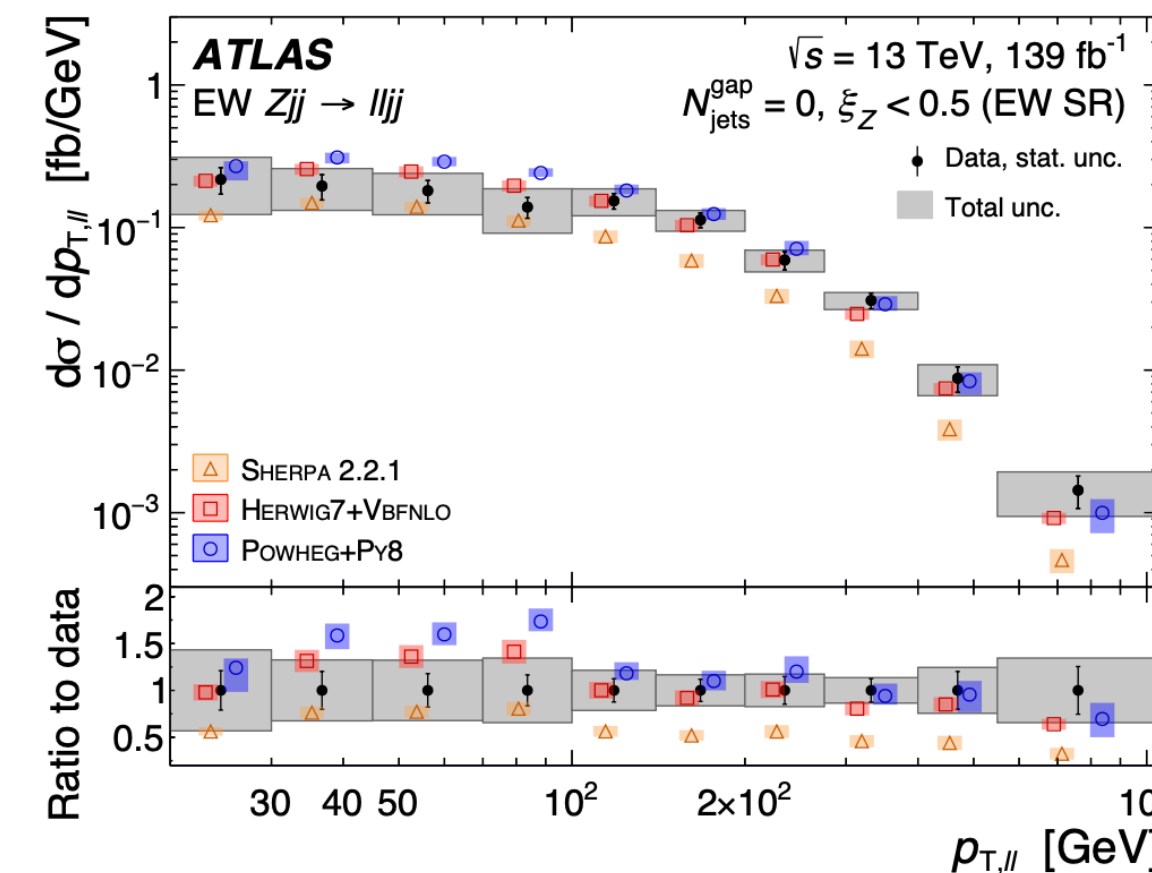
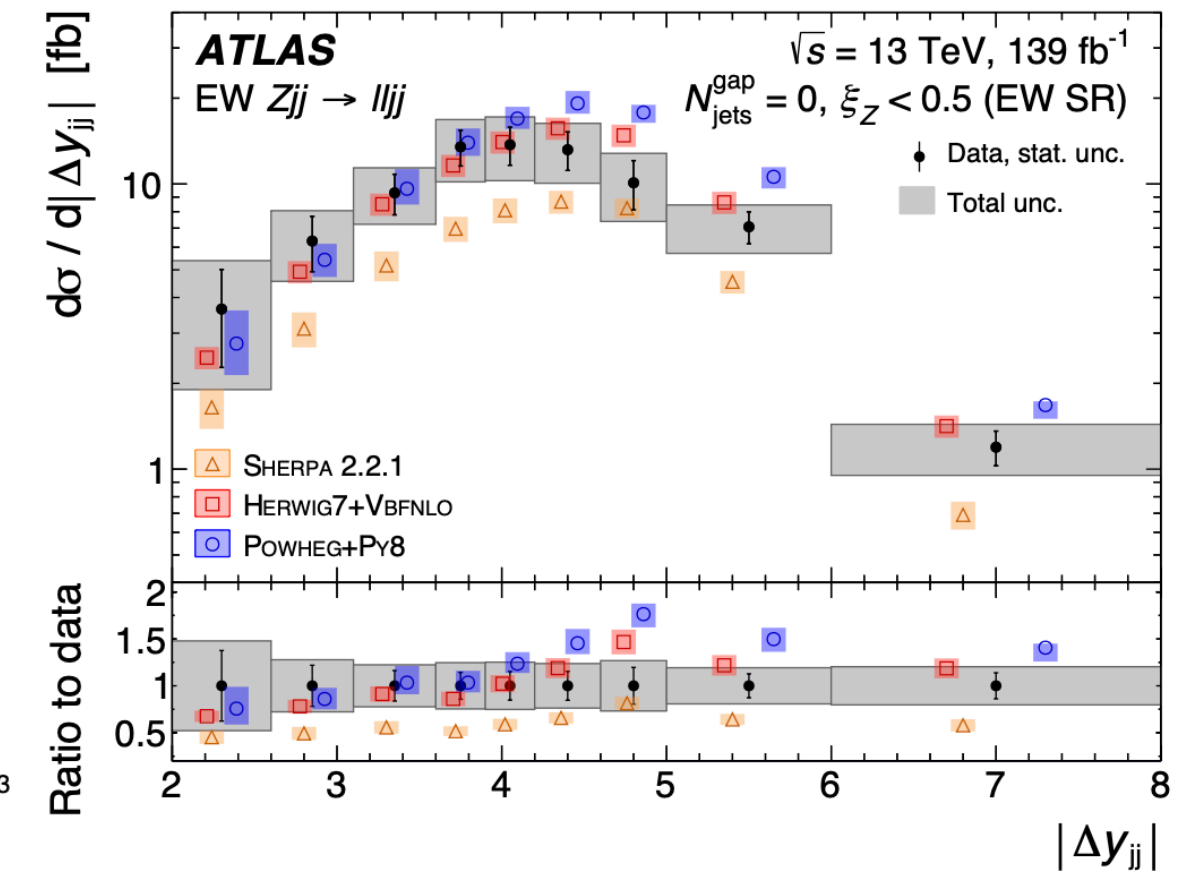
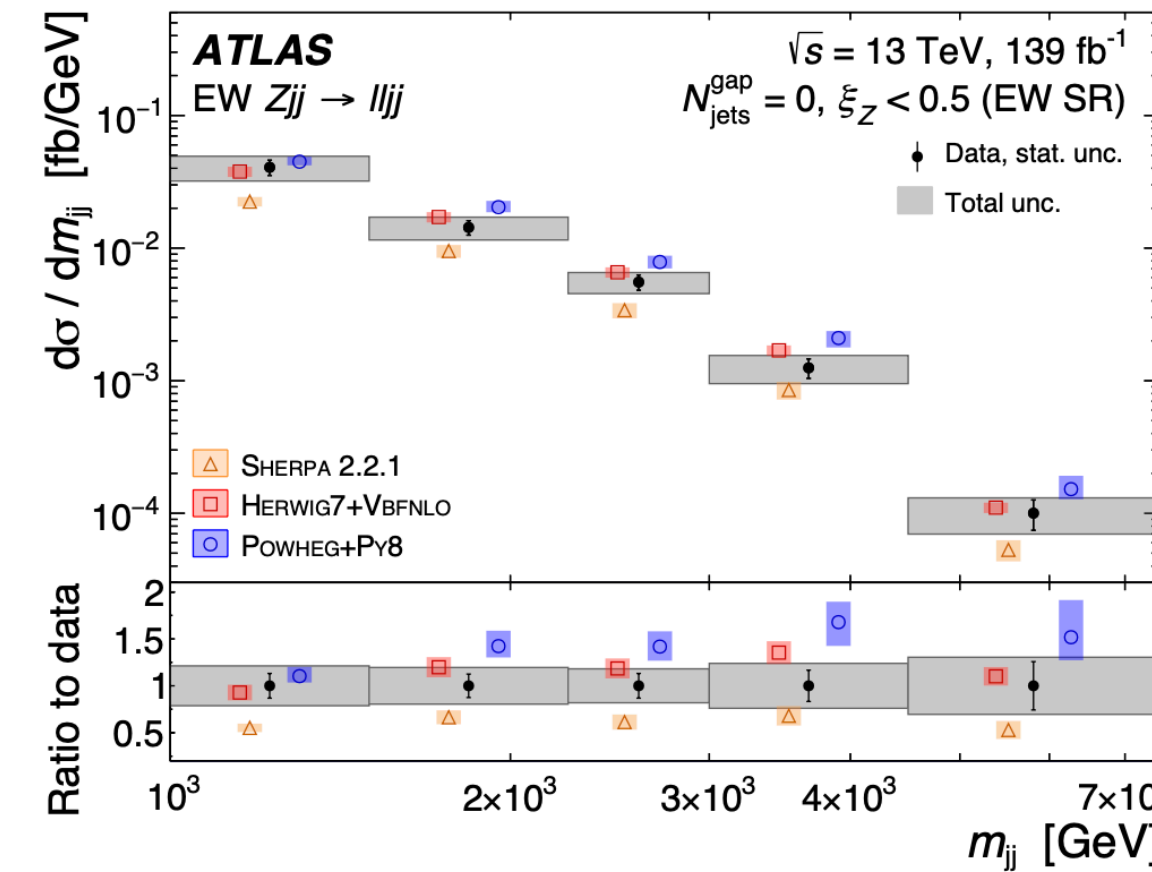
Differential distributions for both EWK and EWK+QCD Zjj are derived as functions of m_{jj} , $|\Delta y_{jj}|$, $p_{T,ll}$ and $\Delta\phi_{jj}$.

- HERWIG7+VBFNLO** predictions are in agreement with data;

Signal	Measured xsec [fb]	Expected* xsec [fb]
EWK Zjj	$37.4 \pm 3.5(\text{stat}) \pm 5.5(\text{syst})$	$39.5 \pm 3.4(\text{scale}) \pm 1.2(\text{PDF})$

*HERWIG7+VBFNLO

- POWHEG+PY8** overestimates EW Zjj cross section (setup of PS when matched to the ME calculation);
- SHERPA** prediction significantly underestimates the measured differential cross section (non-optimal setting of the colour flow).



Summary of other results

$Z\gamma jj$ production

Production of a Z boson (decaying in ee or $\mu\mu$) in association with a photon and two jets.

- Observation with **significance higher than 5σ** for combined channels;
- Differential cross sections (in backup) for 10 different kinematic variables lead to results consistent with SM predictions for both EWK and inclusive $Z\gamma$ production.

Signal	Region	Meas. xsec [fb]	Exp.* xsec [fb]
EWK $Z\gamma$	$m_{jj} > 500$ GeV	3.6 ± 0.5	3.5 ± 0.3
EWK+QCD $Z\gamma$	$m_{jj} > 150$ GeV	$16.8^{+2.0}_{-1.8}$	$15.7^{+5.0}_{-2.6}$

*MG5_aMC@NLO and SHERPA

Reference: [Phys. Lett. B 846 \(2023\) 138222](#)

ssWW production

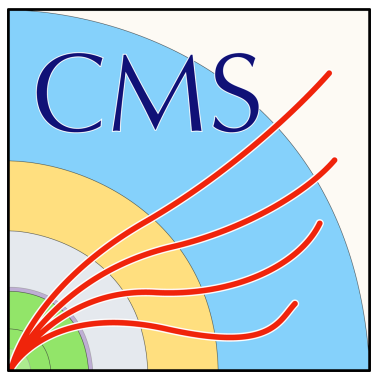
Same-sign W VBS production with Ws decaying in e or μ .

- EWK and inclusive cross section measurement:

Description	$\sigma_{\text{fid}}^{\text{EW}}$ [fb]	$\sigma_{\text{fid}}^{\text{EW+Int+QCD}}$ [fb]
Measured cross section	2.92 ± 0.22 (stat.) ± 0.19 (syst.)	3.38 ± 0.22 (stat.) ± 0.19 (syst.)
MG5_AMC+HERWIG7	2.53 ± 0.04 (PDF) $^{+0.22}_{-0.19}$ (scale)	2.92 ± 0.05 (PDF) $^{+0.34}_{-0.27}$ (scale)
MG5_AMC+PYTHIA8	2.53 ± 0.04 (PDF) $^{+0.22}_{-0.19}$ (scale)	2.90 ± 0.05 (PDF) $^{+0.33}_{-0.26}$ (scale)
SHERPA	2.48 ± 0.04 (PDF) $^{+0.40}_{-0.27}$ (scale)	2.92 ± 0.03 (PDF) $^{+0.60}_{-0.40}$ (scale)
SHERPA \otimes NLO EW	2.10 ± 0.03 (PDF) $^{+0.34}_{-0.23}$ (scale)	2.54 ± 0.03 (PDF) $^{+0.50}_{-0.33}$ (scale)
POWHEG BOX+PYTHIA	2.64	–

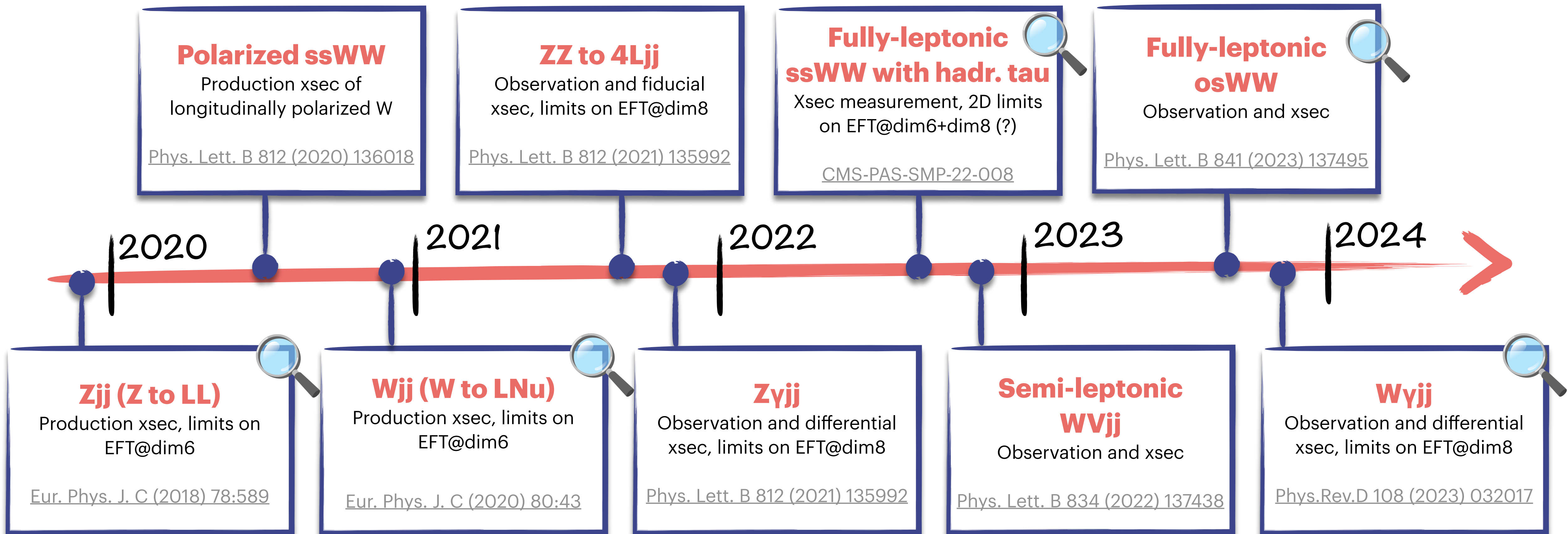
- Differential cross section (in backup);
- Extraction of limits on **EFT dim8** operators w/ unitarity and Search for **double Higgs** boson $H^{\pm\pm}$ produced by VBF and decaying in ssWW (2.5σ @450GeV).

Reference: [JHEP 04 \(2024\) 026](#)



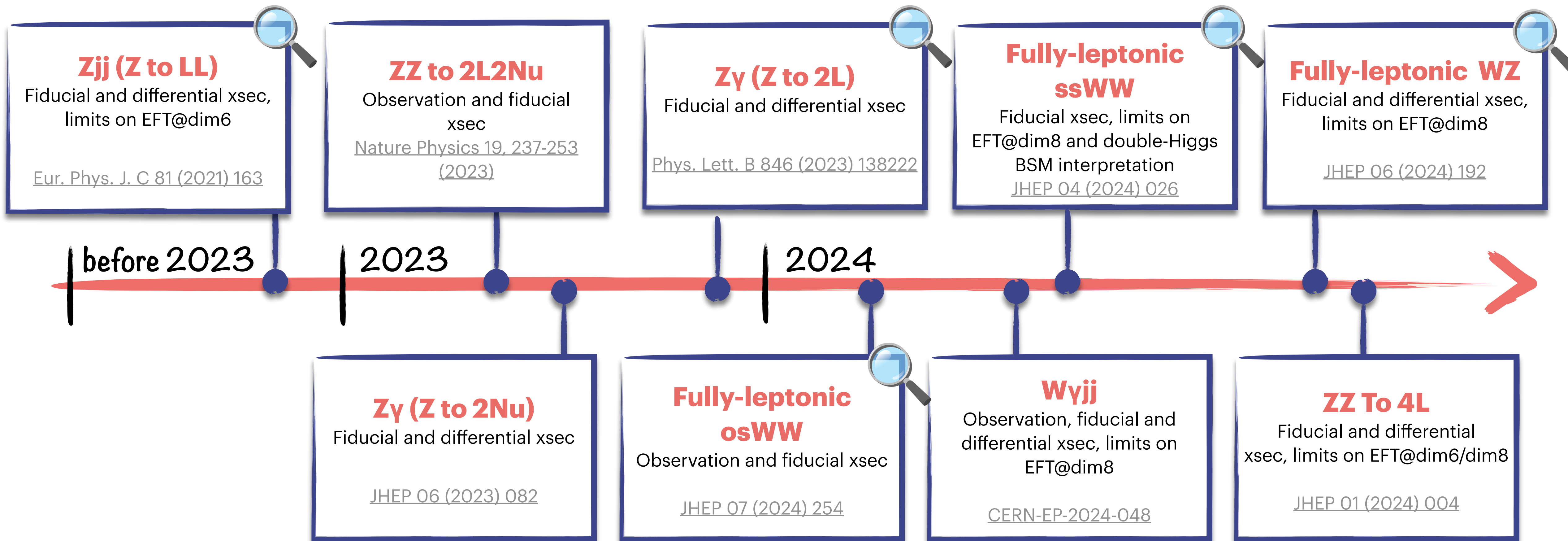
If you want more, from CMS...

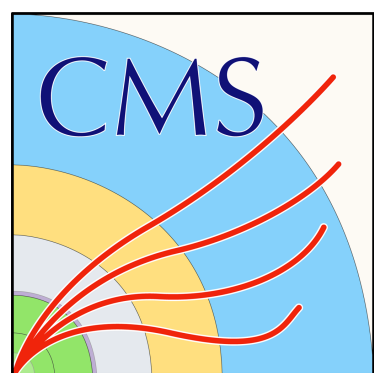
CMS results for VBS (VBF) processes at $\sqrt{s} = 13$ TeV and integrated luminosity of 138 (35.9) fb^{-1}



If you want more, from ATLAS...

ATLAS results for VBS and VBF processes at $\sqrt{s} = 13$ TeV and integrated luminosity of 140 fb^{-1}





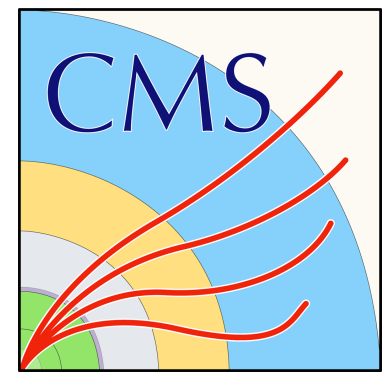
Summary

- Many analyses performed with full Run2 datasets and more to come
- The exploration of Effective Field Theory interpretations is gaining importance in VBS and VBF field
- Recent studies shown a high sensitivity to dim6 EFT operators and this would allow VBS processes to be integrated into the landscape of global EFT interpretations

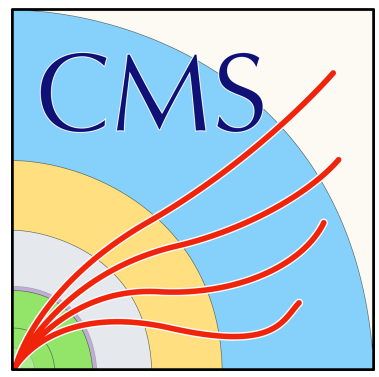
Stay tuned for Run3!



Loading....



Backup

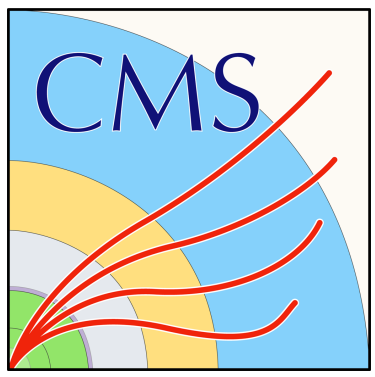


Opposite-sign WW VBS

Uncertainties and yields

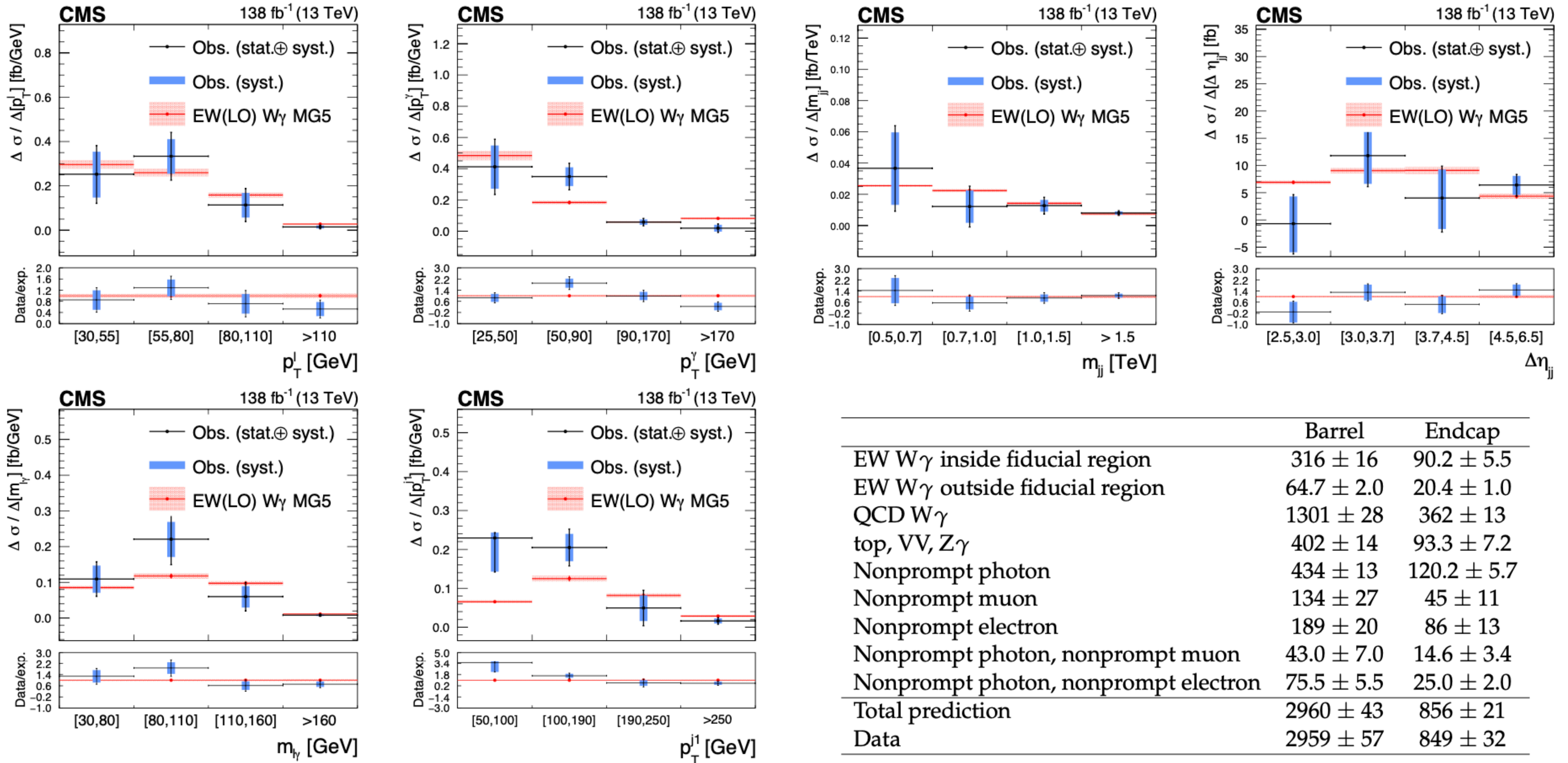
Uncertainty source	Value
QCD-induced W^+W^- normalization	5.3%
$t\bar{t}$ scale variation	5.1%
VBS signal scale variation	5.0%
$t\bar{t}$ normalization	4.9%
b tagging	3.5%
Trigger corrections	3.3%
DY normalization	2.9%
Jet energy scale + resolution	2.6%
Unclustered p_T^{miss}	2.4%
QCD-induced W^+W^- scale variation	2.1%
Integrated luminosity	2.0%
Muon efficiency	2.0%
Pileup	1.8%
Electron efficiency	1.5%
Underlying event	1.3%
Parton shower	1.0%
Other	<1%
Total systematic uncertainty	13.1%
Total statistical uncertainty	14.9%
Total uncertainty	19.8%

Process	SR $e\mu$ $Z_{\ell\ell} < 1$	SR $e\mu$ $Z_{\ell\ell} > 1$	SR $ee - \mu\mu$ $Z_{\ell\ell} < 1$	SR $ee - \mu\mu$ $Z_{\ell\ell} > 1$
DATA	2441	2192	1606	1667
Signal + background	2396.8 ± 98.5	2239.6 ± 106.0	1590.4 ± 49.4	1660.5 ± 43.6
Signal	169.1 ± 20.2	69.9 ± 8.4	98.0 ± 6.5	38.3 ± 2.5
Background	2227.7 ± 96.4	2169.7 ± 105.6	1492.4 ± 48.9	1622.1 ± 43.5
$t\bar{t} + tW$	1629.4 ± 71.4	1452.5 ± 69.5	767.8 ± 14.5	642.5 ± 13.2
WW (QCD)	327.0 ± 61.6	409.3 ± 77.3	111.1 ± 16.6	121.5 ± 17.3
Nonprompt	107.0 ± 18.4	109.9 ± 16.4	30.0 ± 4.9	32.0 ± 4.2
DY no PU jets	—	—	259.5 ± 27.3	408.3 ± 17.1
DY + 1 PU jets	—	—	222.7 ± 33.3	337.4 ± 32.9
DY $\tau^+\tau^-$	69.2 ± 4.6	102.0 ± 5.8	—	—
Multiboson	67.7 ± 6.6	75.6 ± 7.3	60.9 ± 3.8	60.1 ± 4.8
Zjj	1.0 ± 0.2	0.4 ± 0.0	40.5 ± 4.2	20.3 ± 1.3
Higgs	26.6 ± 1.5	20.1 ± 1.0	—	—

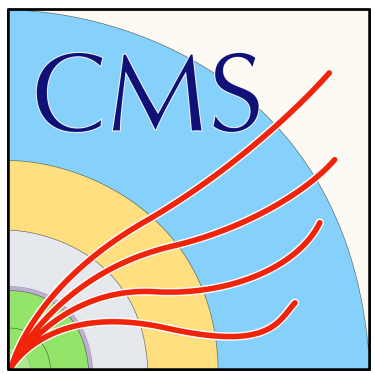


EWK production of $W\gamma + 2\text{jets}$

Differential cross section



	Barrel	Endcap
EW $W\gamma$ inside fiducial region	316 ± 16	90.2 ± 5.5
EW $W\gamma$ outside fiducial region	64.7 ± 2.0	20.4 ± 1.0
QCD $W\gamma$	1301 ± 28	362 ± 13
top, VV, $Z\gamma$	402 ± 14	93.3 ± 7.2
Nonprompt photon	434 ± 13	120.2 ± 5.7
Nonprompt muon	134 ± 27	45 ± 11
Nonprompt electron	189 ± 20	86 ± 13
Nonprompt photon, nonprompt muon	43.0 ± 7.0	14.6 ± 3.4
Nonprompt photon, nonprompt electron	75.5 ± 5.5	25.0 ± 2.0
Total prediction	2960 ± 43	856 ± 21
Data	2959 ± 57	849 ± 32

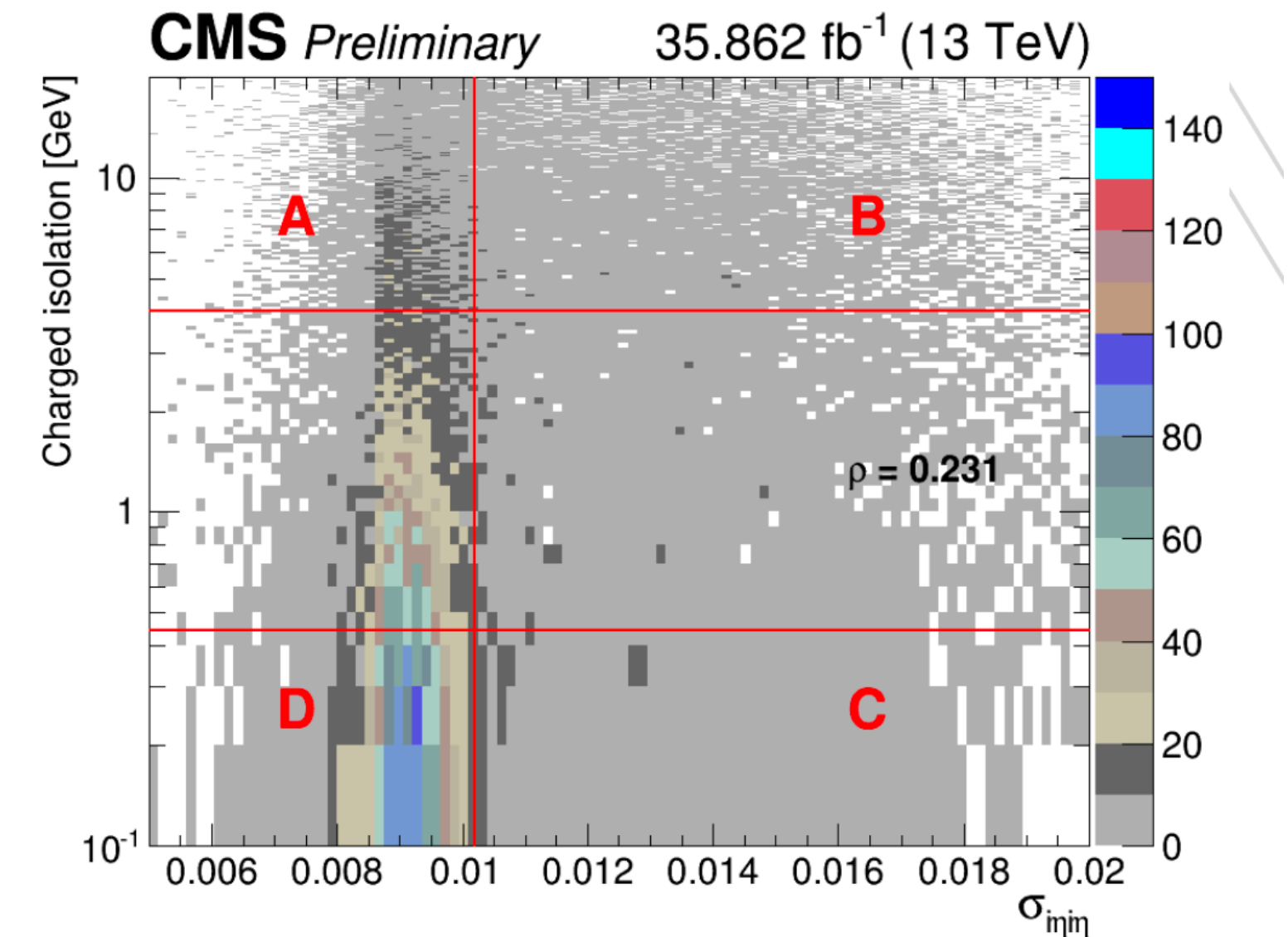


EWK production of $W\gamma + 2\text{jets}$

Discrimination of prompt and non-prompt photons

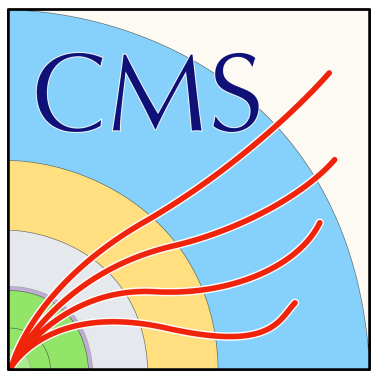
Estimate of fake photons rate is done knowing fake photons fraction.

- prompt photon template and the fake photon template are fit to the data template to get the fake fraction for different photon p_T bins
- $\sigma_{\eta\eta} < 0.01015$ (0.0272) in barrel (endcap)*
 - One loose muon and no other leptons in muon channel, or one veto electron other leptons in electron channel
 - HLT pass
 - missing $ET > 30$ GeV
 - W transverse mass > 30 GeV
 - $\Delta R_{l\gamma} > 0.5$
 - $p_T^{lep} > 30$ GeV, $|\eta^{lep}| < 2.4$ (2.5) muon(ele)
 - $25 \text{ GeV} < p_T^\gamma < 4000$ GeV, $|\eta^\gamma| < 1.4442$ (barrel), $1.566 < |\eta^\gamma| < 2.5$ (endcap)
 - $|M_{l\gamma} - M_Z| > 10$ (ele)
 - Photon pixelseed veto



2D distribution of charge isolation and $\sigma_{\eta\eta}$ of photons (D is the good photon region), in other regions objects don't meet requirements for charge isolation and $\sigma_{\eta\eta}$

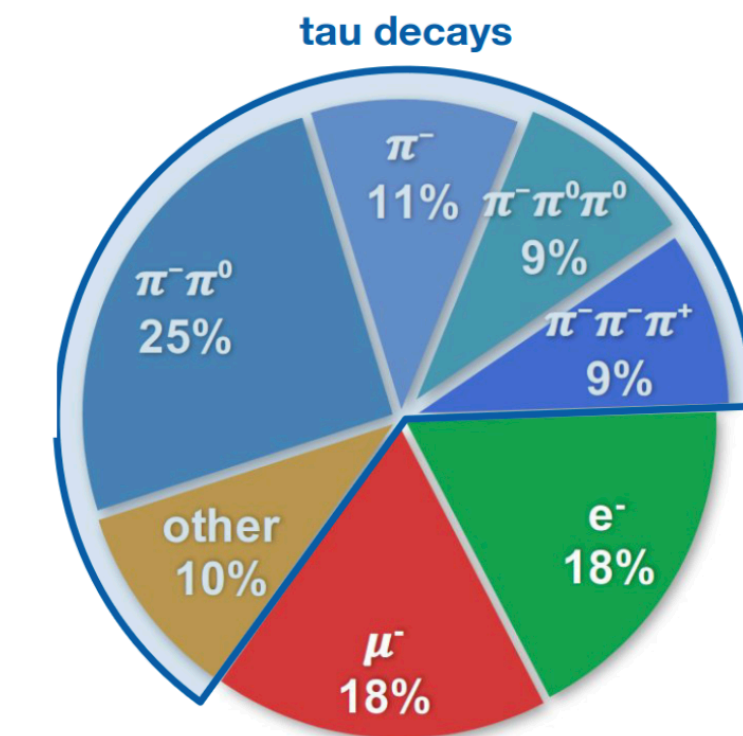
* energy-weighted spread within the 5×5 crystal matrix centered on the crystal with the largest energy deposit in the supercluster



Same-sign WW with hadronic tau

Non-prompt background estimate

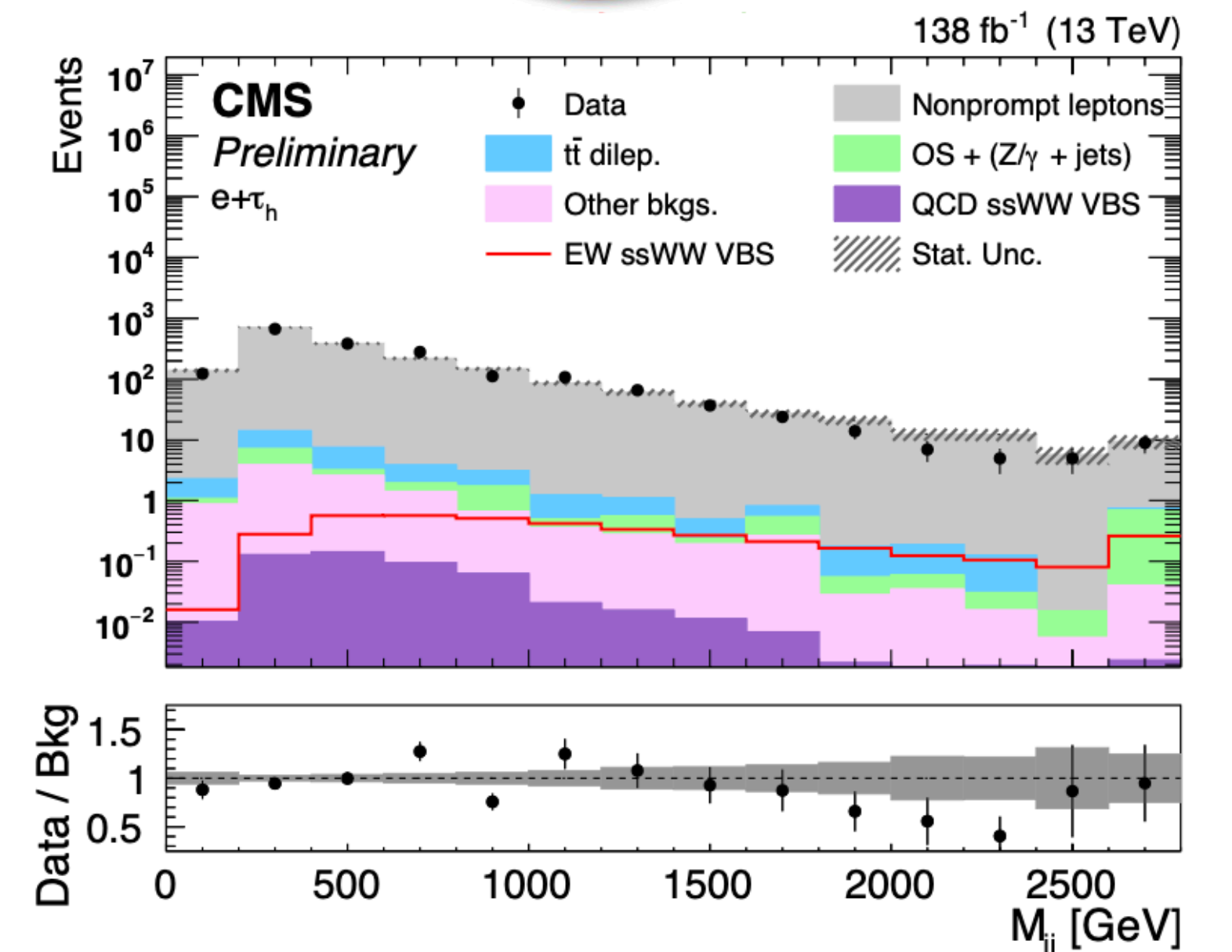
Hadronically decaying taus are reconstructed with hadrons-plus-strips algorithm and identified with DeepTau algorithm based on DNN models, and is capable of discriminating taus from jets, electron and muons using three different classifiers

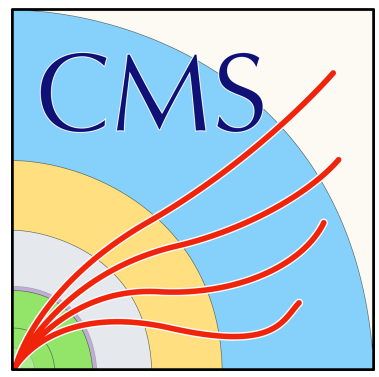


Region	1 ℓ , 1 τ_h , no additional "loose" ℓ		
	same-sign (ℓ, τ_h)	$p_T^{\text{miss}} > 50 \text{ GeV}$	additional requirements
SR	✓	×	$M_{jj} > 500 \text{ GeV}$
Nonprompt CR	✓	×	
$t\bar{t}$ CR	×	✓	b-tagged jet ("medium")
OS CR	×	✓	b-tagged jet veto ("loose")
QCD-enriched CR	1 "loose" $e, \mu, \text{ or } \tau_h$, no add. leptons, $p_T^{\text{miss}} \leq 50 \text{ GeV}, M_T(\ell, p_T^{\text{miss}}) < 50 \text{ GeV}$		

Non-prompt yield estimated from data CRs by pass-fail method.

- QCD-enriched region (data jet-based trigger) is used to perform the first step of estimate, disjoint from other CRs and SR
- Non prompt region validates the bkg estimate.



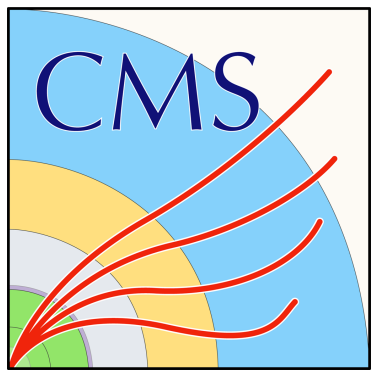


Same-sign WW with hadronic tau

DNN variables and uncertainties

Input variable	SM DNN	dim-6 DNN	dim-8 DNN
$\tau_h p_T$	✓	✓	✓
ℓp_T	✓	✓	✓
$\tau_h \eta$		✓	
$\ell \eta$		✓	
leading VBS jet p_T	✓	✓	✓
subleading VBS jet p_T	✓	✓	✓
leading VBS jet mass		✓	✓
subleading VBS jet mass		✓	✓
VBS jet pair $\Delta\phi$		✓	
M_{jj}	✓	✓	
M_{1T}	✓	✓	✓
M_{o1}	✓	✓	✓
$M_T(\tau_h, \vec{p}_T^{\text{miss}})$			✓
$M_T(\ell, \vec{p}_T^{\text{miss}})$	✓	✓	✓
$M_T(\ell, \tau_h, \vec{p}_T^{\text{miss}})$			✓
$p_T^{\text{rel}}(\ell, j_1)$		✓	
$p_T^{\text{rel}}(\ell, j_2)$		✓	
$p_T^{\text{rel}}(\tau_h, j_1)$		✓	
$p_T^{\text{rel}}(\tau_h, j_2)$		✓	
$\Delta\phi(\ell, j_1)$		✓	
$\Delta\phi(\ell, j_2)$		✓	
$\Delta\phi(\tau_h, j_1)$		✓	
$\Delta\phi(\tau_h, j_2)$		✓	
$p_{T, \text{leading } \tau_h \text{ track}} / p_{T, \tau_h}$	✓	✓	
Zeppenfeld variable		✓	

Uncertainty source	$+\Delta\mu$	$-\Delta\mu$
Theory (PDF, QCD-scale, ISR, and FSR)	+0.157	-0.099
Non-prompt estimation	+0.136	-0.125
$t\bar{t}$ normalization	+0.051	-0.023
Prefiring	+0.105	-0.059
Luminosity	+0.079	-0.092
b -tagging and mistagging	+0.007	-0.004
Jet energy scale and resolution, Pile-up jet ID	+0.079	-0.097
Pileup	+0.152	-0.162
LO-to-NLO VBS corrections	+0.043	-0.025
Unclustered energy	+0.003	-0.010
Hadronic tau energy scale and DEEPTAU	+0.154	-0.152
Charge misidentification	+0.005	-0.010
Lepton reconstruction, identification, and isolation	+0.005	-0.024
MC statistical	+0.324	-0.322
Total systematic uncertainty	+0.344	-0.302
Data statistical uncertainty	+0.522	-0.477
Total uncertainty	+0.625	-0.564



Next to Leading Order corrections

Table 1: Summary of higher-order predictions currently available for the ss-WW channel: at fixed order and matched to parton shower. The symbols \checkmark , \checkmark^* , and \mathbf{X} means that the corresponding predictions are available, in the VBS approximation, or not available yet.

Order	$\mathcal{O}(\alpha^7)$	$\mathcal{O}(\alpha_s \alpha^6)$	$\mathcal{O}(\alpha_s^2 \alpha^5)$	$\mathcal{O}(\alpha_s^3 \alpha^4)$
NLO	\checkmark	\checkmark	\checkmark	\checkmark
NLO+PS	\checkmark	\checkmark^*	\mathbf{X}	\checkmark

Table 7: Summary of higher-order predictions currently available for the os-WW channel: at fixed order and matched to parton shower. The symbols \checkmark , \checkmark^* , and \mathbf{X} means that the corresponding predictions are available, in the VBS approximation, or not yet.

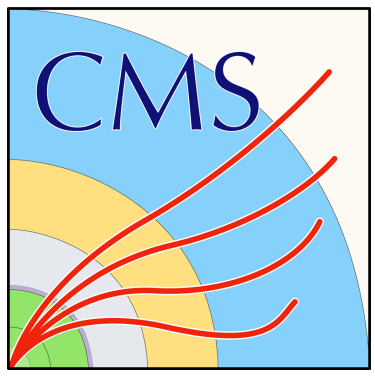
Order	$\mathcal{O}(\alpha^7)$	$\mathcal{O}(\alpha_s \alpha^6)$	$\mathcal{O}(\alpha_s^2 \alpha^5)$	$\mathcal{O}(\alpha_s^3 \alpha^4)$
NLO	\mathbf{X}	\checkmark^*	\mathbf{X}	\checkmark
NLO+PS	\mathbf{X}	\checkmark^*	\mathbf{X}	\checkmark

Table 3: Summary of higher-order predictions currently available for the WZ channel: at fixed order and matched to parton shower. The symbols \checkmark , \checkmark^* , and \mathbf{X} means that the corresponding predictions are available, in the VBS approximation, or not yet.

Order	$\mathcal{O}(\alpha^7)$	$\mathcal{O}(\alpha_s \alpha^6)$	$\mathcal{O}(\alpha_s^2 \alpha^5)$	$\mathcal{O}(\alpha_s^3 \alpha^4)$
NLO	\checkmark	\checkmark	\mathbf{X}	\checkmark
NLO+PS	\mathbf{X}	\checkmark^*	\mathbf{X}	\checkmark

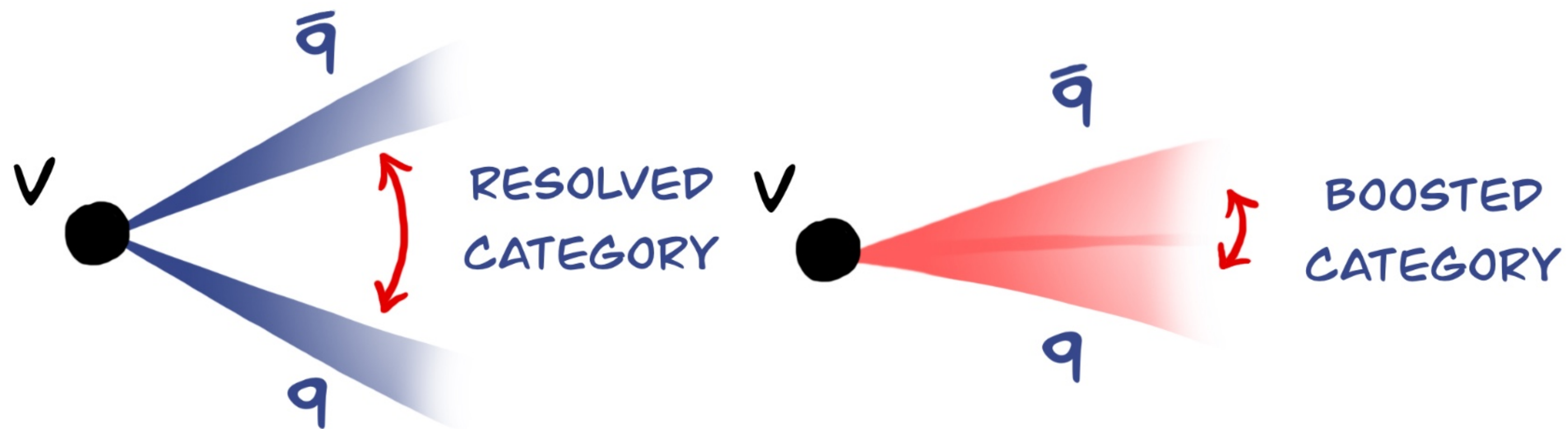
Table 5: Summary of higher-order predictions currently available for the ZZ channel: at fixed order and matched to parton shower. The symbols \checkmark , \checkmark^* , and \mathbf{X} means that the corresponding predictions are available, in the VBS approximation, or not yet.

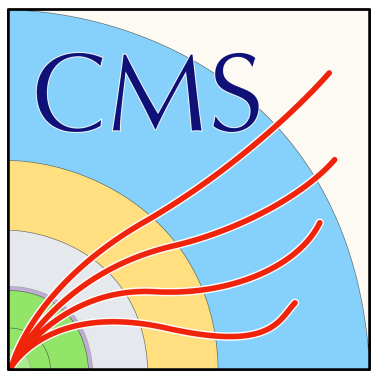
Order	$\mathcal{O}(\alpha^7)$	$\mathcal{O}(\alpha_s \alpha^6)$	$\mathcal{O}(\alpha_s^2 \alpha^5)$	$\mathcal{O}(\alpha_s^3 \alpha^4)$
NLO	\checkmark	\checkmark	\mathbf{X}	\checkmark
NLO+PS	\mathbf{X}	\checkmark^*	\mathbf{X}	\checkmark



WW semi-leptonic

- First evidence for EW production of $WV+2\text{jets}$ ($V = W, Z$) in semi-leptonic channel
- To maximize the efficiency for the signal, different selection requirements are applied depending on jet p_T . Two categories of events, based on reconstruction of hadronically decaying V : resolved (2 distinct jets with dijet mass $\sim V_{\text{mass}}$) or boosted (1 large-radius jet)
- Multivariate ML discriminators optimized to separate signal and bkg





WV semi-leptonic

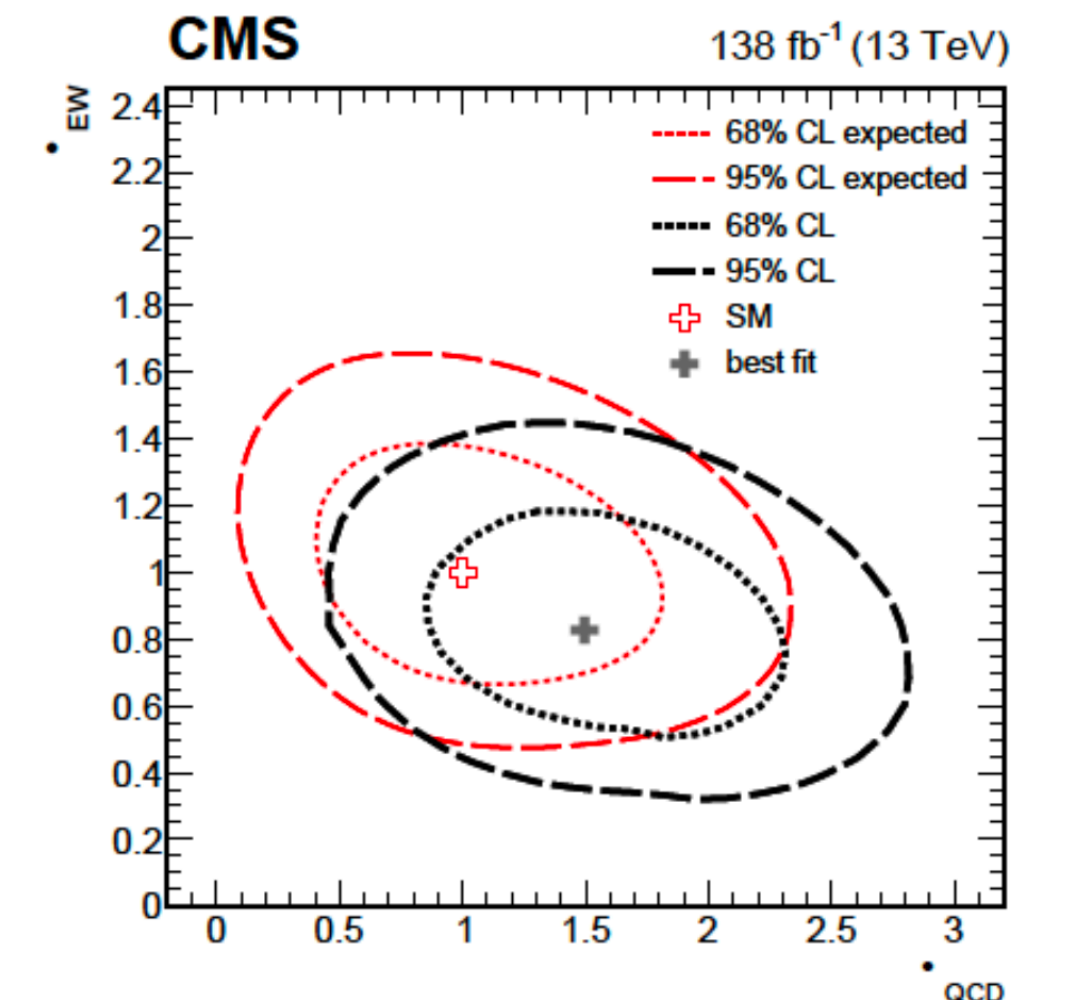
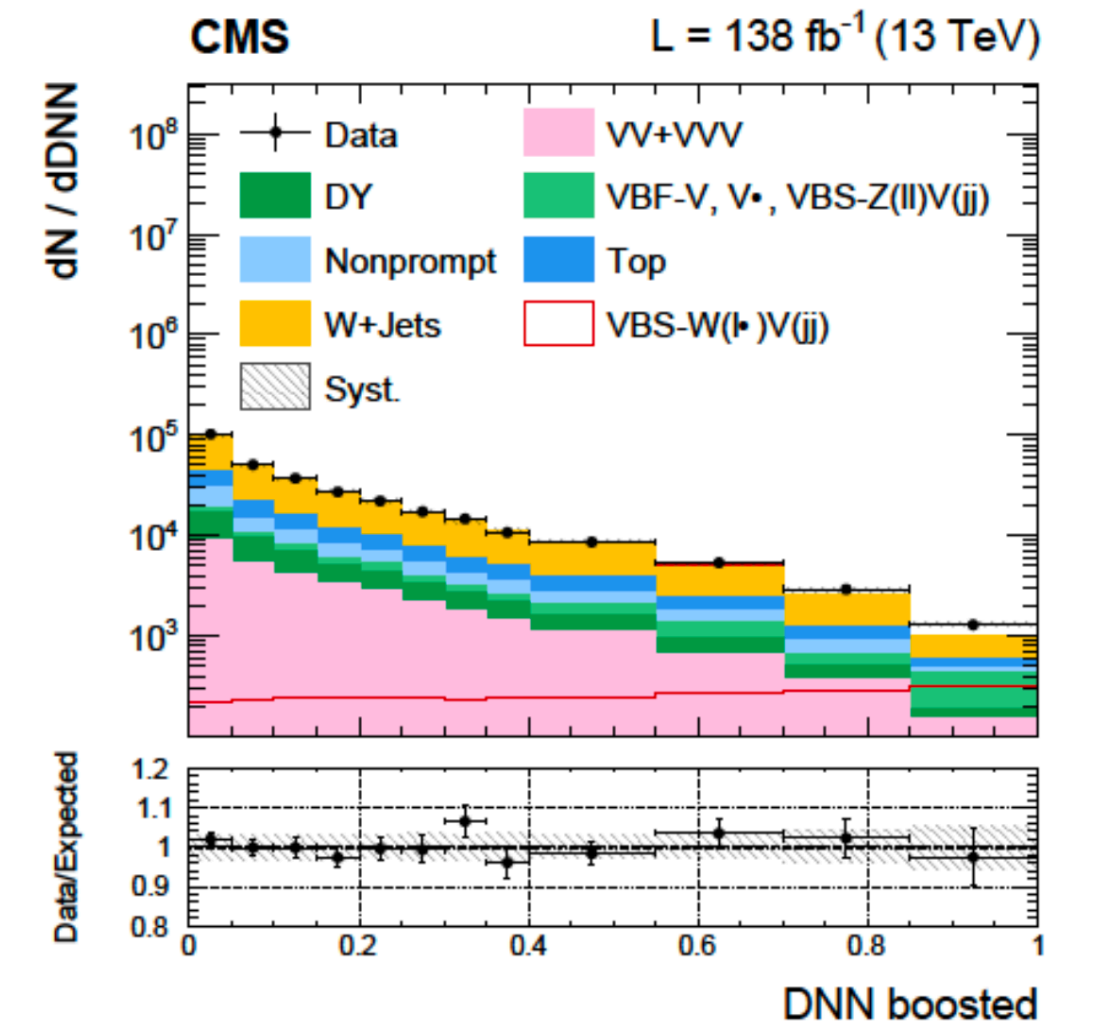
- Measurement of purely EW WV signal strength ($\mu_{\text{QCD}} = 1$) and EWK+QCD WV signal strength (EWK/QCD ratio fixed to SM) in a fiducial phase space region.

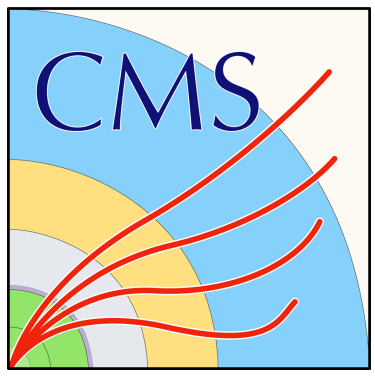
Signal	$\mu = \sigma_{\text{OBS}}/\sigma_{\text{SM}}$	Cross Section [pb]
EWK WV	$0.85 \pm 0.12(\text{stat})_{-0.17}^{+0.19}(\text{syst})$	$1.90_{-0.46}^{+0.53}$
EWK+QCD WV	$0.97 \pm 0.06(\text{stat})_{-0.21}^{+0.19}(\text{syst})$	$16.4_{-2.8}^{+3.5}$

Significance 4.4σ (5.1σ exp.)

- Simultaneous EW and QCD WV production fit: signal strengths of two components are left as free independent parameters.

Agreement with SM predictions within 68% CL





Summary of other CMS results

ZZ to 4L + 2jets

		Perturbative order	SM σ (fb)	Measured σ (fb)
		ZZjj inclusive		
EW	LO		0.275 ± 0.021	$0.33^{+0.11}_{-0.10}$ (stat) $^{+0.04}_{-0.03}$ (syst)
	NLO QCD		0.278 ± 0.017	
	NLO EW		$0.242^{+0.015}_{-0.013}$	
EW+QCD			5.35 ± 0.51	$5.29^{+0.31}_{-0.30}$ (stat) ± 0.47 (syst)
		VBS-enriched (loose)		
EW	LO		0.186 ± 0.015	$0.180^{+0.070}_{-0.060}$ (stat) $^{+0.021}_{-0.012}$ (syst)
	NLO QCD		0.197 ± 0.013	
EW+QCD			1.21 ± 0.09	$1.00^{+0.12}_{-0.11}$ (stat) ± 0.07 (syst)
		VBS-enriched (tight)		
EW	LO		0.104 ± 0.008	$0.09^{+0.04}_{-0.03}$ (stat) ± 0.02 (syst)
	NLO QCD		0.108 ± 0.007	
EW+QCD			0.221 ± 0.014	$0.20^{+0.05}_{-0.04}$ (stat) ± 0.02 (syst)

$$-0.24 < f_{T0}/\Lambda^4 < 0.22$$

$$-0.31 < f_{T1}/\Lambda^4 < 0.31$$

$$-0.63 < f_{T2}/\Lambda^4 < 0.59$$

$$-0.43 < f_{T8}/\Lambda^4 < 0.43$$

$$-0.92 < f_{T9}/\Lambda^4 < 0.92$$

Most stringent limits to date on FT8 and FT9 dim-8 operators.

Polarized ssWW

Process	$\sigma \mathcal{B}$ (fb)	Theoretical prediction (fb)
$W_L^\pm W_L^\pm$	$0.32^{+0.42}_{-0.40}$	0.44 ± 0.05
$W_X^\pm W_T^\pm$	$3.06^{+0.51}_{-0.48}$	3.13 ± 0.35
$W_L^\pm W_X^\pm$	$1.20^{+0.56}_{-0.53}$	1.63 ± 0.18
$W_T^\pm W_T^\pm$	$2.11^{+0.49}_{-0.47}$	1.94 ± 0.21

WW CoM frame

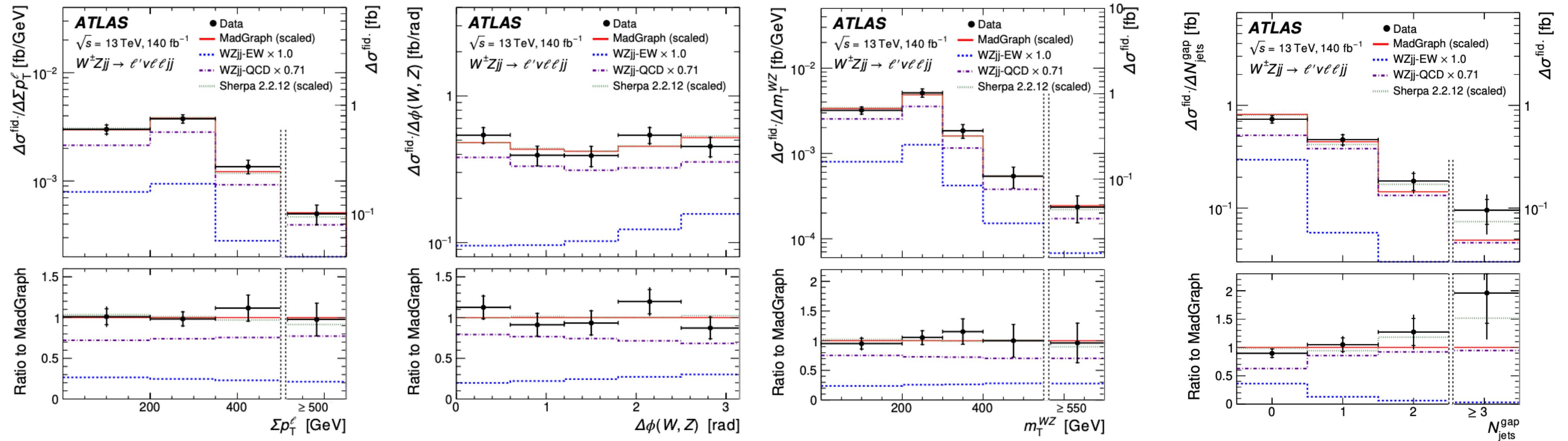
Process	$\sigma \mathcal{B}$ (fb)	Theoretical prediction (fb)
$W_L^\pm W_L^\pm$	$0.24^{+0.40}_{-0.37}$	0.28 ± 0.03
$W_X^\pm W_T^\pm$	$3.25^{+0.50}_{-0.48}$	3.32 ± 0.37
$W_L^\pm W_X^\pm$	$1.40^{+0.60}_{-0.57}$	1.71 ± 0.19
$W_T^\pm W_T^\pm$	$2.03^{+0.51}_{-0.50}$	1.89 ± 0.21

p-p CoM frame

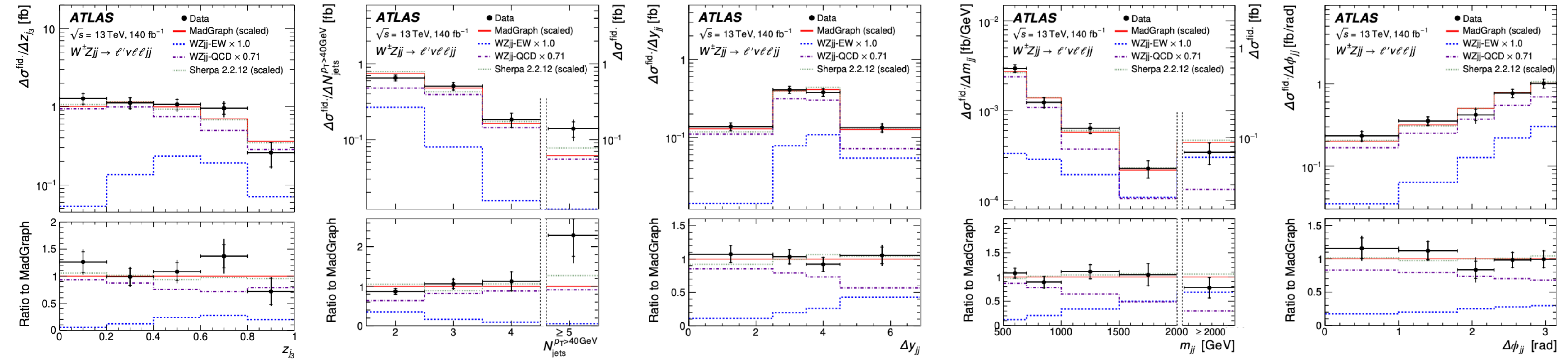
Observed (expected) CL@95% upper limit on xsec for L-polarized ssWW: **1.17 (0.88) fb** (WW CoM frame)

EWK production for ssWW (at least one W longitudinally polarized) lead to observed (expected) significance of **2.3 (3.1) σ** .

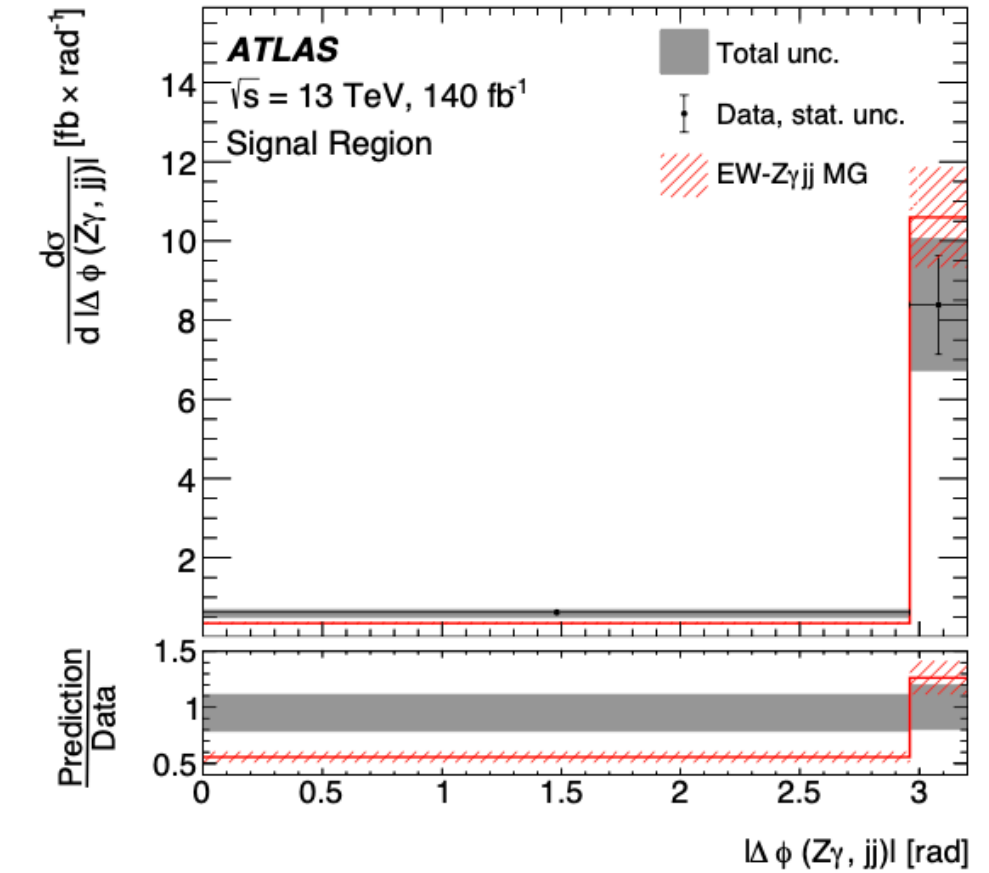
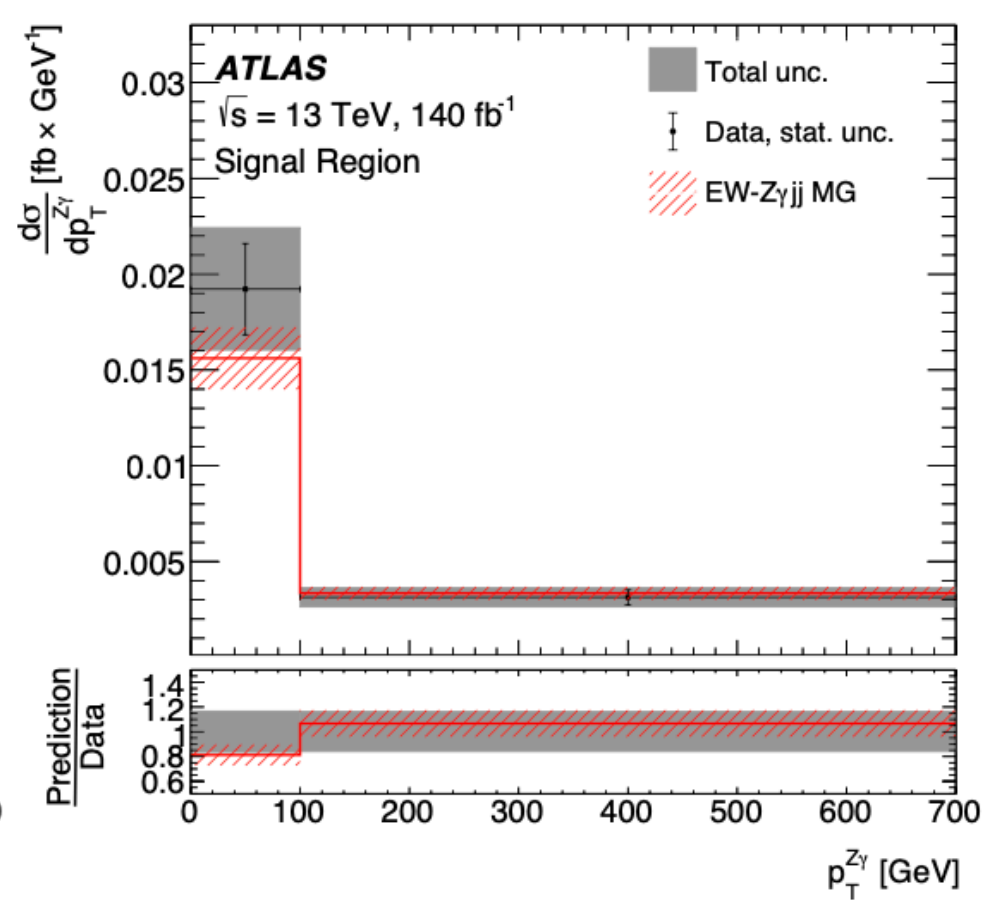
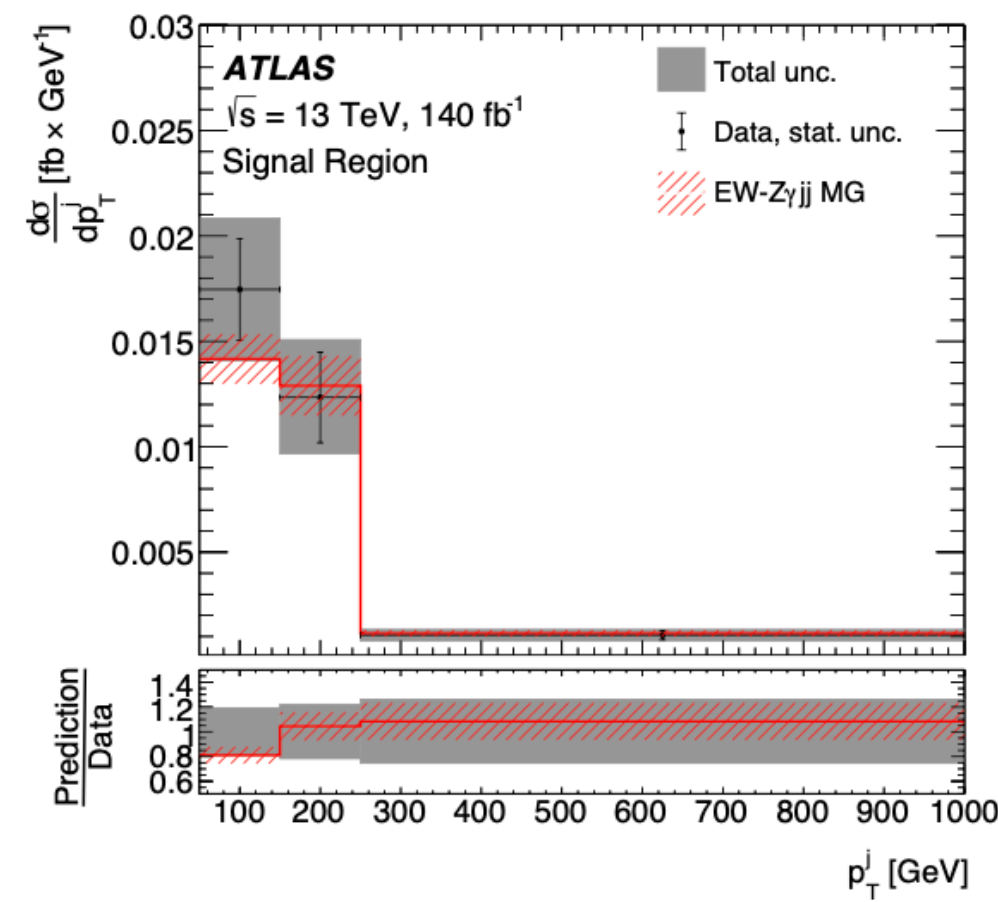
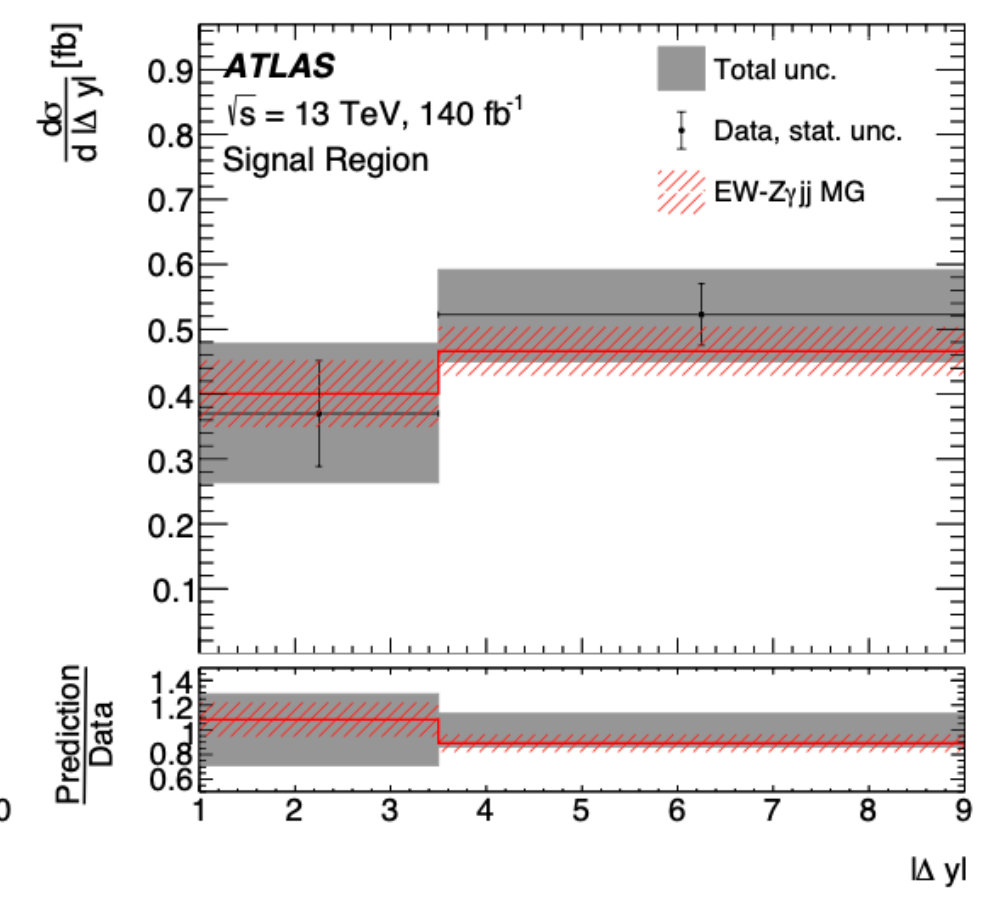
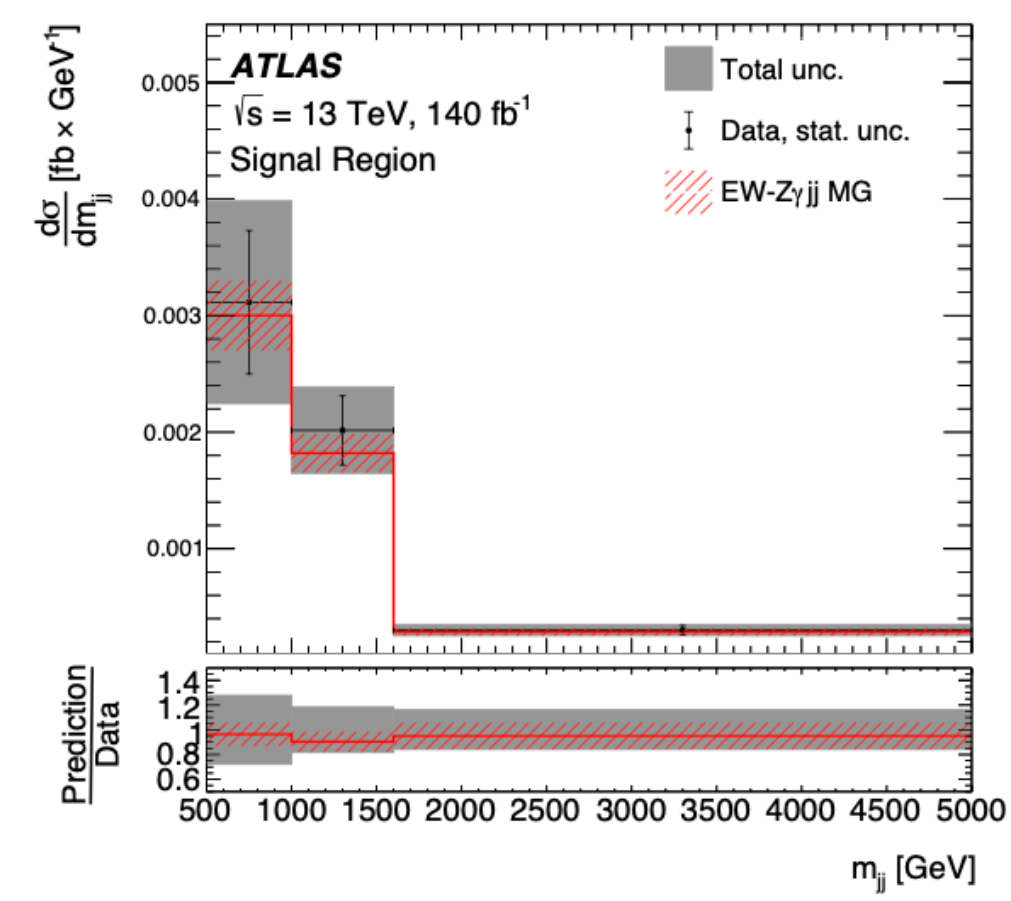
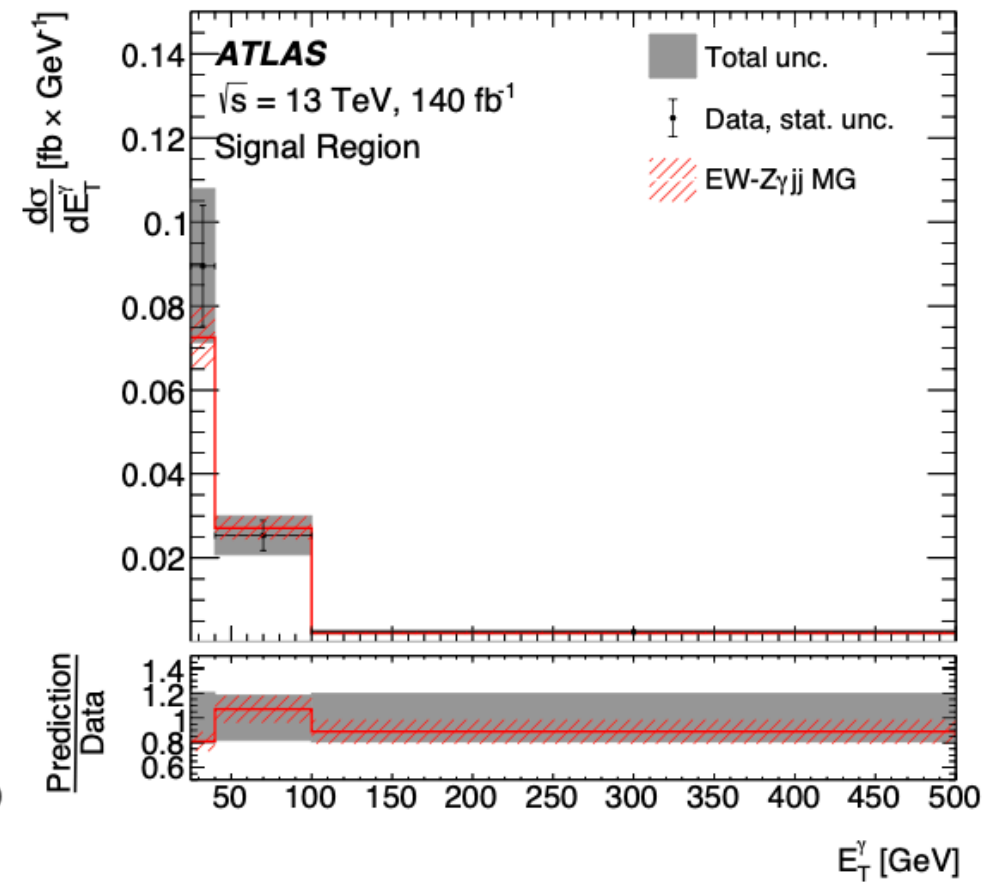
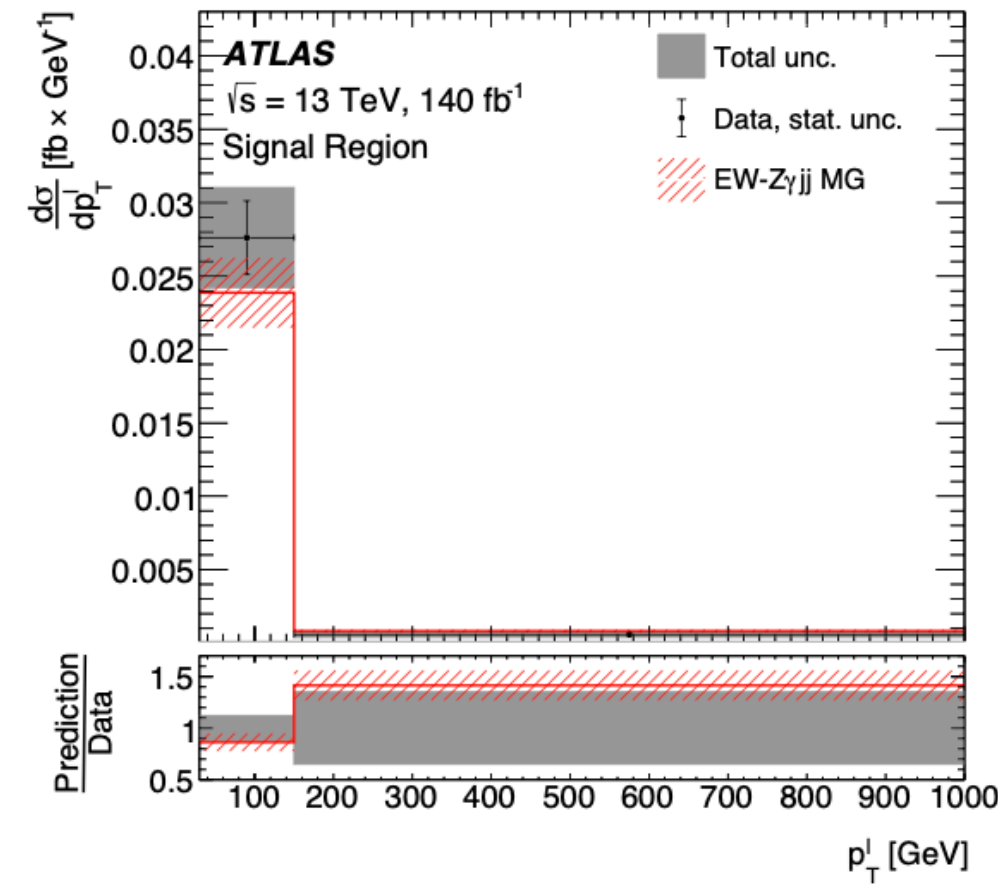
VBS WZ - differential distributions (1)



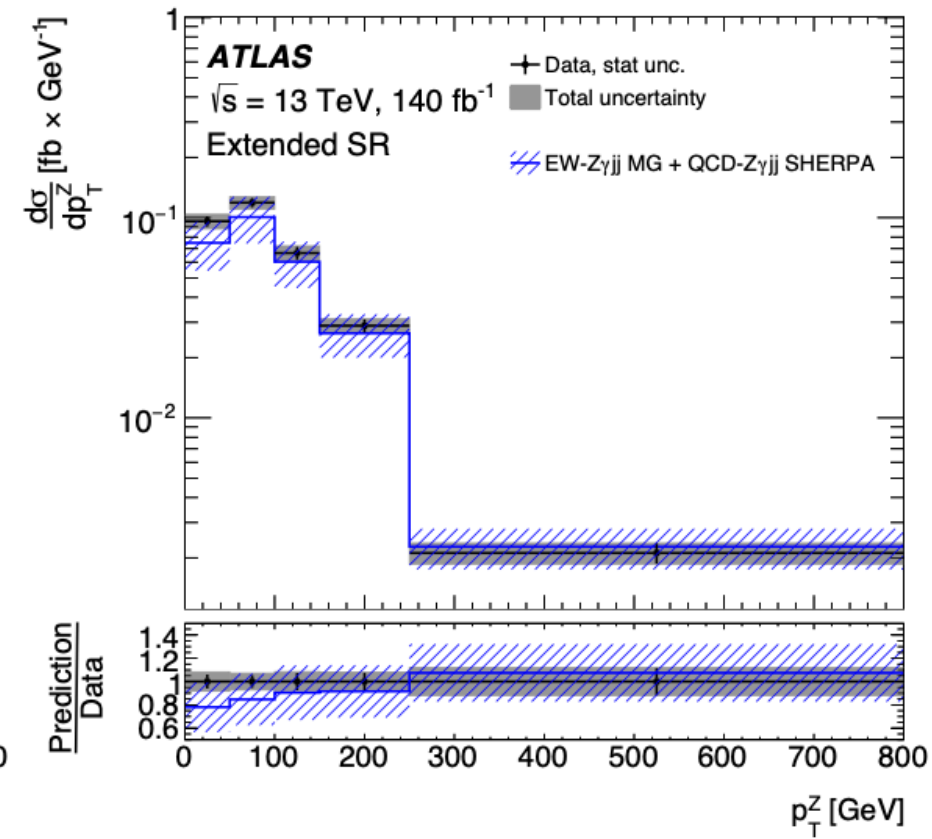
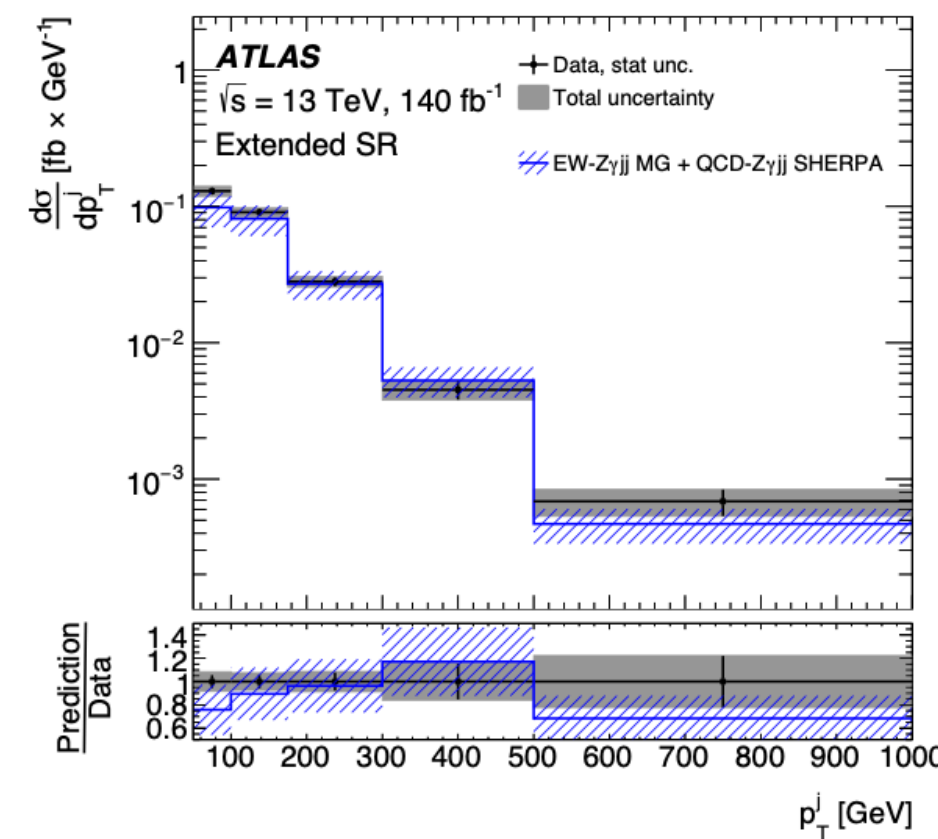
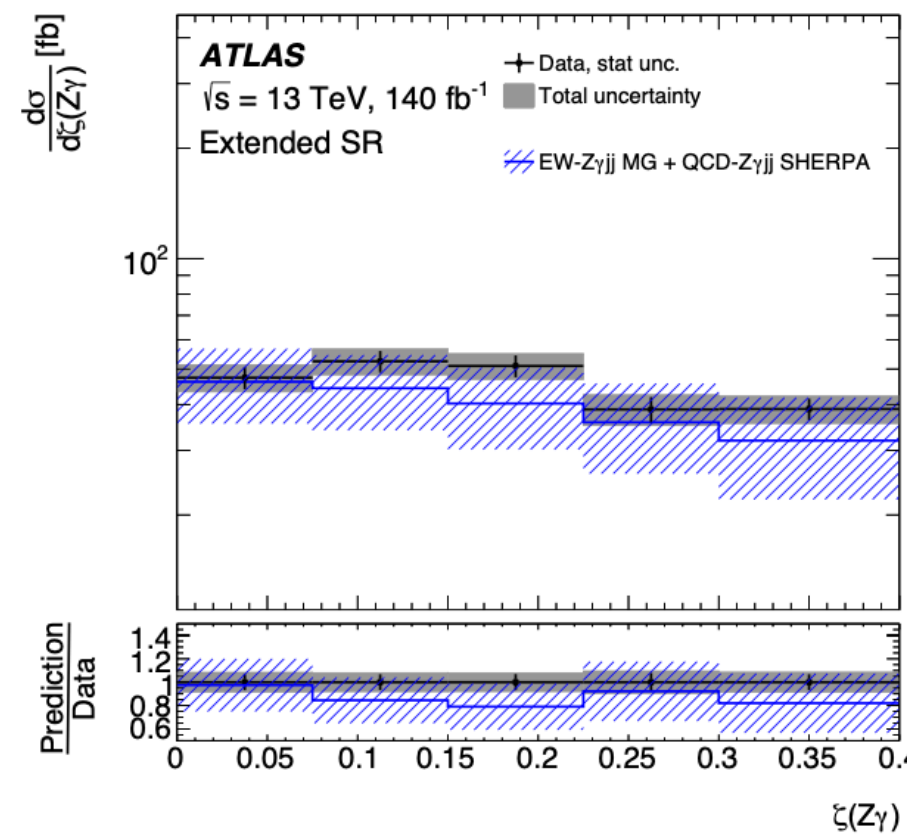
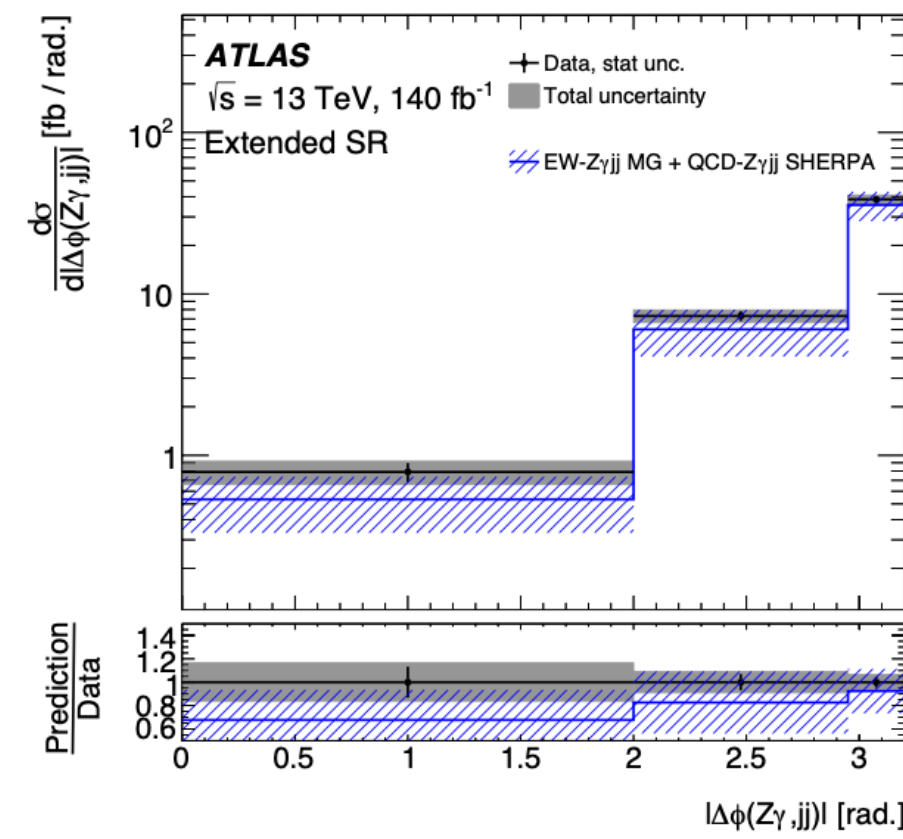
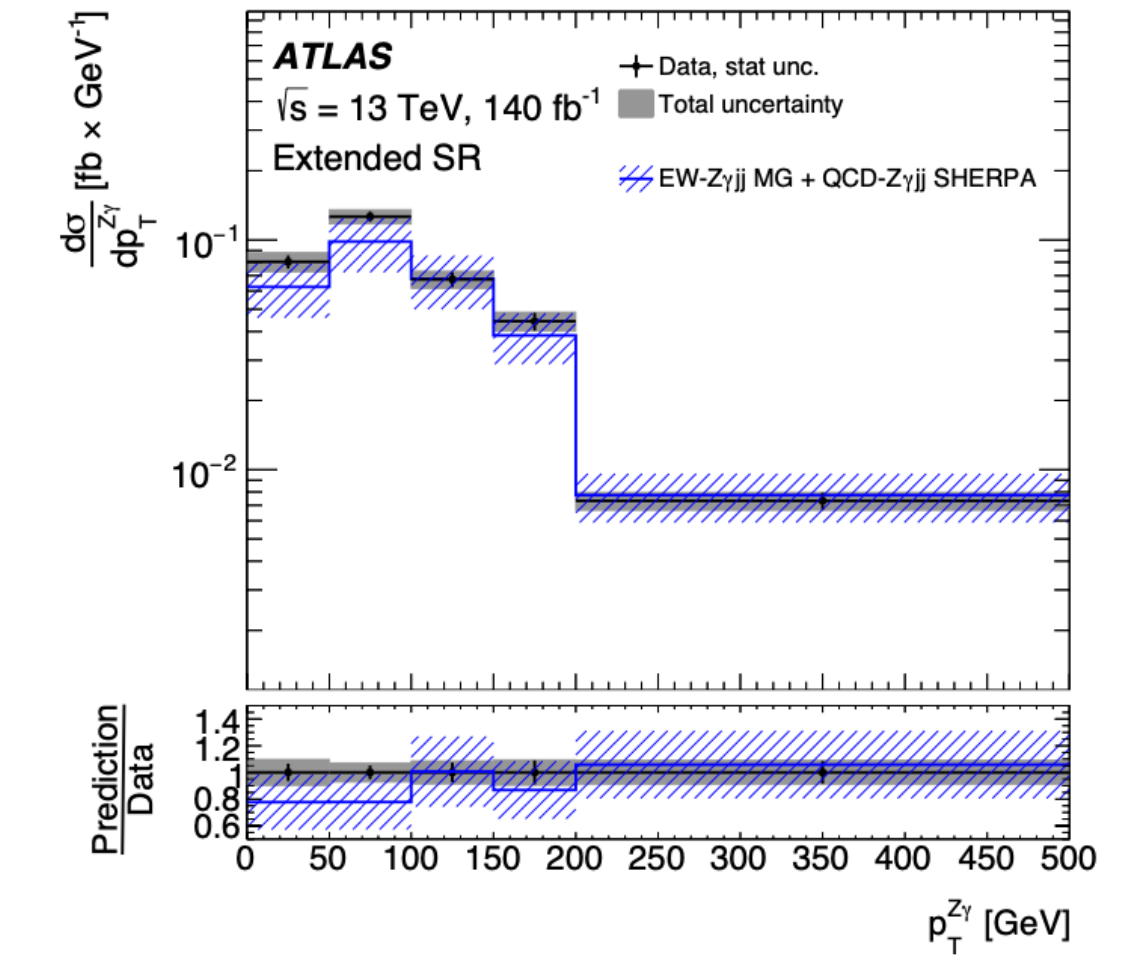
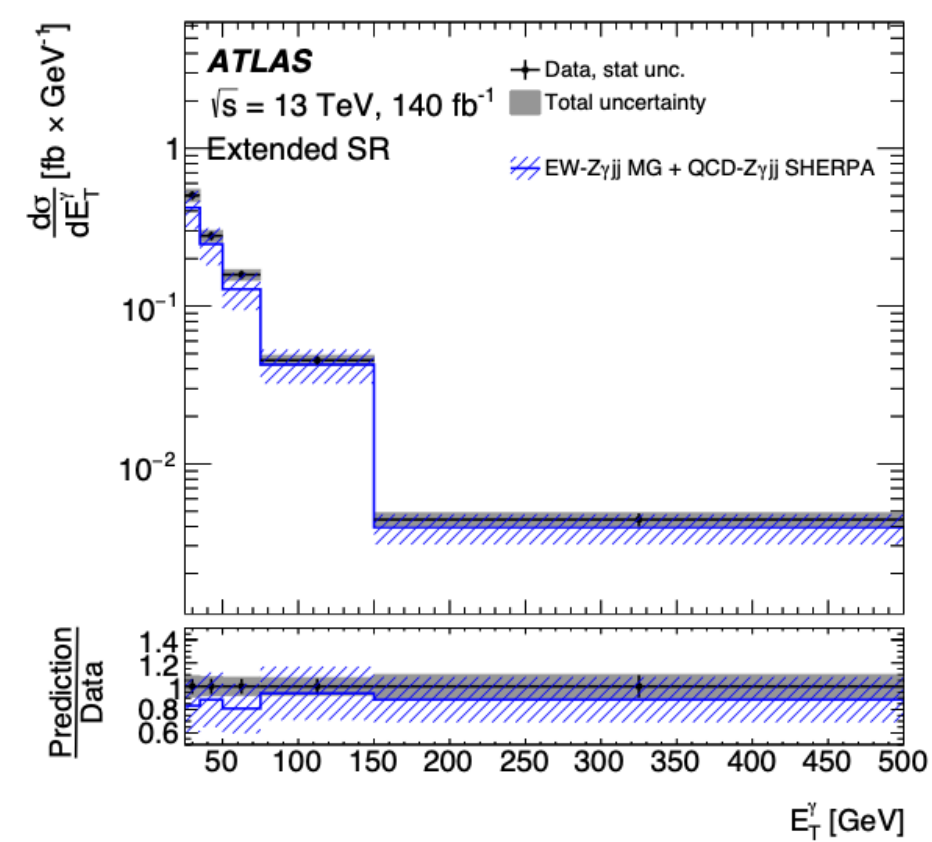
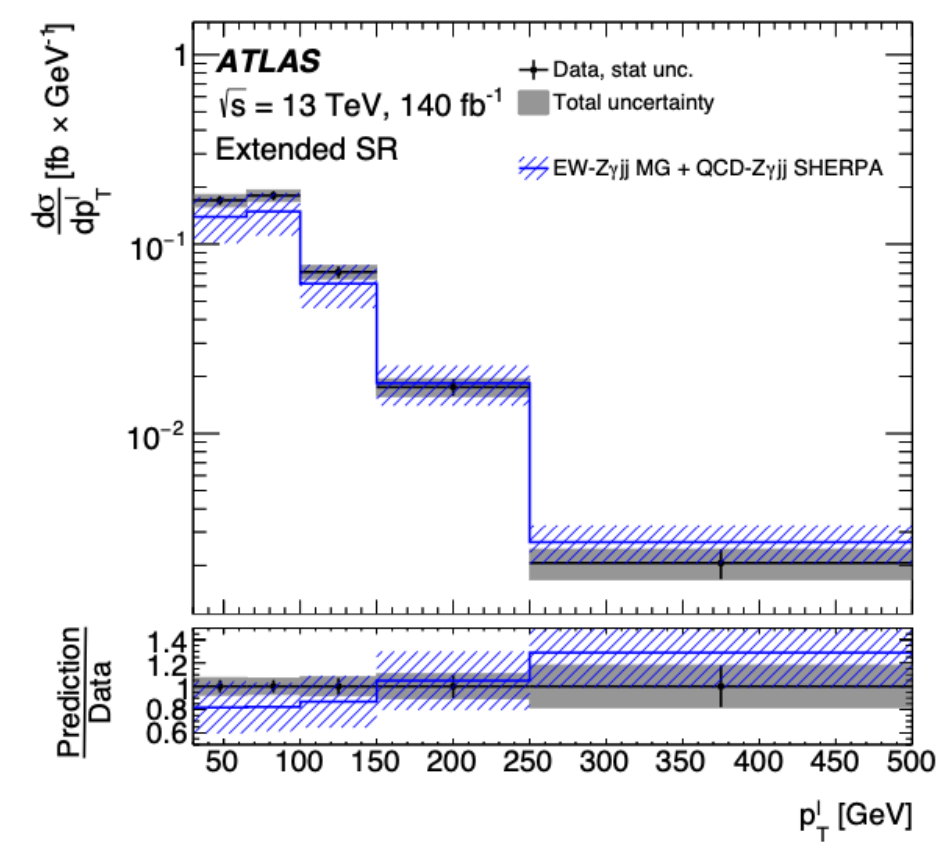
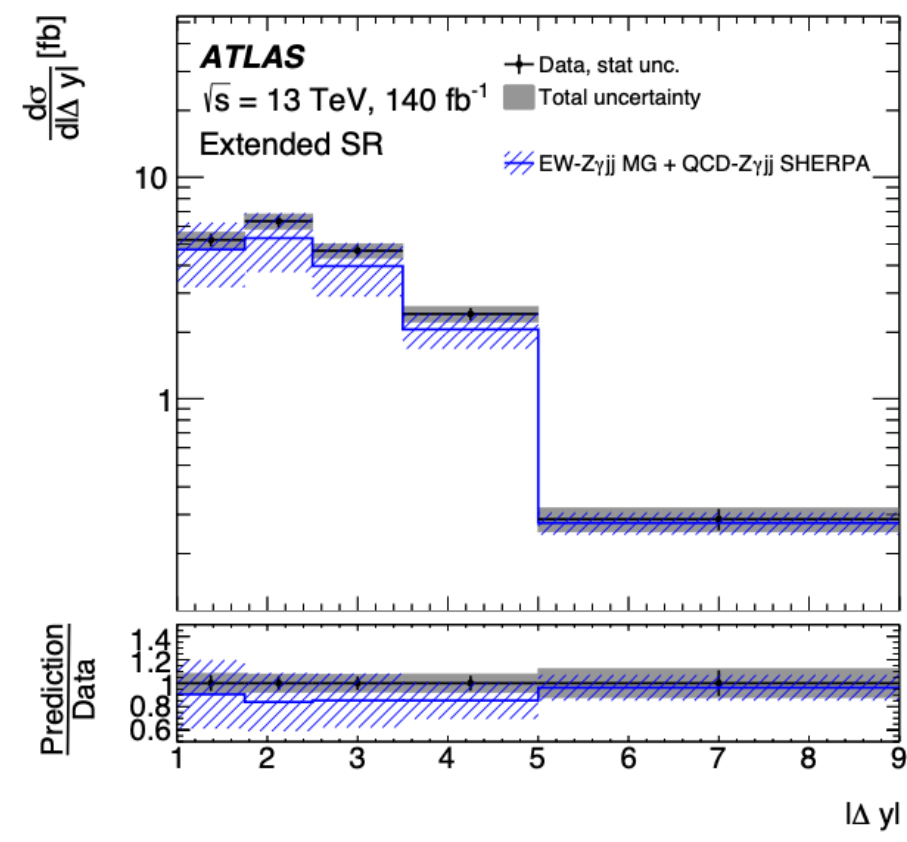
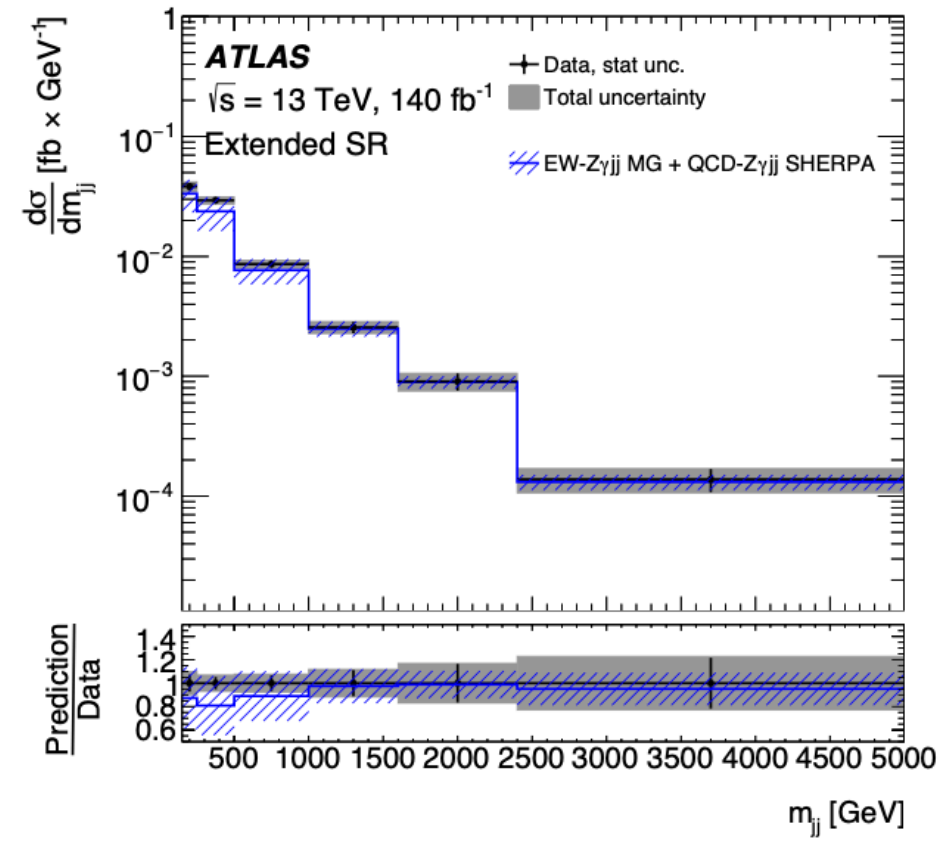
VBS WZ - differential distributions (2)



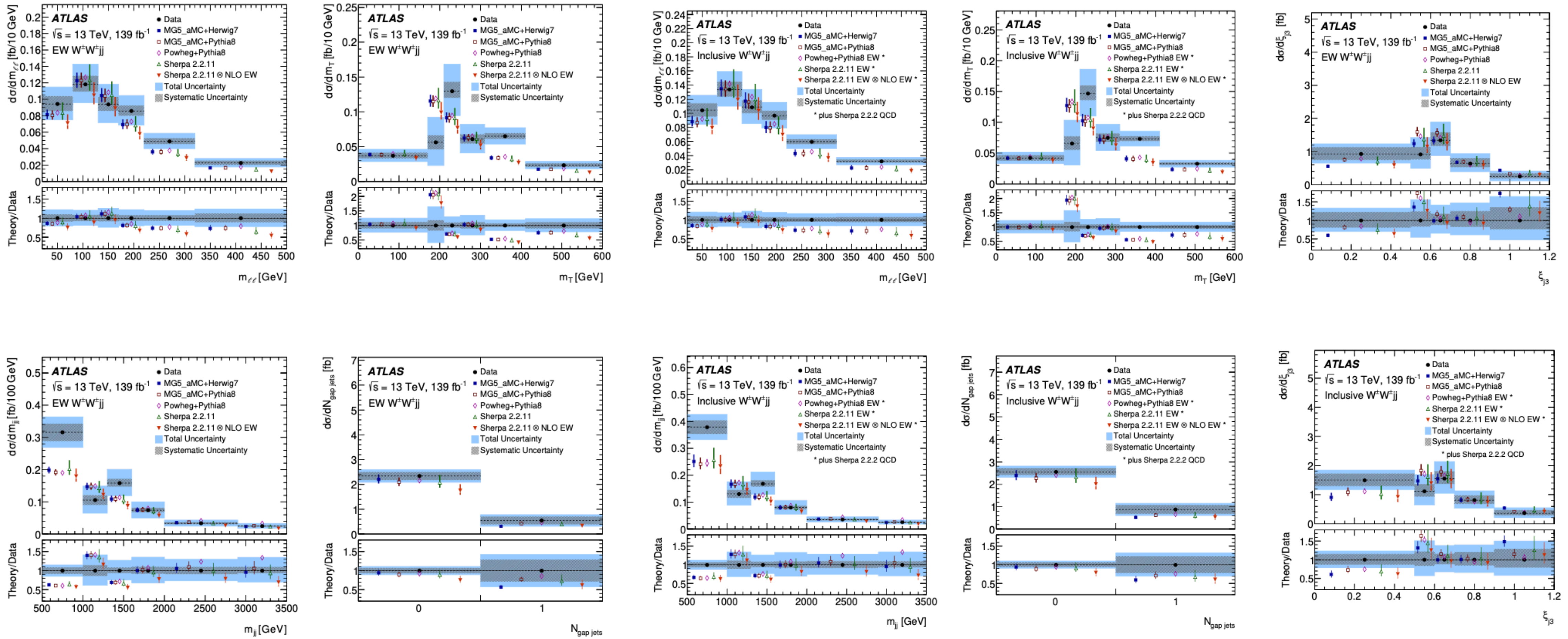
$Z\gamma jj$ - results (1)



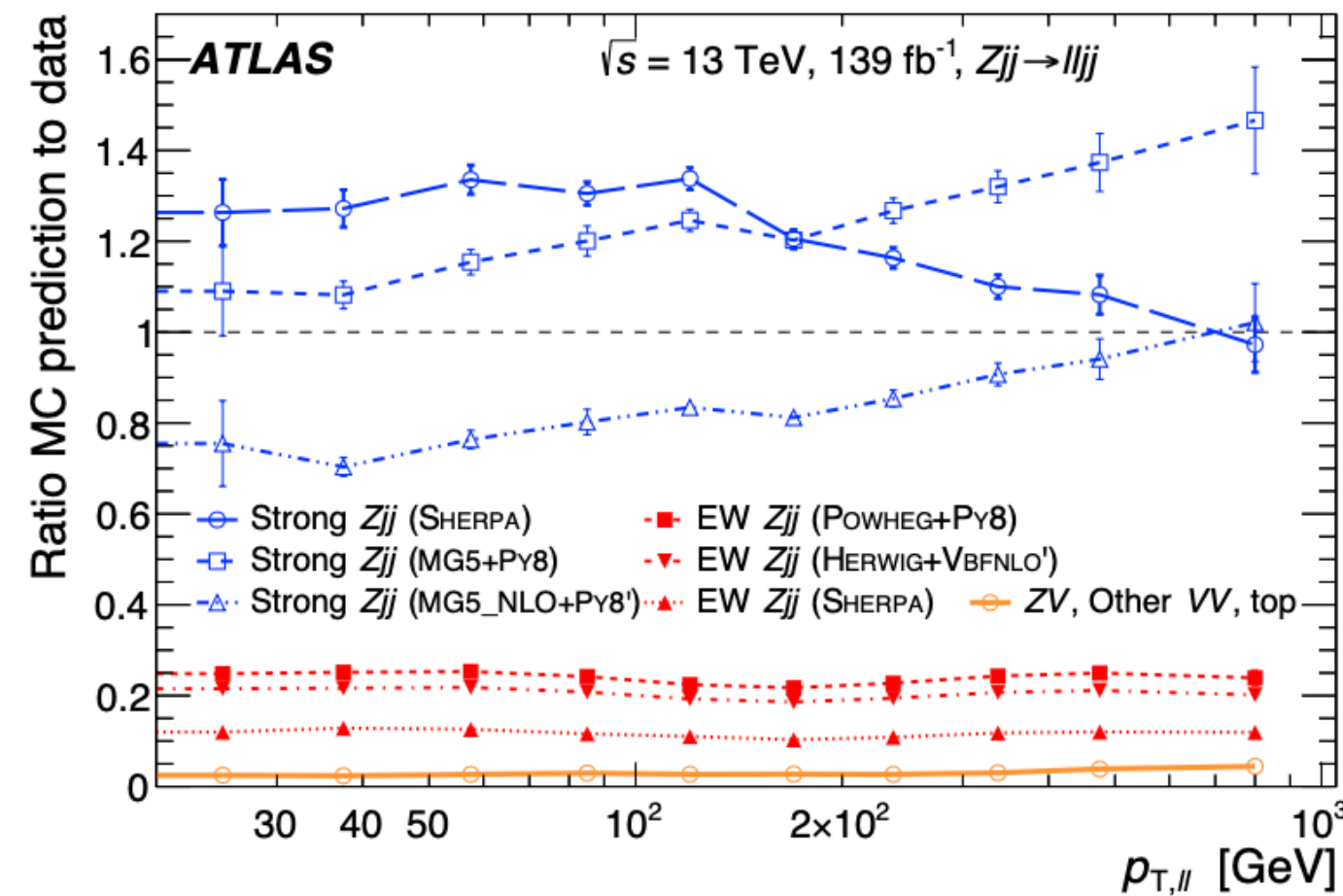
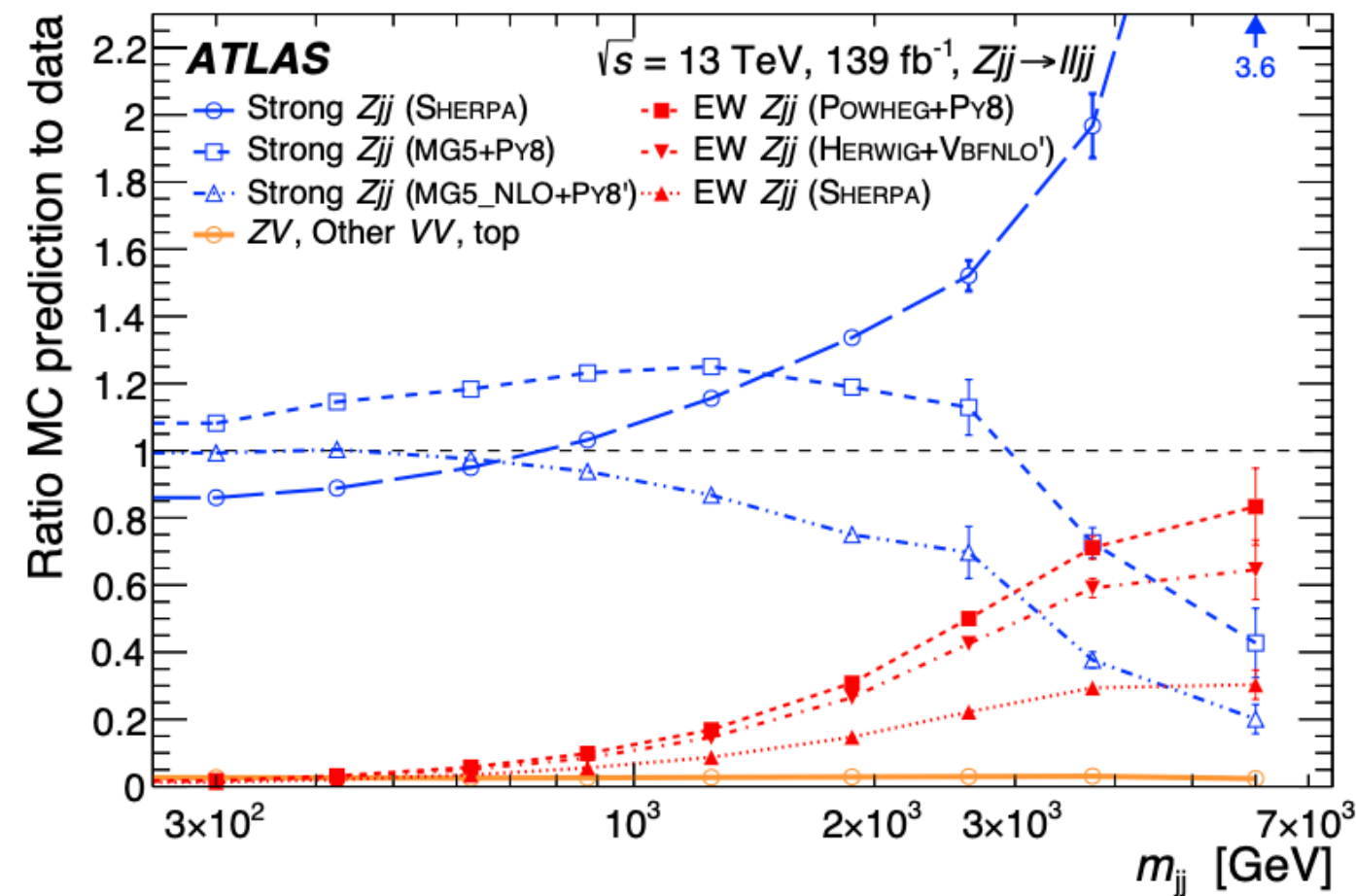
$Z\gamma jj$ - results (2)



Same-sign WW - results (1)



VBF Zjj - some detail

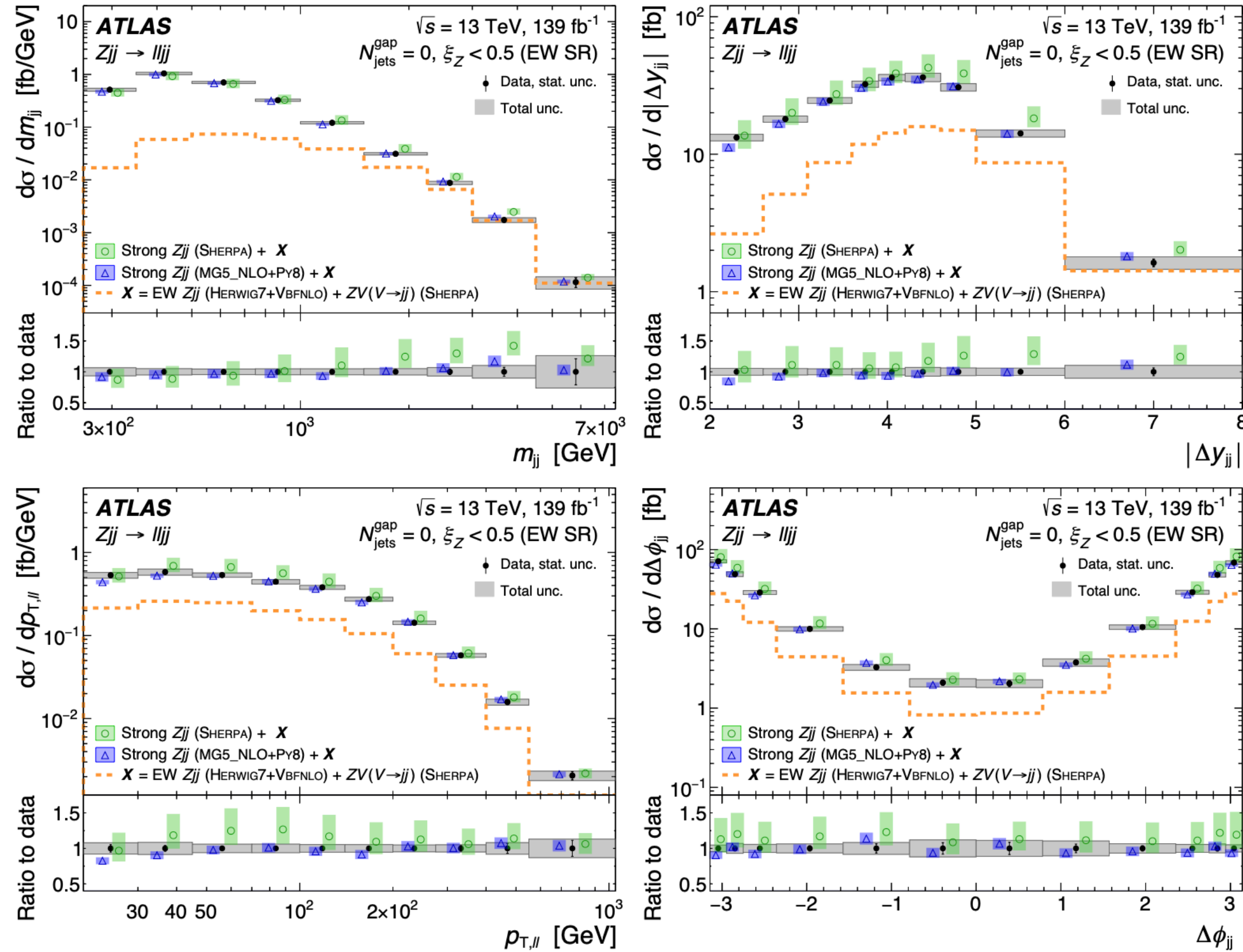


Deviation from data before fit
for different generators

Dressed muons	$p_T > 25 \text{ GeV}$ and $ \eta < 2.4$
Dressed electrons	$p_T > 25 \text{ GeV}$ and $ \eta < 2.47$ (excluding $1.37 < \eta < 1.52$)
Jets	$p_T > 25 \text{ GeV}$ and $ y < 4.4$
VBF topology	$N_\ell = 2$ (same flavour, opposite charge), $m_{\ell\ell} \in (81, 101) \text{ GeV}$ $\Delta R_{\min}(\ell_1, j) > 0.4$, $\Delta R_{\min}(\ell_2, j) > 0.4$ $N_{\text{jets}} \geq 2$, $p_T^{j1} > 85 \text{ GeV}$, $p_T^{j2} > 80 \text{ GeV}$ $p_{T,\ell\ell} > 20 \text{ GeV}$, $p_T^{\text{bal}} < 0.15$ $m_{jj} > 1000 \text{ GeV}$, $ \Delta y_{jj} > 2$, $\xi_Z < 1$
CRa	VBF topology $\oplus N_{\text{jets}}^{\text{gap}} \geq 1$ and $\xi_Z < 0.5$
CRb	VBF topology $\oplus N_{\text{jets}}^{\text{gap}} \geq 1$ and $\xi_Z > 0.5$
CRc	VBF topology $\oplus N_{\text{jets}}^{\text{gap}} = 0$ and $\xi_Z > 0.5$
SR	VBF topology $\oplus N_{\text{jets}}^{\text{gap}} = 0$ and $\xi_Z < 0.5$

SR and CR definition

VBF Zjj - other results

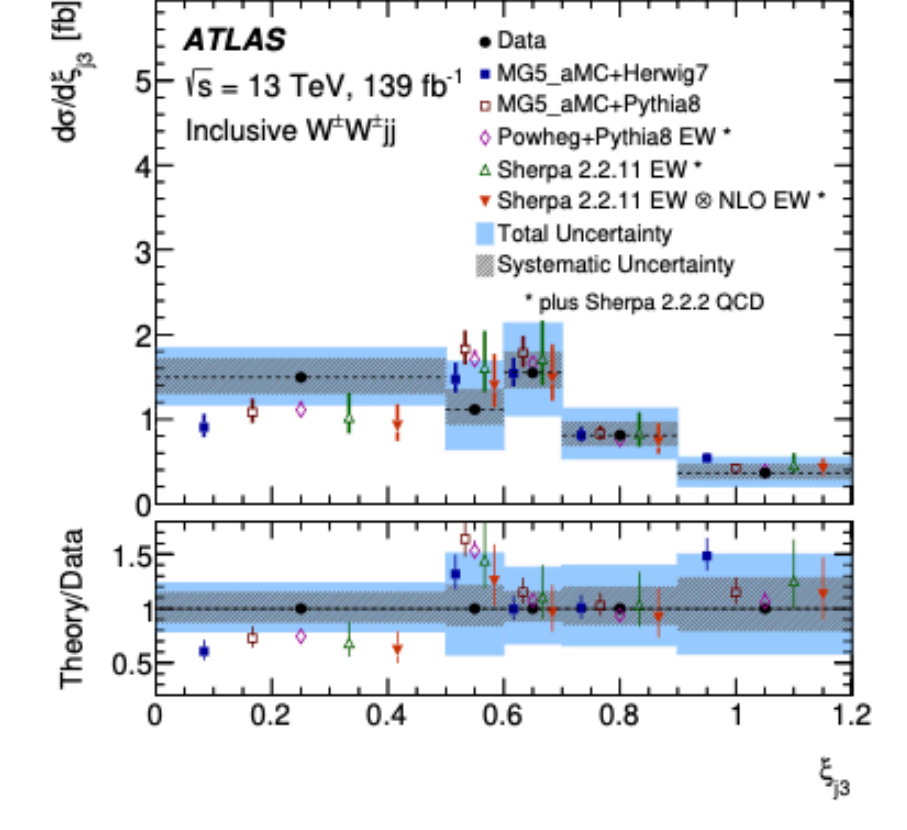
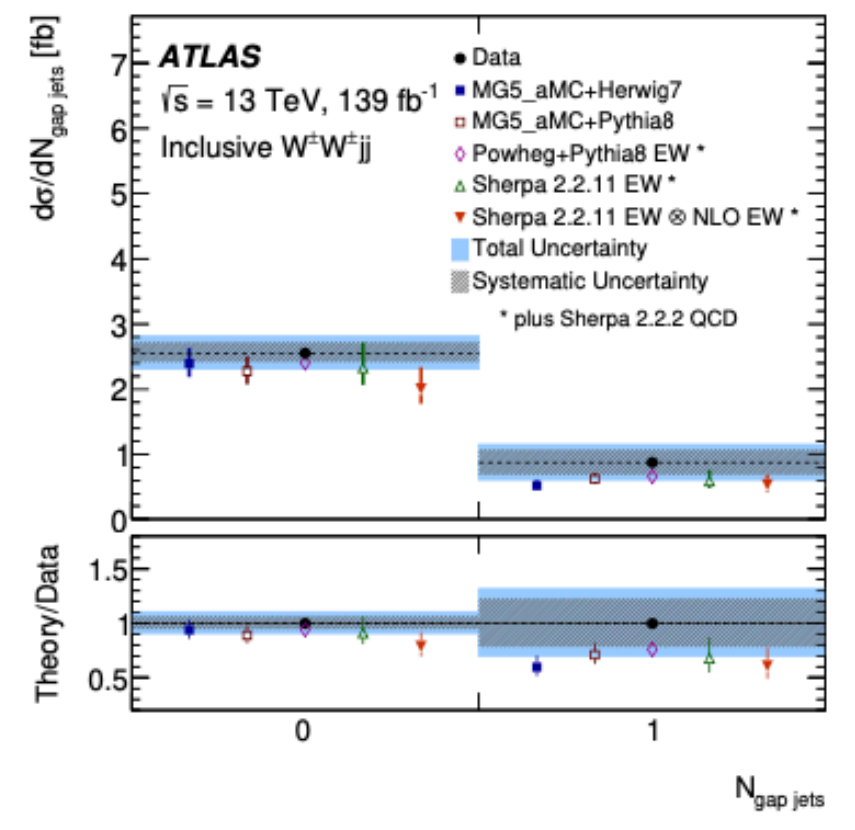
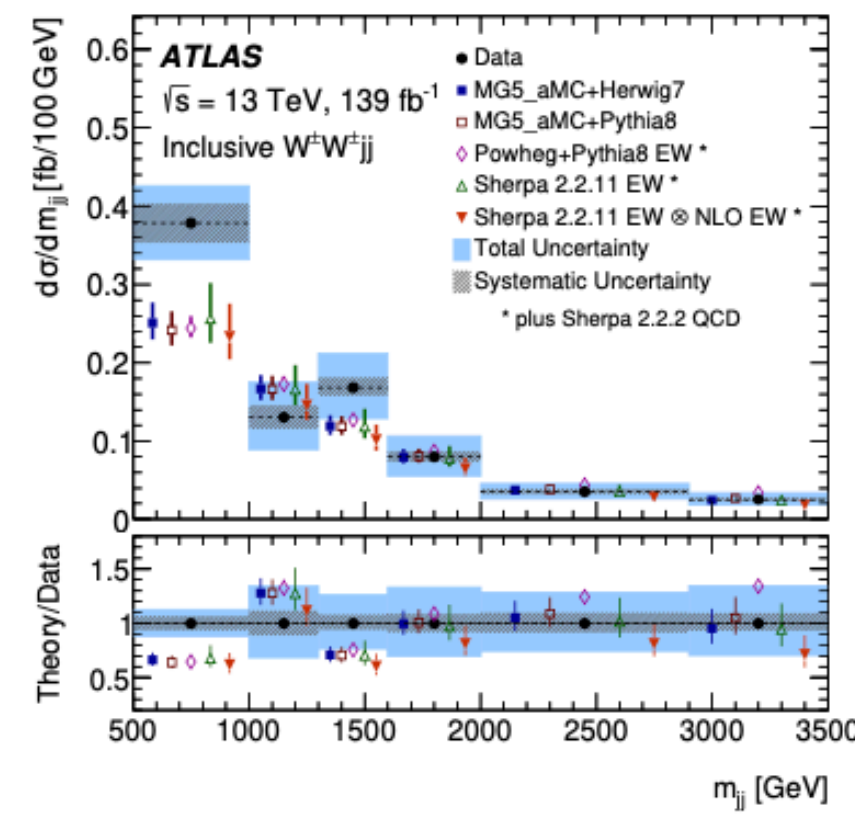
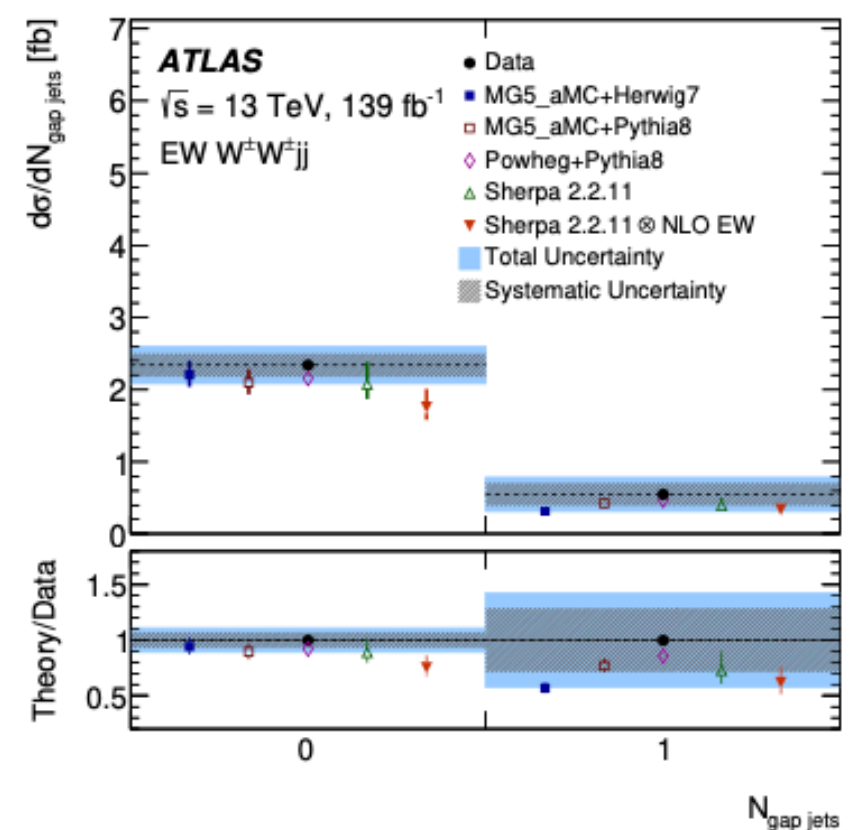
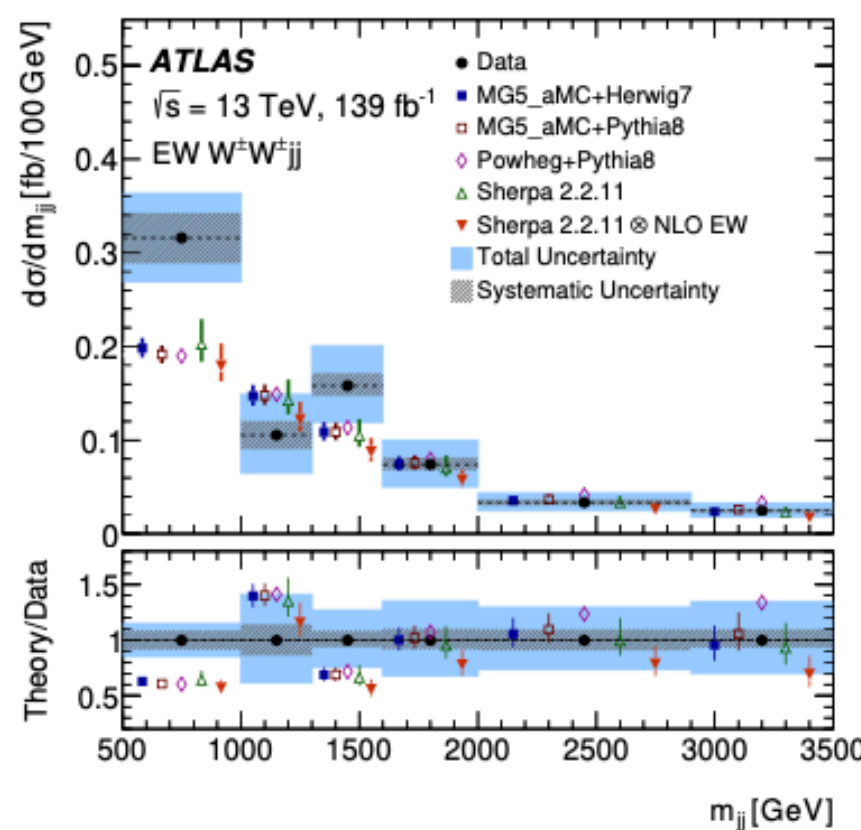
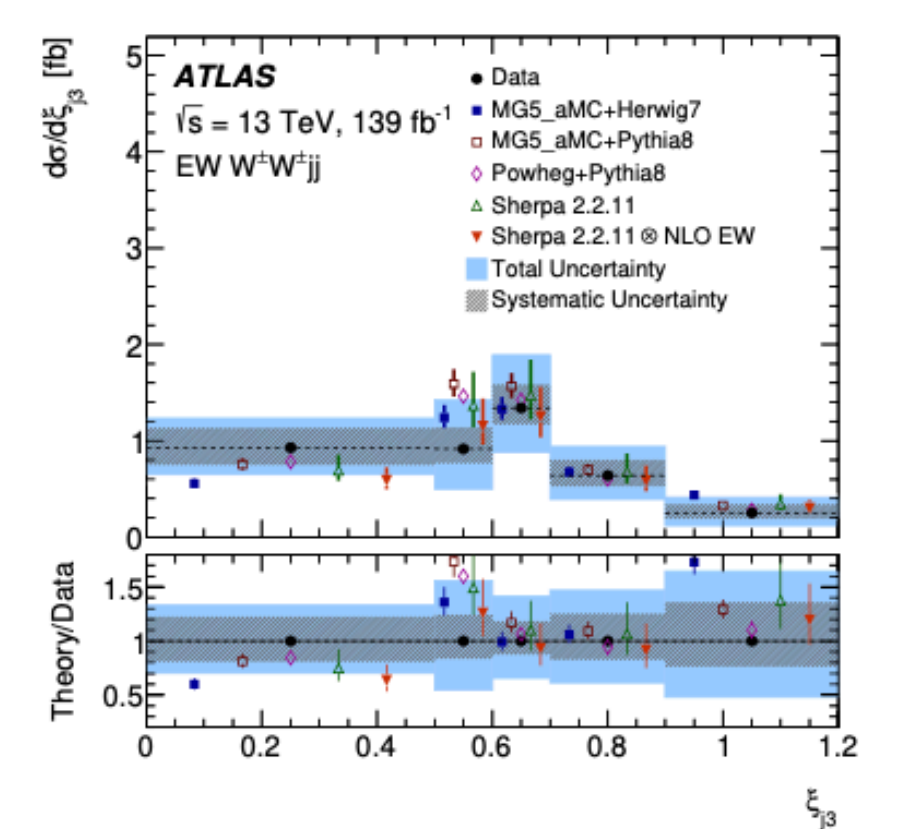
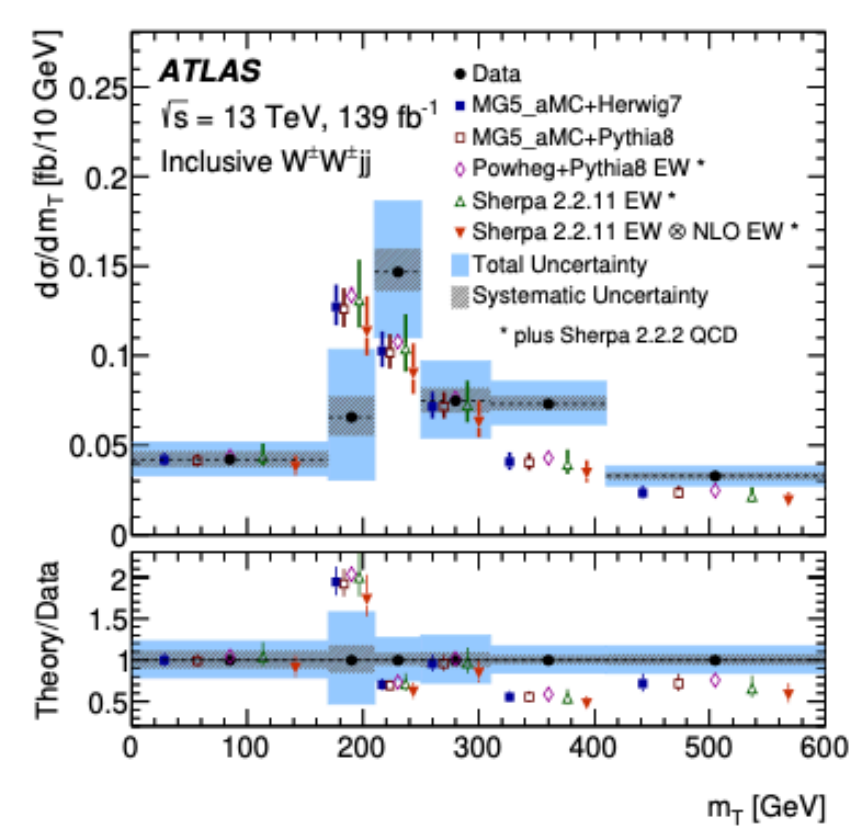
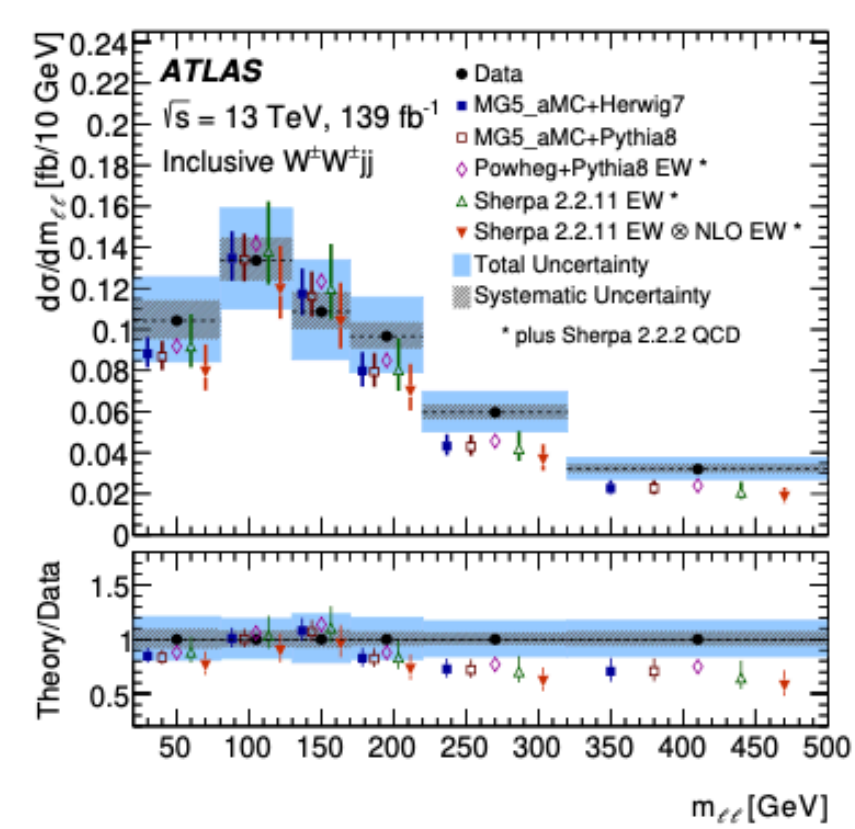
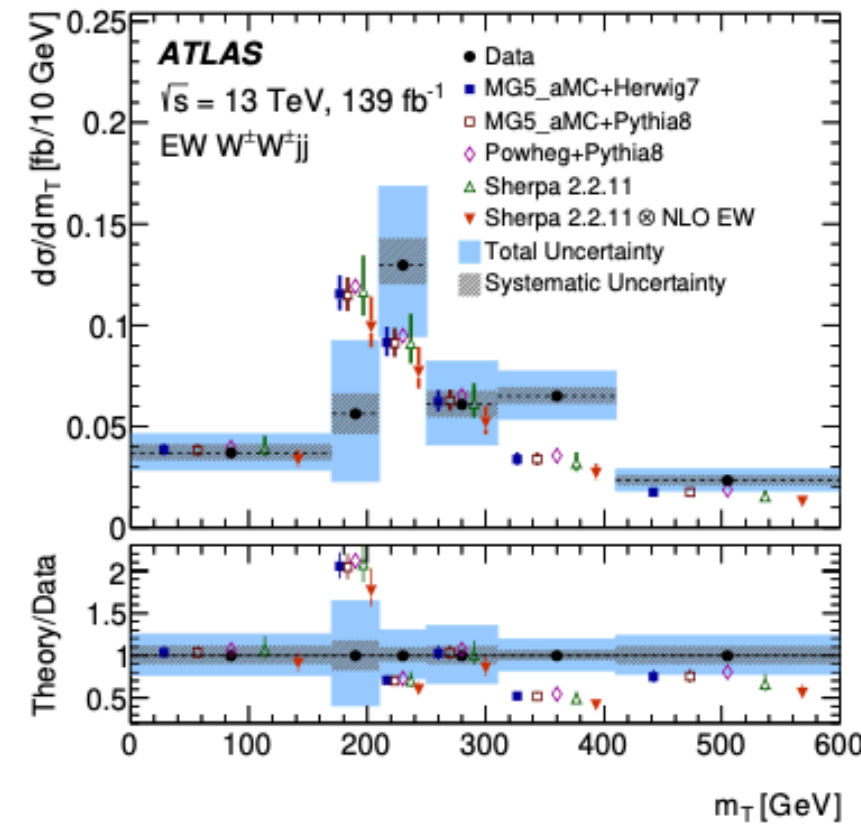
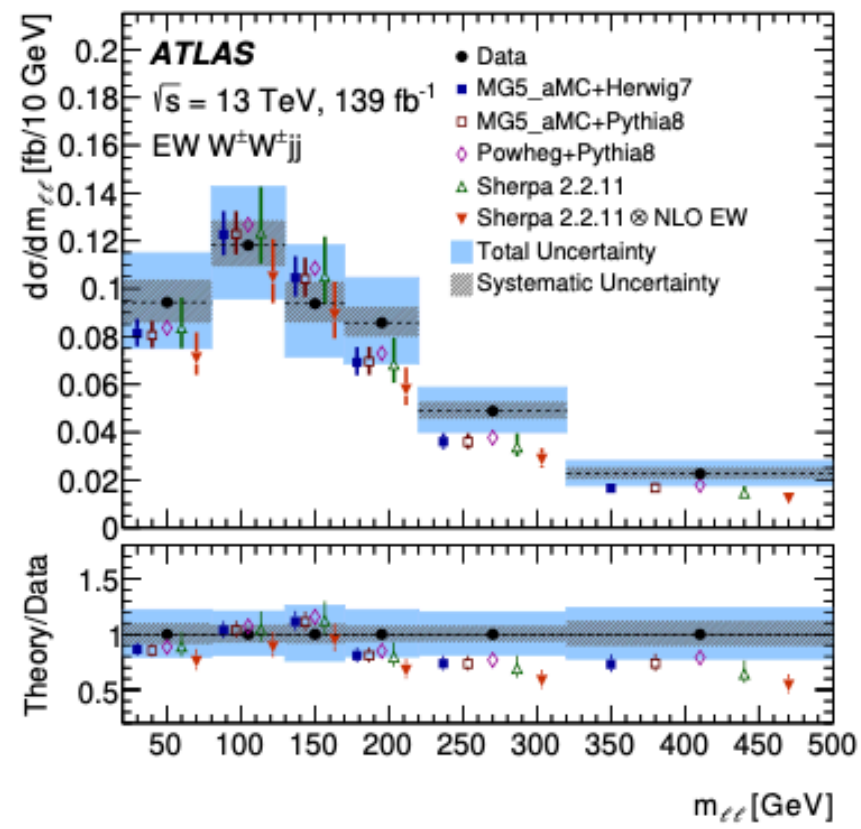


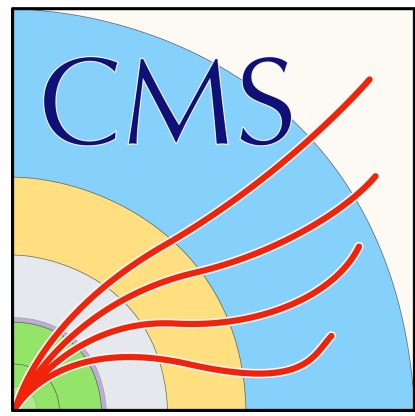
Wilson coefficient	Includes $ \mathcal{M}_{d6} ^2$	95% confidence interval [TeV ⁻²] Expected	95% confidence interval [TeV ⁻²] Observed	p -value (SM)
c_W/Λ^2	no	[-0.30, 0.30]	[-0.19, 0.41]	45.9%
	yes	[-0.31, 0.29]	[-0.19, 0.41]	43.2%
\tilde{c}_W/Λ^2	no	[-0.12, 0.12]	[-0.11, 0.14]	82.0%
	yes	[-0.12, 0.12]	[-0.11, 0.14]	81.8%
c_{HWB}/Λ^2	no	[-2.45, 2.45]	[-3.78, 1.13]	29.0%
	yes	[-3.11, 2.10]	[-6.31, 1.01]	25.0%
$\tilde{c}_{HWB}/\Lambda^2$	no	[-1.06, 1.06]	[0.23, 2.34]	1.7%
	yes	[-1.06, 1.06]	[0.23, 2.35]	1.6%

EFT Dimension 6 constraints

Inclusive Zjj - differential distributions

Same-sign WW - results (1)





VBF-H at CMS and ATLAS

Some literature

ATLAS